U.S. Department of Transportation
Federal Aviation Administration

Impact of Alternative Jet Fuel and Fuel Blends on Non-Metallic Materials Used in Commercial Aircraft Fuel Systems

Continuous Lower Energy, Emissions and Noise (CLEEN) Program

Submitted by The Boeing Company

DOT/FAA/AEE/2014-10

NextGEN

The Continuous Lower Energy, Emissions and Noise (CLEEN) Program is a Federal Aviation Administration NextGen effort to accelerate development of environmentally promising aircraft technologies and sustainable alternative fuels. The CLEEN Program is managed by the FAA's Office of Environment and Energy.

The report presented herein is an updated final report deliverable submitted by The Boeing Company for a project conducted under the CLEEN Program to evaluate the feasibility of selected alternative fuels as viable drop-in replacements to petroleum jet fuel. The initial study, completed in July 2011, examined the impact of aromatic molecules on fuel system materials. In a subsequent study, completed in December 2013 (and included in this updated report) work continued to examine the impact of cycloparaffin molecules on fuel system materials. This project was conducted under FAA other transaction agreement (OTA) DTFAWA-10-C-0030. This is report number DOT/FAA/AEE/2014-10 by the FAA's Office of Environment and Energy and it updates previously issued report number DOT/FAA/AEE/2012-01.

Note to the reader: Boeing refers to these fuels throughout the report as synthetic paraffinic kerosene (SPK). The classification of synthetic paraffinic kerosene encompasses alternative fuels derived from both the Fischer-Tropsch (FT) process and those classified as Hydroprocessed Esters and Fatty Acids (HEFA). Both of these fuel types are approved for use in commercial aviation at up to a 50% blend with petroleum jet fuel.

Final Report for Alternative Fuels Task: Impact of SPK Fuels and Fuel Blends on Non-metallic Materials used in Commercial Aircraft Fuel Systems

July 29, 2011

Updated December 18, 2013

Prepared for:

FAA Office of Environment and Energy under

CLEEN OTA Number: DTFAWA-10-C-0030

Prepared by:

The Boeing Company, and

University of Dayton Research Institute

Authors:

John L. Graham

University of Dayton Research Institute

Timothy F. Rahmes*, Mark C. Kay, Jean-Philippe Belières, James D. Kinder, Steven A. Millett, Jean Ray, William L. Vannice*, John A. Trela*

The Boeing Company

*-corresponding authors

Executive Summary

A study has been completed to examine the overall effect of SPK and SPK fuel blends on non-metallic materials used in commercial aircraft fuel systems. The primary measure of performance was the volume swell of dry source materials immersed in fuel for 40 hours at room temperature. Supporting data was obtained in the form of an analysis of the fuel absorbed by each test material using either thermogravimetric analysis or by thermal desorption gas chromatography-mass spectrometry. The volume swell and fuel absorbed using a set of 12 Jet-As and 4 SPKs were used as the primary basis for comparison. The Jet-As were selected to span a broad range of aromatics (from 8.7% to 23.1%) while the SPKs were selected from a variety of sources, though they were processed into 4 very similar fuels with 0% aromatics. To evaluate the relative importance of the molecular structure of fuel components in general, and aromatics in particular, the activity of 10 aromatics selected to emphasize the relative roles of molar volume, polarity, and hydrogen bonding were measured and compared with the reference Jet-As. Furthermore, data was obtained on a set of fuels consisting of 50% SPK/Jet-A fuel blends to assess the effect of these fuels on fuel system materials regardless of their aromatic content as well as the effect of those blends with 8% aromatics. This work was presented at the CRC annual meeting in Seattle in May, 2011, prior to the updated ASTM D7566-11 fuel specification approval of up to 50% SPK blends, released on July 1, 2011.

The overall response to the aromatic content of the fuel was found to be material-dependent with the greatest effect being shown by a nitrile rubber O-ring material, a polythioether and a polysulfide sealant. A fluorocarbon O-ring material was found to be relatively inert while two epoxy coatings and a nylon and a Kapton® film were found to be essentially inert in all of the test fuels. A fluorosilicone O-ring material was found to show moderate volume swell behavior, however the volume swell of this material was a very weak function of the aromatic content. Although the volume swell of the test materials tended to increase with the aromatic of the fuel, only the nitrile rubber O-ring and a polythioether and polysulfide sealant materials showed a volume swell character in the SPKs that was lower that of Jet-A based on the reference fuels used. It is very important to note that these results should be considered a statistical prediction as to whether the volume swell of a given blend would fall within the predicted ‘normal’ range for Jet-A.

With respect to the influence of the molecular structure of the fuel; volume swell was found to increase as the molar volume of the fuel components decreases and as their polarity and hydrogen bonding increases. Amongst these three factors (molar volume, polarity, hydrogen bonding) molar volume had the least influence on the volume swell followed by polarity and hydrogen bonding. Furthermore, the influence of hydrogen bonding tended to be significantly higher than that of polarity. This suggests that the volume swell of jet fuel will increase as the boiling range skews towards lower temperatures (lower molecular weight) and as the overall polarity and hydrogen bonding increases, and vice versa. Noting that the bulk of Jet-A and all of typical SPKs are paraffinic and therefore non-polar, the polarity and hydrogen bonding character of the fuel will be dominated by the aromatics. However, emphasizing that the bulk of the fuel is paraffinic, particularly as the aromatic content is lowered, the influence of the molecular weight distribution of the fuel must be considered. This emphasizes the importance of taking into

account the composition of a fuel as a whole when considering how it interacts with non-metallic materials and not focusing on one class fraction of the fuel such as aromatic content alone. Close inspection of the volume swell character of the neat SPK fuels shows that even though they span a boiling range similar to that of the reference JET-A fuels, their volume swell was less than the value expected by extrapolating the volume swell of the reference fuels. This has the effect of depressing the volume swell of blends prepared from these fuels. Prior studies have shown this to be a common phenomenon with paraffinic alternative fuels and that this may result from the absence of cycloparaffins.

Consequently, a follow-on study was performed in 2013 to evaluate the role of cycloparaffins in alternative fuels. It was found that cycloparaffins are smaller than comparable linear and branched paraffins and show relatively weak polarity, both factors that would contribute volume swell character to alternative fuels. A systematic study of cycloparaffins showed that modest volume swell activity is common to cycloparaffins, though much lower than aromatics. Furthermore, non-substituted cycloparaffins exhibit higher volume swell activity than substituted cycloparaffins. The addition of active cycloparaffins, such as decalin or cyclodecane, at levels comparable to what naturally occurs in conventional jet fuel (30% v/v) can elevate the volume swell character of SPKs to levels near that of a low aromatic Jet-A. This suggests that the addition of cycloparaffins to SPKs could reduce, or even eliminate, the need for aromatics in these fuels. The results of this follow-on study are contained within Appendix L.

Table of Contents

Index of Tables and Figures

Figures:

Tables:

1 Introduction and Background

1.1 Introduction

In 2010 the Federal Aviation Administration (FAA) initiated the Continuous Lower Energy, Emissions and Noise (CLEEN) program to develop technologies to assist in reducing the environmental impact of commercial aviation. One of several technology areas that are being examined for achieving this goal is the use of "drop-in" alternative jet fuels such as synthetic paraffinic kerosene (SPK), which is also known as hydrotreated renewable jet (HRJ). This fuel has the potential to be used in existing engines without modification. SPKs are unique in that they can be obtained from a variety of non-petroleum sources such as coal, natural gas, algae, agriculture, and biomass. The latter are particularly interesting in that they offer the potential for reduced lifecycle greenhouse gas emissions. A significant challenge facing the widespread use of low aromatic jet fuels is fully characterizing the impact of their use in systems that have evolved for use with petroleum distillate fuels. A concern focuses on lower aromatics content in these fuels compared to current fuels in use, which may cause polymeric materials such as O-ring seals and sealants to shrink, harden, and fail. Current industry experience has determined that a minimum of 8% aromatic content is required in synthetic jet fuel blends. Moreover, there is limited knowledge as to the influence of the types of aromatics on the strength of the interaction between the fuel and the various polymeric fuel system materials. However, it is known that while aromatics have a large influence on seal-swell, they are not the only fuel component affecting it. Oxygenates, sulfur-containing compounds, and acidic compounds are some examples of molecules that can also affect materials properties. This report summarizes the results of a study to evaluate the impact of low aromatic jet fuels on the volume swell of selected polymeric materials commonly used in commercial aircraft fuel systems. Appendix L extends this analysis to cycloparaffins which could reduce or eliminate the need for aromatics in future jet turbine fuels, significantly reducing the environmental impact of these fuels.

1.2 Background

In the absence of chemical reactions, when a new polymeric material is exposed to fuel for the first time two processes can occur. First, the material may absorb components from the fuel (alkanes, aromatics, additives, etc.) which by itself would generally cause the material to swell and soften. (Complete dissolution of the material would be a limiting case of this process.) Second, the fuel may extract components from the material (plasticizers, processing aids, residual solvents, etc.) which would generally cause the material to shrink and harden. The overall effect the fuel has on the material will be the balance of these two processes. Once the material has been in service for some time the fuel-extractable components will have been removed and all subsequent changes in physical properties will result from a shifting equilibrium between the material and the overlying fuel which in turn will depend on the composition of the fuel.

At its most fundamental level, the absorption of fuel by a polymeric material is governed by the chemical physics of polymer solutions, specifically the processes that occur very early in the formation of a polymer solution where the fluid first wets, then penetrates the polymer matrix.

Thermodynamically, this process can be described as a series of discrete steps beginning with the separation of fuel molecules from the bulk fluid through the breaking of fuel-fuel intermolecular bonds. Next, a cavity large enough to accept the fuel molecule must be opened in the polymer by breaking polymer-polymer intermolecular bonds on adjacent polymer strands, a process that imparts elastic strain on the polymer surrounding the penetration site. Finally, the fuel molecule is inserted into the polymer, creating polymer-fuel bonds. (The cavity left behind in the fuel must also be closed, though this step is often disregarded.) Energetically, this process can be expressed as the breaking of fuel-fuel intermolecular bonds (requiring energy), the separation of the polymer-polymer intermolecular bonds (requiring energy), and the making of polymer-fuel intermolecular bonds (releasing energy). Considering the overall energy balance of these processes, the strength of interaction between the fuel and polymer depends on the size and shape of the fuel molecules, the intermolecular bonding of the polymer, the intermolecular bonding of the fuel, and the intermolecular bonds that form between the polymer and the fuel penetrants.

One method of expressing the intermolecular bonding of polymers and solvents (in this case the fuel molecules) is through the use of Hansen solubility parameters (HSPs). Briefly, HSPs summarize the relative contributions of dispersion (van der Waals forces), polarity (dipole-dipole interactions), and hydrogen bonding (specific electrostatic interactions) to the overall intermolecular bonding of pure species (fuel-fuel and polymer-polymer interactions). The HSPs for selected fuel components are summarized in Table 1-1. These show that alkanes tend to be relatively large molecules that are non-polar and do not participate in hydrogen bonds. In contrast, aromatics (alkyl benzenes) are more compact, they can exhibit some polarity and they can form weak hydrogen bonds. The diaromatics (alkyl naphthalenes) are also relatively compact and can exhibit significant polar and hydrogen bonding character. Given that most fuel system polymers obtain their fuel resistance by virtue of relatively high polarity and hydrogen bonding it has been found that in very general terms the strength of interaction between a fuel and a polymeric fuel system material tends to increase as the molar volume of the fuel components decrease and as their polarity and hydrogen bonding increases. Based on these factors, the HSPs listed in Table 1-1 suggest that alkanes will have the weakest interactions with fuel-resistant polymeric materials followed by aromatics and diaromatics, which is consistent with the general observation that physical properties such as volume swell tends to vary with the aromatic content of jet turbine fuels. However, it is important to note that the extent of interaction will be very material dependent as well as a function of the specific components present in the fuel. Furthermore, it is important to note that while the interactions between the alkanes and fuel-resistant materials is expected to be weak, the alkanes are the largest single class of compounds in a typical jet fuel and they can also have an influence on the overall strength of interaction between the fuel and polymer.

With respect to the material compatibility of jet fuels, including alternative fuels, it would be beneficial if there were tabulations of the allowable limits function critical physical properties (volume change, modulus, glass transition temperature, etc.) but unfortunately this information is not available. This is a consequence of the historical background of how fuel system materials have been developed; that is the implicit assumption that they would be used in service with petroleum distillate fuels whose properties are set by the respective fuel specifications which in

turn limits the variation in both composition and the range of interactions these fuel have on polymeric materials. In the absence of defensible, quantitative limits on physical properties an alternative approach to assessing material compatibility has been developed. Briefly, it is assumed that all fuel system materials currently in use have passed their respective qualification requirements and no further certification is necessary. Furthermore, in the course of normal service fuel system polymers are exposed to a variety of fuels with a commensurate range of compositions and range of interactions with the fuel system materials. By default, even though the range of the real in-service variation in the physical properties of these polymers may be unknown, they are considered acceptable by virtue of the fact that they do not adversely affect current in-service performance. Consequently, the overall approach used in this study is to establish a reference population using a set of representative jet fuels and to compare the behavior of the test fuels and fuel blends with this reference set. If the variation of the selected physical property resulting from the exposure to the test fuel falls within the range of the reference population then the test fuel is likely to be compatible with conventional fuels. If the variation of the physical property resulting from the exposure to the test fuel falls outside the range of the reference population the extent of deviation can form the basis for making a determination as the material compatibility of the test fuel.

Table 1-1 Hansen Solubility Parameters ($MPa^{1/2}$) for Selected Fuel Components

Compound Class	Fuel Component	Hansen Solubility Parameters			MV
		Dispersion	Polar	H-Bond	mL/mol
Alkanes	Nonane	15.7	0.0	0.0	180
	Decane	15.7	0.0	0.0	196
	Dodecane	16.0	0.0	0.0	229
	Hexadecane	16.3	0.0	0.0	294
Aromatics	Benzene	18.4	0.0	2.0	89
	Toluene	18.0	1.4	2.0	107
	o-Xylene	17.8	1.0	3.1	121
	Ethyl Benzene	17.8	0.6	1.4	123
	1,2,3-Trimethylbenzene	17.8	0.4	1.0	134
	1,3,5-Trimethyl Benzne	18.0	0.0	0.6	140
	o-Diethyl Benzene	17.7	0.1	1.0	154
	p-Diethyl Benzene	18.0	0.0	0.6	157
	N-Butylbenzene	17.4	0.1	1.1	157
	o-N-Butyltoluene	17.6	0.1	1.0	171
	p-N-Butyltoluene	17.4	0.1	1.0	174
Diaromatics	Naphthalene	19.2	2.0	5.9	112
	1-Methyl Naphthalene	20.6	0.8	4.7	139

2 Experimental Methods

2.1 Volume Swell

The physical property of fuel system materials selected for analysis in this study is volume swell. Volume swell is a basic response of a polymeric material when exposed to jet fuel and an important physical property for components such as O-ring seals, sealants, and coatings. Volume swell was measured using a technique described as optical dilatometry (see J.L. Graham, R.C. Striebich, K.J. Myers, D.K. Minus, W.E. Harrison, "The Swelling of Nitrile Rubber by Selected Aromatics Blended in a Synthetic Jet Fuel," *Energy and Fuels*, *20* (2), 2006, pp. 759-765). As illustrated in Figure 2-1, and shown in Figure 2-2 an optical dilatometer consists of an optical cell positioned over a small digital camera and illuminated from above with a small flat panel LED. For each analysis small samples measuring approximately 2mm x 2mm were placed in the optical cell along with 10 mL of the test fuel. (As described below and listed in Table 2-2, the thickness of the samples varied depending on the source material.) The samples were positioned near the center of the cell and rested on the bottom of the vessel. Starting at 2 minutes after being immersed in the fuel the samples were digitally photographed every 20 seconds for the next 3 minutes. At 6 minutes total elapsed time the samples were photographed every 15 minutes for the next 40 hours. During the exposure the fuel was static and at room temperature (75°F +/- 5°F). After the aging period was complete the cross-sectional area of each sample was extracted from the digital images, which in turn was taken as a characteristic dimension proportional to the volume (isotropic volume swell was assumed for the amorphous materials used here). The final volume swell for each sample is taken as the average of the last five data points in each set (the last hour of the exposure). The final volume swell for each test material is taken as the average of 2 or more samples.

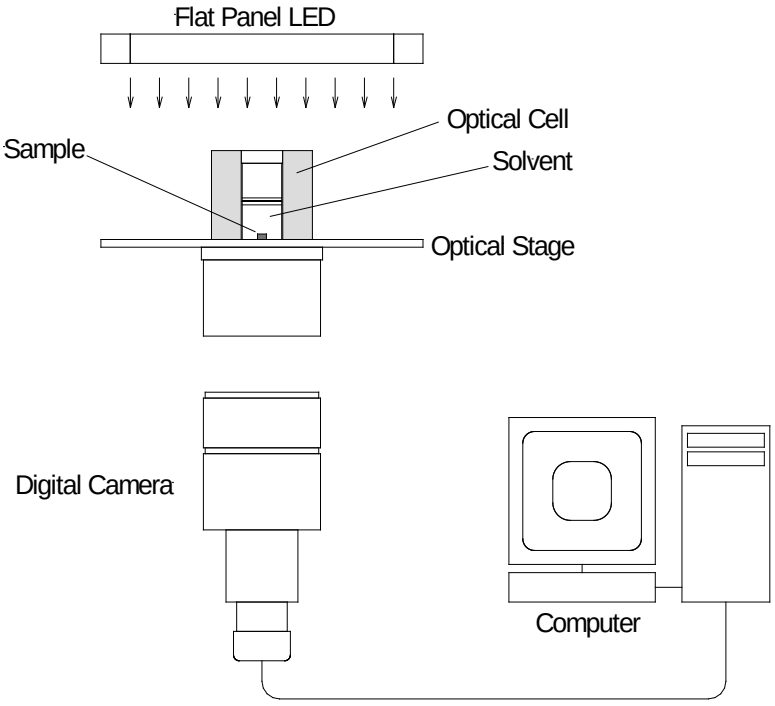

Figure 2-1. Schematic of an optical dilatometer.

Figure 2-2. An early example of an optical dilatometer.

Note that in some cases (see the appendices) the volume swell of the test material was not at equilibrium by the end of the 40-hour aging period. However, the progression of the volume swell was considered sufficient to establish the relative response of each material to the test fuel. Furthermore, the scope of this study was intended to examine the acute response of the test materials to each of the test fuels.

2.2 Analysis of Absorbed Fuel

Although volume swell was the primary measure of a material's overall response to a fuel, additional supporting data in the form of the mass fraction of fuel absorbed as measured by thermogravimetric analysis (TGA) as well as the composition of the absorbed fuel as determined by gas chromatography-mass spectrometry (GC-MS). For the latter the composition of the absorbed fuel is determined by direct thermal desorption GC-MS of small samples weighing approximately 1mg sectioned from the volume swell samples and returned to the fuel for 7-10 days. An identical analysis was performed on the fuel in which the material was aged allowing the relative solubility of the major class fractions of the fuel to be expressed in terms of their partition coefficients (Kpf, the ratio of the concentration in the material to the concentration in the overlying fuel). The Kpf values reflect the relative solubility of each class fraction in the specific test material. The Kpf values were also used to estimate the overall composition of the absorbed fuel to reflect how each class fraction contributes to the observed volume swell. For this study the major class fractions were taken as the alkanes, aromatics (alkyl benzenes), naphthalene, and naphthalenes (alkyl naphthalenes). These class fractions are obtained from the total ion chromatograms (TICs) using extracted ions taken as being characteristic of each class; 43 amu (atomic mass units) for the alkanes, 105 amu for the alkyl benzenes, 128 amu for naphthalene, and 141 amu for the alkyl naphthalenes.

2.3 Statistical Analysis of the Volume Swell and Mass Fraction of Fuel Absorbed

Once the volume swell and mass fraction of fuel absorbed had been obtained for all of the reference Jet-A's the mean (using a linear fit to the data), 90% confidence interval, and 90% prediction interval for all Jet-A's with an aromatic content of 10%-25% was estimated using SAS v9.2 (SAS Institute, Inc.). Although 8% has been proposed as a lower limit for the aromatic content of alternative jet turbine fuels, the range of 10%-25% was selected as being representative of the range in which 95% of all jet turbine fuels lie based on an analysis of JP-8 purchased by the U.S. Air Force (see "Properties of Fischer-Tropsch (FT) Fuel Blends for Use in Military Equipment", SAE Document Number 2006-01-0702). This approach results in an analysis that is somewhat more conservative than the proposed 8% lower limit.

In addition to describing the statistical distribution of the reference populations, a similar analysis was applied to 50% SPK/Jet-A fuel blends. The overlap between the 90% prediction intervals (P.I.) of the reference and test fuel populations was taken as;

$$\text{Overlap } 90\%\text{ PI} = \frac{\text{(UL Test Fuel) - (LL Reference Fuels)}}{\text{(UL Test Fuel) - (LL Test Fuel)}} \times 100\% \qquad (1)$$

Here UL and LL are the upper limit and lower limit of the respective 90% confidence intervals. A similar metric was used to quantify the relative difference between the average point values for the SPKs and the reference populations as;

$$\text{Relative Difference} = \frac{\text{(Point Value) - (LL Reference Fuels)}}{\text{(UL Reference Fuels) - (LL Reference Fuels)}} \times 100\% \qquad (2)$$

Finally, each of the reference data sets was fit with a linear regression model of the volume swell versus the aromatic content of the fuel and summarized in terms of the intercept (estimated volume swell in a Jet-A with 0% aromatics), slope (also referred to as the specific swell; %swell/%aromatics), and coefficient of determination (R^2).

2.4 Source Materials

The fuels selected for use in this study are listed in Table 2-1. These included 12 Jet-A fuels with 8.7% to 23.1% aromatics. All reference fuels used were taken from commercial providers, without modification, with the exception of the lowest aromatic sample (SRI-1), which, after clay treating was examined for the presence of residual diEGME using extracted ion chromatograms taking mass fragments with m/e of 45 and 90 amu as being characteristic of this additive. This analysis showed that if present, diEGME in SRI-1 was below the detection limit of approximately 1 ppm. Furthermore, the fuel absorbed by each elastomer was also examined for the presence of diEGME and none was observed.

The materials selected for these are listed in Table 2-2, and included 4 O-ring materials, 2 sealants, 2 coatings, and 2 films. Note that the nitrile rubber material was examined in two variants; as-received N0602 and as a version with its plasticizer extracted and re-designated as N0602e. Briefly, the N0602e O-ring samples were prepared by soaking them in acetone for 24 hours, rinsing them with fresh acetone, and repeated 3 times. After the final wash with fresh acetone the samples were air-dried for 24 hours, then dried in a force-convection oven at 60ºC for 1 hour.

Table 2-1 Fuels Used in This Study

Fuel	ID	Aromatics	Naphthalenes	Notes
Jet-A	SRI-1	8.7%	0.2%	Clay-treated JP-8
	4597	15.0%	1.9%	
	5245	15.5%	0.2%	
	3166	17.6%	2.5%	
	4598	17.6%	1.4%	
	4600	17.7%	1.3%	
	4658	17.7%	1.3%	
	4626	17.9%	0.6%	
	5661	18.1%	0.6%	
	4877	19.6%	0.4%	
	4599	19.9%	1.4%	
	3602	23.1%	1.1%	
Average		17.4%	1.1%	
SPK	SPK-1	0.0%	0.0%	Jatropha
	SPK-2	0.0%	0.0%	Camelina
	SPK-3	0.0%	0.0%	Jatropha-Camelina-Algae
	SPK-4	0.0%	0.0%	Bio-Oil Derived SPK

*Naphthalenes, **Synthetic Paraffinic Kerosene

Table 2-2 Materials Used in This Study

Component	Material	Sample ID	Sample Thickness
O-Rings	Nitrile Rubber	N0602	1mm
	Extracted Nitrile Rubber*	N0602e	1mm
	Fluorosilicone	L1120	1mm
	Low Temp Fluorocarbon	V0835	1mm
Sealants	Lightweight Polysulfide	PR 1776	1mm
	Polythioether	PR 1828	1mm
Coatings	Epoxy	BMS 10-20	0.2mm
	Epoxy	BMS 10-123	0.04mm
Films	Nylon (6,6)	Nylon	1mm
	Kapton	Kapton	0.08mm

3 Results and Discussion

3.1 Volume Swell of Reference Jet-A and SPK

The volume swell of the test materials in the reference fuels and SPKs are summarized in Table 3-1 and Figure 3-1. through Figure 3-4. Each of the data figures shows the average volume swell for each of the test fuels and the 90% confidence interval for each data point (i.e. error bars). The overall statistical analysis includes the line of best fit through the reference data set and the 90% confidence interval for the regression line. The analysis also shows the 90% prediction interval which is a statistical prediction for the volume swell of 90% of all individual Jet-As based on the distribution of the reference fuels. Each graph gives the equation for the line of best fit and the coefficient of determination (R^2). The intercept of this line gives the statistical prediction of the volume swell of a Jet-A with 0% aromatics (the volume swell of the alkane fraction of the fuel in the absence of aromatics), the average strength of interaction between Jet-A and the test material in terms of the slope (specific swell), and how strongly the strength of interaction correlates with the aromatic content of the fuel (the R^2 value).

Table 3-1 Overall Summary of the Volume Swell Results for the Neat Fuels

Component	Sample ID	Material	Jet-A 90% PI*		Average SPK	Relative Diff.	Specific Swell**	R^2
			LL	UL				
O-Rings	N0602	Nitrile Rubber	3.72%	17.40%	0.15%	-26%	0.549	0.724
	N0602e	Nitrile Rubber	15.25%	33.24%	9.98%	-29%	0.690	0.679
	L1120	Fluorosilicone	4.00%	8.03%	6.44%	60%	0.057	0.076
	V0835	Fluorocarbon	0.18%	1.30%	0.25%	7%	0.024	0.201
Sealants	PR 1776	Polysulfide	-2.20%	0.98%	-2.56%	-11%	0.102	0.498
	PR 1828	Polythioether	2.00%	6.85%	0.17%	-38%	0.153	0.481
Coatings	BMS 10-20	Epoxy	-0.17%	0.19%	-0.03%	39%	-0.005	0.071
	BMS 10-123	Epoxy	-0.14%	0.18%	-0.03%	35%	0.000	0.000
Films	Nylon	Nylon	-0.32%	0.15%	-0.14%	39%	-0.014	0.406
	Kapton	Kapton	-0.21%	0.20%	-0.14%	16%	0.006	0.073

***PI = Prediction Interval, **Specific Swell = Slope of Volume Swell vs. Aromatic Content**

Considering the four O-ring materials (Figure 3-1.), the nitrile rubbers show the strongest response (dependence) to the aromatic content in the reference Jet-As. Specifically, the 90% prediction interval for the as-received nitrile rubber (Figure 3-1.) varies from 3.7% to 17.4% (a span of 13.7%) while the extracted nitrile rubber varies from 15.3% to 33.2% (a span of 18.0%). The slightly wider span of the extracted nitrile rubber is thought to result from the partial extraction of plasticizer from the as-received nitrile rubber by the jet fuel. Specifically, as the aromatic content of the fuel increases, it becomes a better solvent for the plasticizer which tends to depress the volume swell line for the new O-ring material. This effect is absent from the extracted nitrile rubber which is thought to give a better representation of the behavior on in-service nitrile rubber O-rings. Both of the nitrile rubber materials show a strong influence from the aromatics present in the reference fuels with specific swells of 0.549 and 0.690 for the as-received and extracted nitrile rubbers, respectively. Both show modest correlation between the

volume swell and the aromatic content with R^2 values of 0.724 and 0.679 for the as-received and extracted nitrile rubbers, respectively. Note that the 90% confidence intervals on the individual data points is quite small showing that the variation in the data is largely due to real differences in the volume swell character of the different fuels. Finally, note that the volume swell of the SPKs is below the range predicted for Jet-A indicating that the volume swell of the neat SPKs (0% aromatics) would be lower than what is expected with a low-aromatic jet fuel.

The fluorosilicone O-ring material was interesting in that it shows moderate volume swell (from 4 to 8% based on the 90% prediction interval), but only a weak dependence on the aromatic content of the fuel. The specific swell was found to be only 0.0569 with an R^2 value of 0.0764. Furthermore, the average volume swell for the SPKs was found to be near the average for the reference Jet-As; 6.4% for the average of the four SPKs versus 6.0% for the average of the 12 Jet-As. The 90% confidence intervals for the individual data points are much wider than what was observed for the nitrile rubber, though this is typical for this material. Additional data would likely reduce the 90% confidence intervals, however the overall conclusion is not expected to change; fluorosilicone O-rings should be suitable for service in both Jet-A and the SPKs used here.

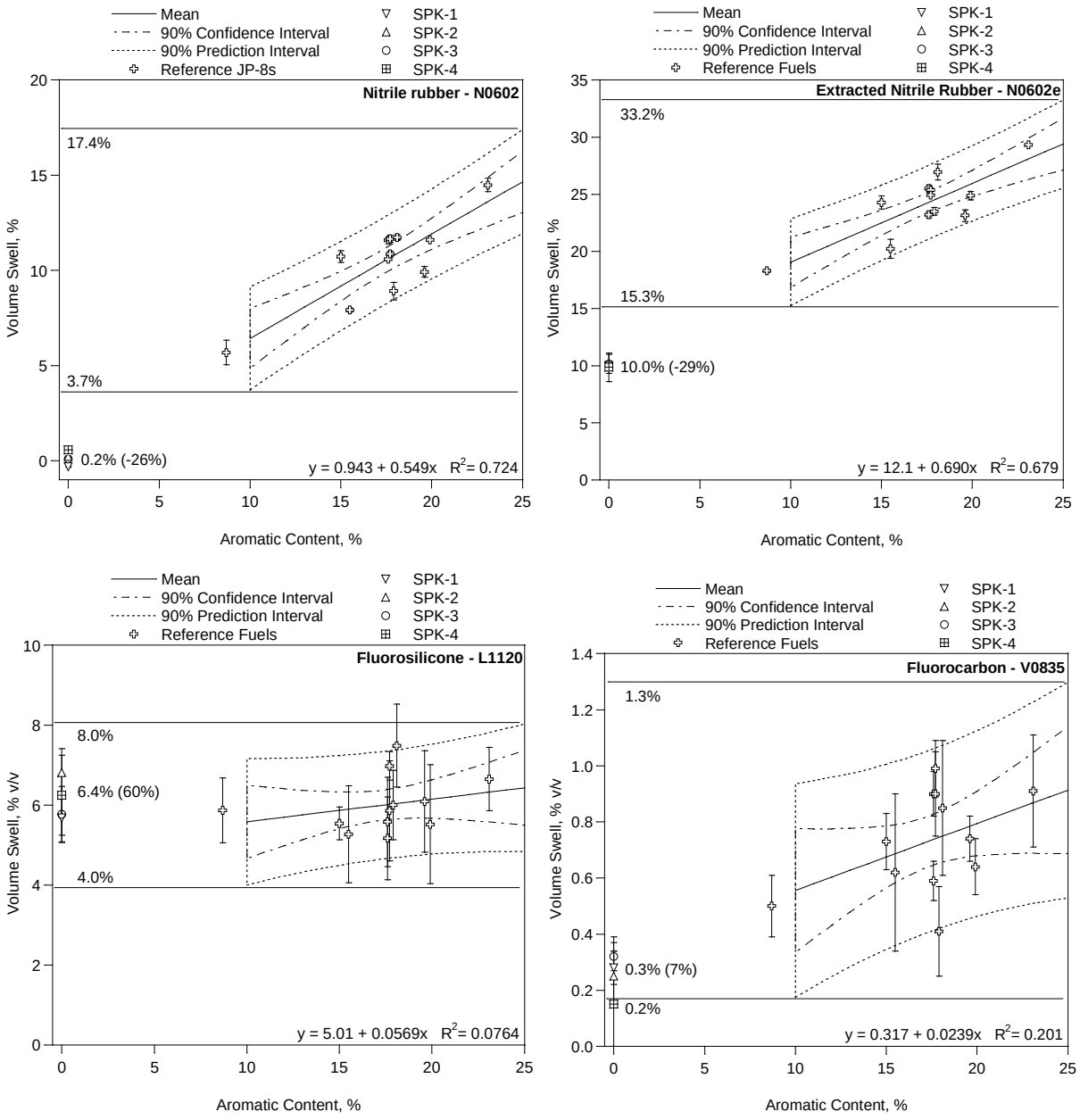

Figure 3-1. The volume swell of the O-ring materials after 40 hours at room temperature. Note the relative difference between the average SPK and the Jet-A 90% prediction interval is in parentheses

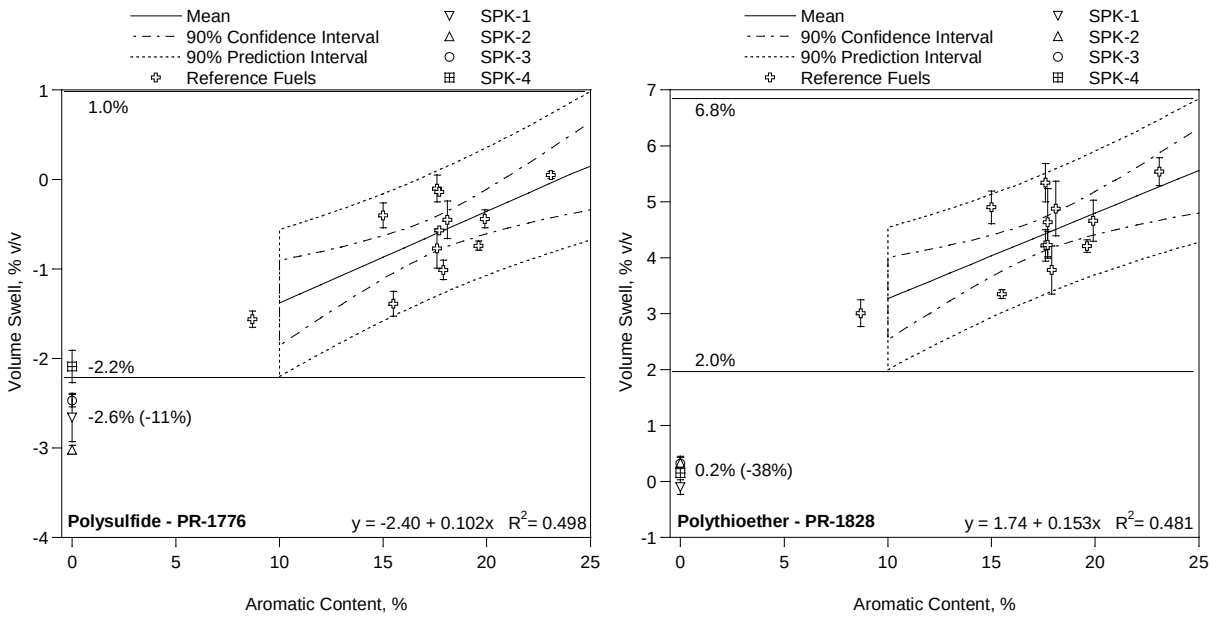

Figure 3-2. The volume swell of the sealant materials after 40 hours at room temperature. Note the relative difference between the average SPK and the Jet-A 90% prediction interval is in parentheses

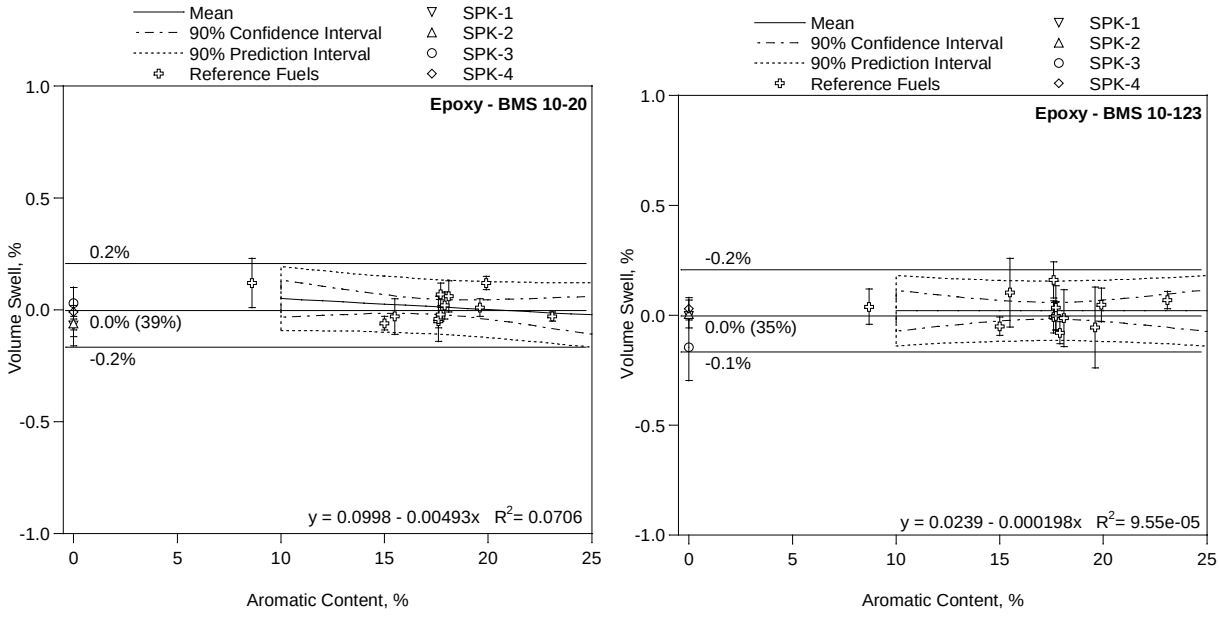

Figure 3-3. The volume swell of the coating materials after 40 hours at room temperature. Note the relative difference between the average SPK and the Jet-A 90% prediction interval is in parentheses

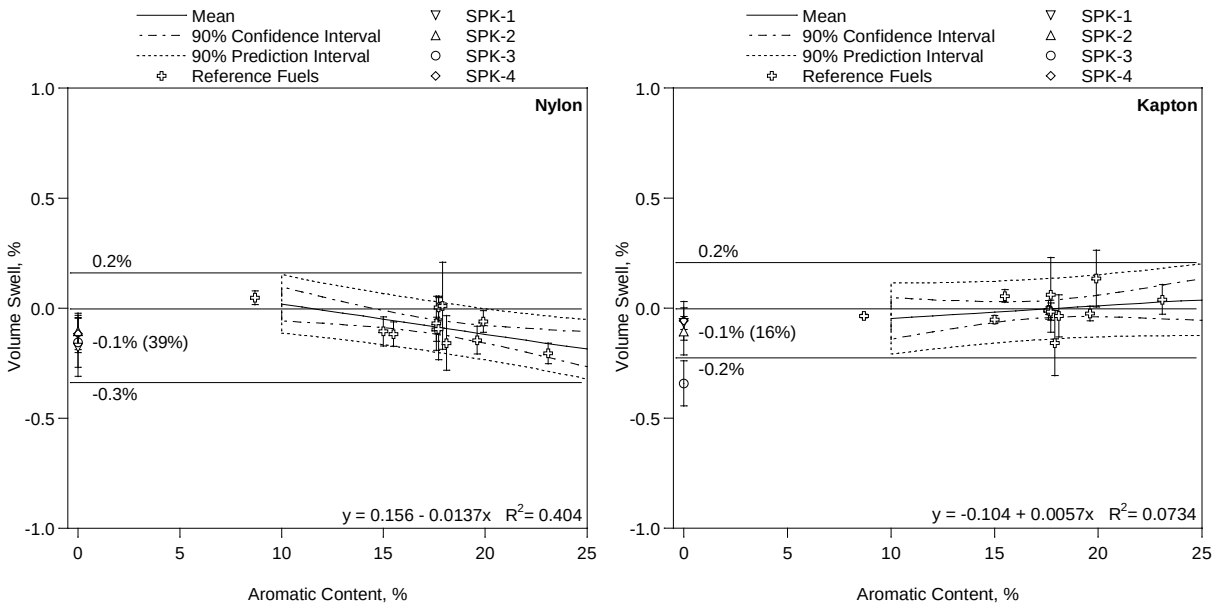

Figure 3-4. The volume swell of the film materials after 40 hours at room temperature. Note the relative difference between the average SPK and the Jet-A 90% prediction interval is in parentheses

The volume swell of the fluorocarbon was found not only to be a relatively weak function of the aromatic content but also to span a relatively narrow range. Specifically, the 90% prediction interval for the volume swell was found to vary from 0.2% to 1.3% with a specific swell of 0.0239 and an R^2 value of 0.201. The average volume swell for the SPKs was found to be within the lower bound of this range with a value of 0.3% suggesting that fluorocarbon O-rings should be suitable for service in both Jet-A and the SPKs used here.

The two sealants showed an interesting range of behavior (Figure 3-2) with the polysulfide PR-1776 shrinking in most of the test fuels and the polythioether showing behavior that was similar to nitrile rubber. The polysulfide showed a modest response to the aromatic content of the reference fuels with the 90% prediction interval varying from -2.2% to 1.0% (a span of 3.2%) and a specific swell of 0.102 and an R^2 value of 0.498. The polythioether showed a somewhat stronger response with the 90% prediction interval varying from 2.0% to 6.8% (a span of 4.8%) and a specific swell of 0.153 and an R^2 value of 0.481. In both materials the volume swell of the SPKs was below the 90% prediction intervals for Jet-A indicating that these materials would shrink to some extent if exposed to these SPKs after being in service with Jet-A, however, given that the polysulfide shrinks even when exposed to Jet-A it is not clear if this would be a problematic response for these materials.

The two coatings and two films (Figure 3-3 and Figure 3-4, respectively) proved to be relatively inert when exposed to the Jet-As and SPKs used in this study. Furthermore, in each case the average volume swell of the SPKs was within range of the reference Jet-As indicating that these materials should be suitable for service in both Jet-A and the SPKs used here.

The overall results from the analysis of the volume swell of the test materials in the reference fuels and neat SPKs is summarized in Table 3-1 and Figure 3-5 in terms of the R^2 values and the specific swell. In this figure the strength of interaction between the fuel and material increases from left to right and the strength of the correlation between the effect and the aromatic content increases from bottom to top. Therefore, materials to the upper right are of highest importance as they show a strong effect that correlates with the aromatic content, while those in the lower left show a relatively weak effect and a poor correlation with the aromatic content. This shows that amongst the materials tested here the nitrile rubbers and sealants are of highest concern for service in low aromatic fuels.

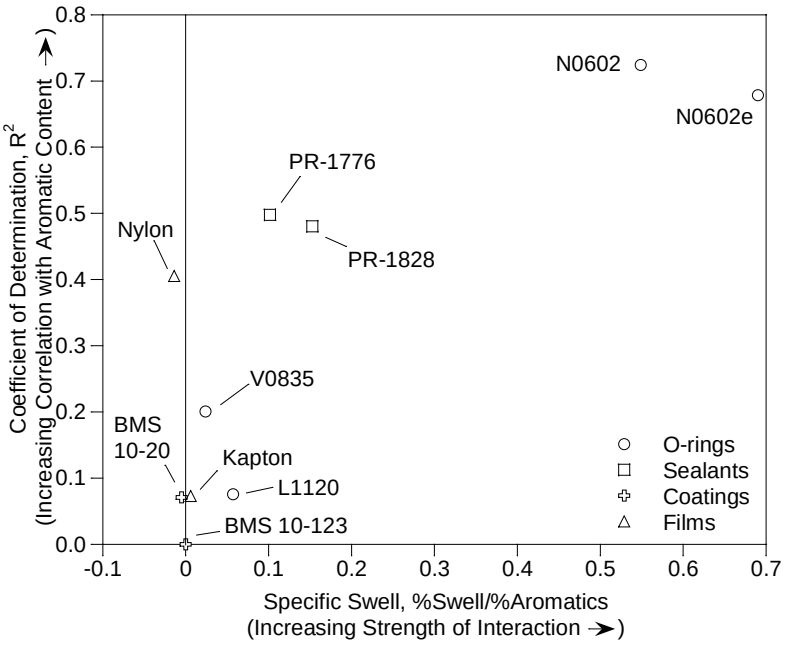

Figure 3-5. The coefficient of determination (R^2) versus the specific swell (slope of the volume swell in the reference Jet-As versus their aromatic content)

3.2 Thermogravimetric Analysis (Mass Fraction) of Absorbed Fuel

The volume swell measurements described above provide valuable information as to how each material responds to the test fuels. However, by itself, volume swell may not accurately reflect the true strength of interaction between the fuel and polymer. Of particular concern are those materials that contain a significant fraction of components such as plasticizers, processing aids, oligomers (partially cured elastomers), and residual solvents that may be extracted by the fuel. For these materials the volume swell measurement may be a convolution of volume gained by the absorption of fuel and volume lost by the extraction of mobile components. This is very common in O-ring materials such as nitrile rubber which is why the plasticizer was removed for one of the materials used in this study. Another very good example is the PR-1776 polysulfide sealant; since this material shrank in nearly all of the fuels used in this study the true strength of

interaction between the fuel and polymer cannot be assessed by the volume swell alone. Another factor is how to evaluate materials for which measuring the volume swell is problematic; materials such as foams and non-curing groove sealants being examples. For these materials an alternative method for measuring the strength of interaction between the fuel and material may be needed.

An alternative to volume swell (or as a supplement to volume swell) is to measure the mass fraction of fuel absorbed by a material using thermogravimetric analysis (TGA). An example of such an analysis is shown in Figure 3-6.

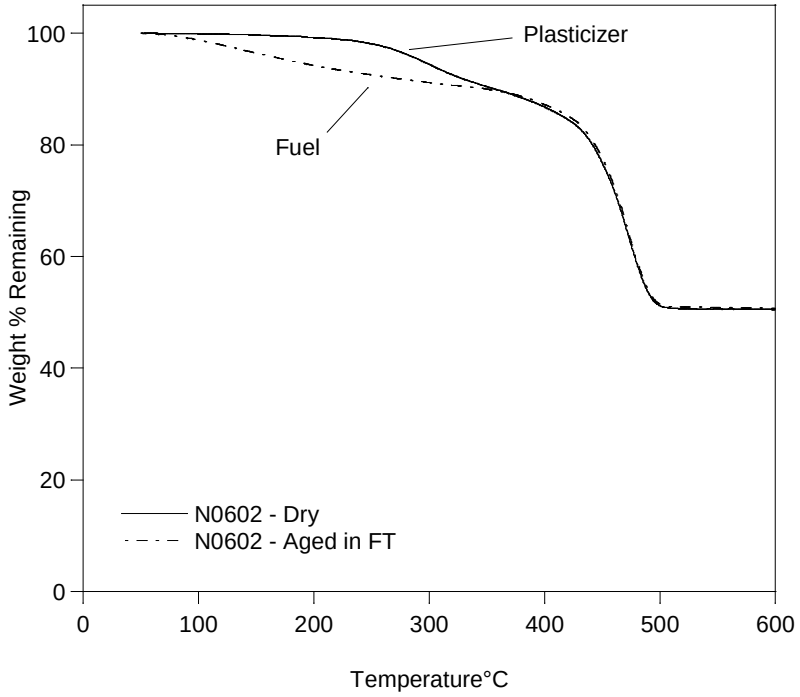

Figure 3-6. An example TGA trace for dry nitrile rubber and nitrile rubber aged in a Fischer-Tropsch (FT) fuel showing the mass of plasticizer extracted by the fuel is similar to the mass of fuel absorbed

The TGA results for the O-ring and sealant materials are summarized in Figure 3-7 and Figure 3-8, respectively. (Note that the coatings and films did not absorb enough fuel to be analyzed by this method). Comparing the TGA and volume swell data shows that the two approaches give very similar results with respect to comparing the mass fraction of the SPK fuel absorbed with the 90% prediction intervals for the mass fraction of Jet-A absorbed. However, there are some informative differences. For example, the results compare very well for the materials that do not have a significant extractable fraction. This includes the extracted nitrile rubber, fluorosilicone, and fluorocarbon O-ring materials. This is because the volume fraction and mass fraction of fuel absorbed are related through the density of the polymer and fuel so that while the two methods may give numerically different results, the comparative results should be the same. For materials that do have a significant extractable fraction the TGA results compare well with the volume

swell results in terms of comparing the SPK and reference Jet-As, however the TGA results more accurately reflect the true strength of interaction between the fuels and elastomers. For example, the volume swell results for the as-received nitrile rubber (Figure 3-1.) shows only 0.2% volume swell for the average SPKs suggesting that only 0.2% v/v fuel is absorbed and that the interaction between the SPKs and nitrile rubber was very weak. However, the TGA results show that 6.4%m/m fuel was actually being absorbed indicating a much stronger level of interaction between the SPK and nitrile rubber. Similarly, the volume swell data for the PR-1828 polythioether also showed an average of only 0.2%v/v, but the TGA data showed an average of 1.3%m/m of the SPKs were being absorbed. Finally, since nearly all of the PR-1776 polysulfide samples shrank when exposed to the SPKs and Jet-As this data reveals very little about the true strength of interaction between the fuels and this material. However, the TGA data shows that an average of 2.0%m/m of the SPKs was being absorbed by this material. Finally, by comparing the TGA results for the as-received and extracted nitrile rubbers (Figure 3-7) shows that removing the plasticizer did not affect the absorption of fuel by this material.

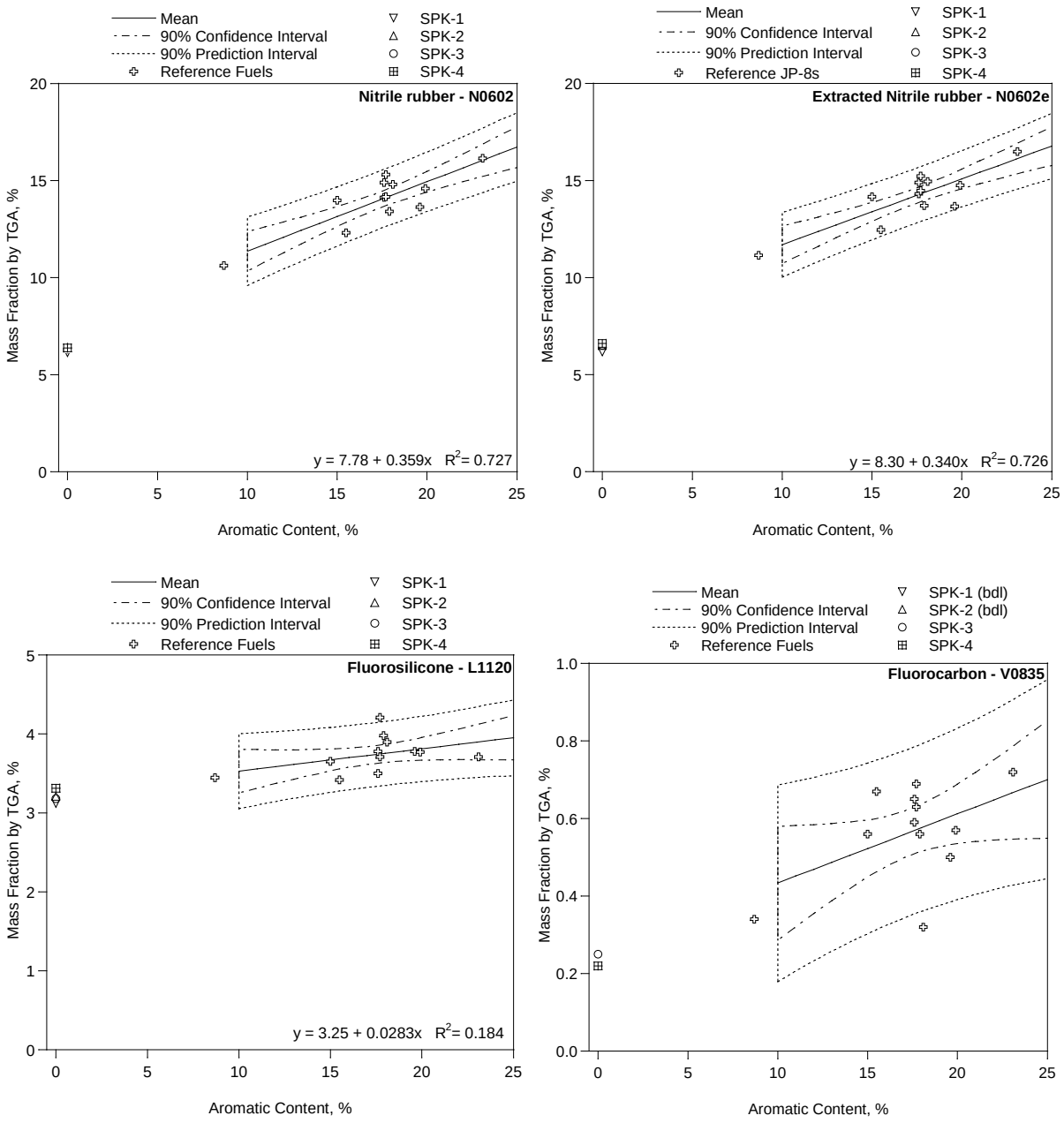

Figure 3-7. Summary of TGA results for the O-ring materials

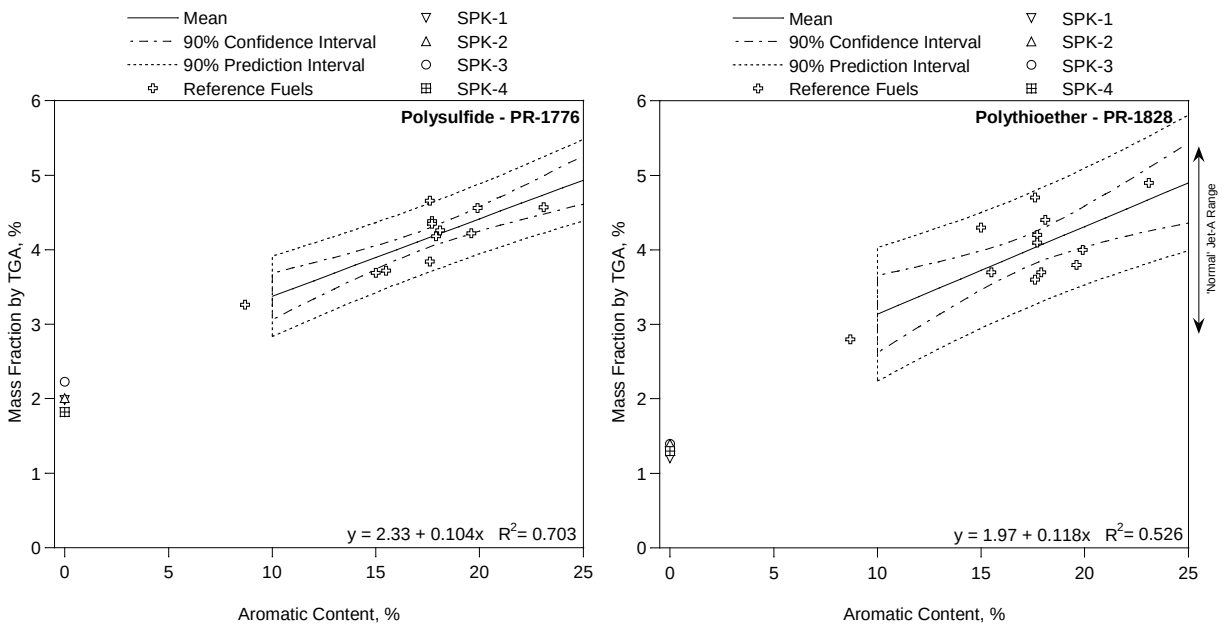

Figure 3-8. Summary of TGA results for the sealant materials

3.3 GC-MS Analysis of Absorbed Fuel

This discussion above illustrates that useful information may be obtained using a relatively simple method such as TGA to measure the mass fraction of fuel being absorbed by polymers aged in jet fuel. However, this technique has limited sensitivity (about 0.1%m/m) and may be challenged by interferences from semi-volatile components that cannot be clearly discriminated from fuel in the source weight loss data. By itself TGA also does not provide any information as to the composition of the absorbed fuel. However, this information may be obtained by analyzing the absorbed fuel using gas chromatography-mass spectrometry (GC-MS). Furthermore, comparing the analysis of the fuel absorbed with the fuel in which the sample was aged allows the relative solubility of the major class fractions and even individual fuel components in terms of their polymer-fuel partition coefficients (Kpf). This same data can be used to estimate the overall composition of the absorbed fuel which in turn reflects how each class fraction contributes to the observed volume swell.

Example GC-MS chromatograms for the fuel absorbed by the O-ring and sealant materials as well as the fuel in which they were aged are shown in Figure 3-9 to Figure 3-13. (Note that the coating and film materials did not absorb enough fuel to be analyzed by the method used here.) The average partition coefficients for the alkanes, alkyl benzenes (Alkyl Bz), naphthalene (Naph), and alkyl naphthalenes (Naphs) are summarized in Table 3-2. The estimated average composition of the fuel absorbed by each material is summarized in Table 3-3.

Overall, the chromatograms shown in Figure 3-9 to Figure 3-13 show that the fuel absorbed by each material is very complex and in most cases is as complex as the fuel itself. This illustrates

that the fuel as a whole participates in the volume swell process and not just the aromatics. Close examination shows that the aromatics are absorbed with a higher degree of selectivity as compared to the alkanes, but not to the exclusion of the alkanes. With respect to the alkanes, examining the chromatograms for the example SPK (SPK-2) illustrates how each material responds to the molar volume of the fuel components. Specifically, since the alkanes are non-polar and cannot participate in hydrogen bonds (see Table 1-1) the only mechanism of selectivity by the materials is molar volume. Specifically, each of the chromatographic traces for the SPK absorbed by the test materials shows some degree of selectivity towards the low molecular weight components (those on the left end of the chromatograms). This is most notable in the data for the fluorocarbon O-ring material (V0835 in Figure 3-11) which shows a high degree of selectivity towards the light end of the chromatogram.

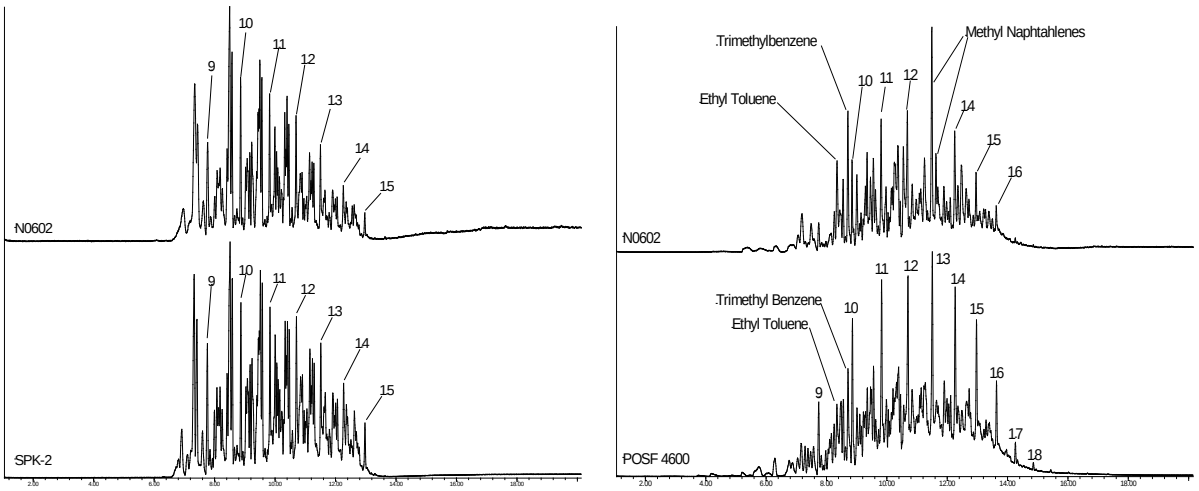

Figure 3-9. Example chromatograms comparing the fuel absorbed by the nitrile rubber (N0602) O-ring material (top) and the fuel in which they were aged (bottom). Note that normal alkanes are labeled with their carbon number

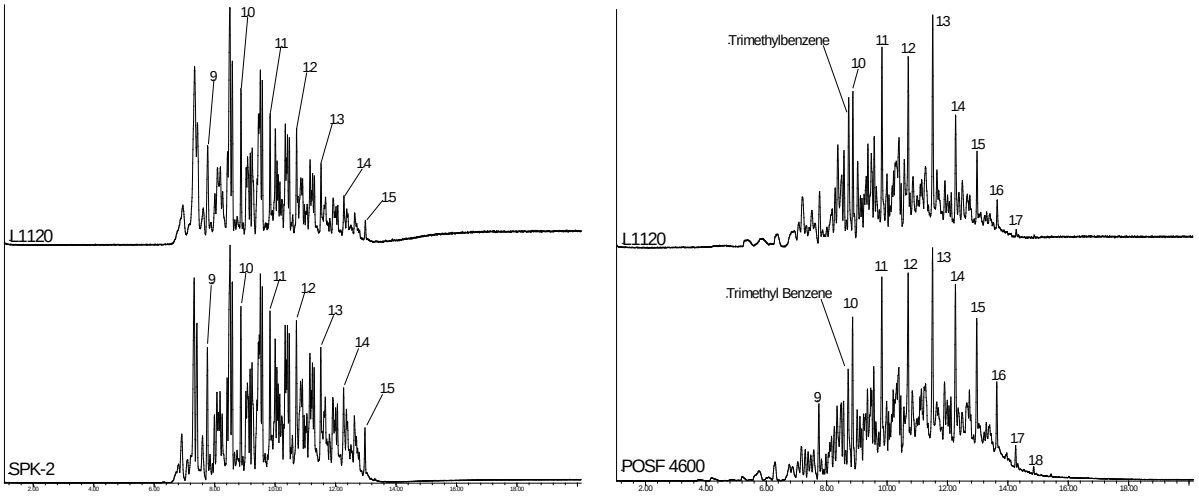

Figure 3-10. Example chromatograms comparing the fuel absorbed by the fluorosilicone (L1120) O-ring material (top) and the fuel in which they were aged (bottom). Note that normal alkanes are labeled with their carbon number

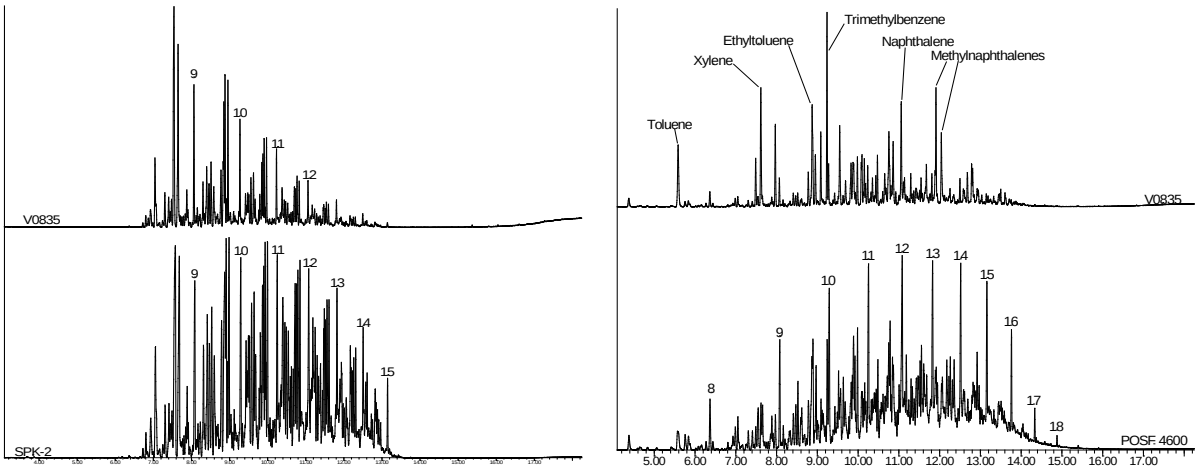

Figure 3-11. Example chromatograms comparing the fuel absorbed by the fluorocarbon (V0835) O-ring material (top) and the fuel in which they were aged (bottom). Note that normal alkanes are labeled with their carbon number

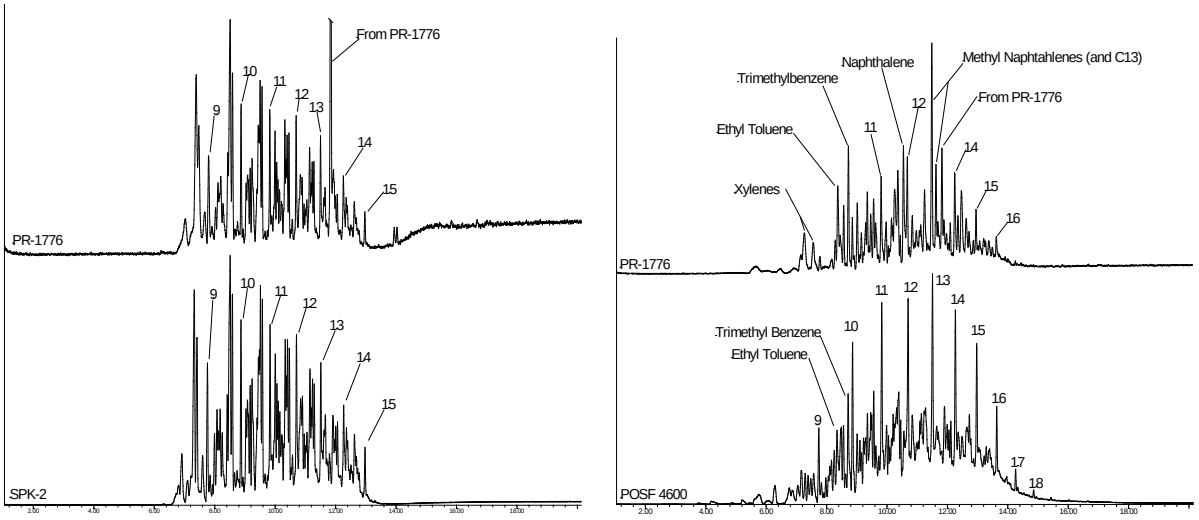

Figure 3-12. Example chromatograms comparing the fuel absorbed by the polysulfide (PR-1776) sealant material (top) and the fuel in which they were aged (bottom). Note that normal alkanes are labeled with their carbon number

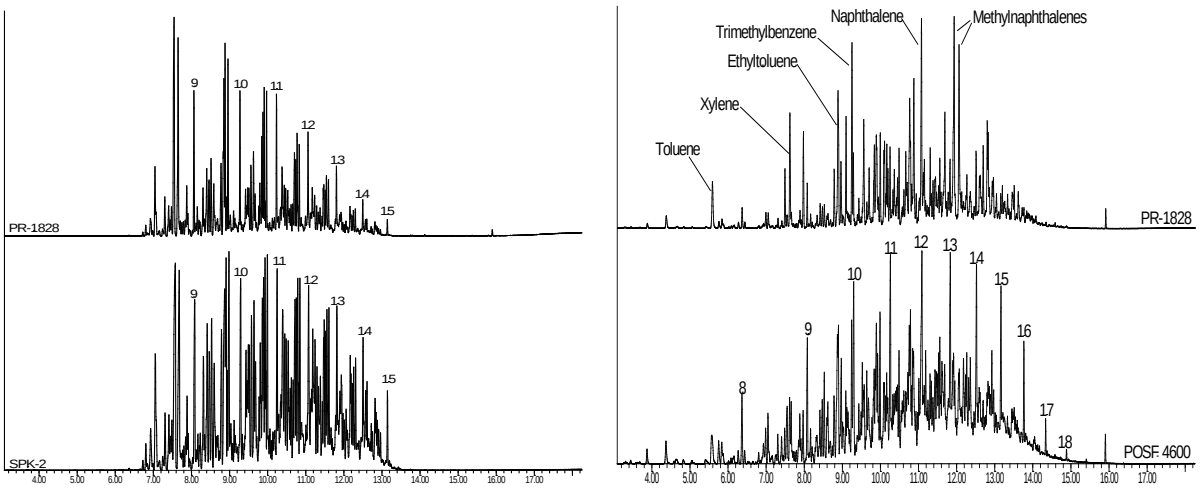

Figure 3-13. Example chromatograms comparing the fuel absorbed by the polythioether (PR-1828) material (top) and the fuel in which they were aged (bottom). Note that normal alkanes are labeled with their carbon number

Table 3-2 Average Polymer/Fuel Partition Coefficients

Component	Material ID	SPK Alkanes	Averaged Jet-A				Alkyl Bz/ Alkane
			Alkanes	Alkyl Bz	Naph*	Naphs**	
O-rings	N0602	0.103	0.126	0.422	1.065	0.705	3.35
	L1120	0.077	0.059	0.121	0.220	0.131	2.05
	V0835	0.011	0.011	0.085	0.230	0.124	7.73
Sealants	PR-1776	0.035	0.044	0.181	0.796	0.389	4.11
	PR-1828	0.027	0.029	0.189	0.775	0.419	6.52
All	Average ratio of Kpf(Alkyl Benzenes)/Kpf(Alkanes)						4.75

*Naph = Naphthalene
**Naphs = Alkyl Naphthalenes

Table 3-3 Estimated Average Composition of Absorbed Fuel

Component	Material ID	Alkanes	Alkyl Bz	Naphs
O-rings	N0602	58.1%	37.9%	4.9%
	L1120	69.8%	28.2%	2.4%
	V0835	38.1%	56.1%	6.9%
Sealants	PR-1776	52.3%	42.1%	6.8%
	PR-1828	41.4%	51.6%	8.5%
All	Average	51.9%	43.2%	5.9%
Fuel	Average Jet-A	82.6%	16.3%	1.1%

With respect to the aromatics, the partition coefficients shown in Table 3-2 shows that the solubility of the class fractions examined here increase as alkanes, alkyl benzenes, alkyl naphthalenes, and naphthalene. This order of selectivity is a consequence of the molecular

characteristics of these fuel components. As shown in Table 1-1 the alkanes are the largest molecules present in jet fuel and exhibit only dispersive (non-polar) intermolecular bonding. The alkyl benzenes are smaller and exhibit some polarity and hydrogen bonding. The alkyl naphthalenes can exhibit polarity and hydrogen bonding that is somewhat higher than the alkyl benzenes, and naphthalene (one of the smallest aromatics found in jet fuel, and limited to 3%) exhibits the highest level of hydrogen bonding.

The highest degree of selectivity towards the aromatics versus the alkanes was found for fluorocarbon O-ring material (V0835) as shown in Table 3-2. Specifically, this Table shows that the solubility of the aromatics from Jet-A was an average of 7.73 times higher than the alkanes for this material. However, the absolute value of the solubility as reflected by the Kpf values is quite low so that this selectivity does not result in significant overall volume swell. The lowest selectivity was found for the fluorosilicone O-ring material (L1120) with the solubility of the aromatics from Jet-A being an average of 2.05 times higher than the alkanes. This is consistent with the volume swell results which showed a very weak correlation between the volume swell and the aromatic content of the fuel for this material. On-average, as shown in Table 3-2, it was found that aromatics from Jet-A were 4.75 times more soluble than the alkanes in the O-ring and sealant materials used here. However, as shown in Table 3-3, the alkanes are estimated to contribute approximately half of the volume swell to these materials. This is a consequence of the fact that while the alkanes are less soluble than the aromatics, they make up the majority of the fuel. Furthermore, based on the analysis described above, as the alkane distribution shifts to smaller and lighter molecules their influence on volume swell increases, and vice versa. This emphasizes the importance of considering the composition of the fuel as a whole and not focusing in on one particular class fraction of the fuel.

3.4 Volume Swell of 50% SPK/Jet-A Fuel Blends

At the time this study was proposed, our consideration was focused on fuels with low aromatic content (approximately 8%). The purpose of this task was to examine the volume swell of the test materials in fuels consisting of 50% blends of SPK-1 and the reference Jet-As and to examine the overlap between the 90% prediction intervals of the blends and reference fuels. This would include observing the overlap of the overall population of blends without regard to the aromatic content of the blend and the estimated volume swell for 50% SPK-1 blends with 8% aromatics.

The volume swell results for this study are summarized in Table 3-4 and in Figure 3-14 through Figure 3-17. These results show that amongst the test materials used here only the nitrile rubber O-ring material and the two sealant materials show any significant potential for exhibiting a volume swell character that is lower than the predicted range for Jet-A fuels used in this study when blended with 50% SPK-1 regardless of the aromatic content. When the aromatic content is restricted to 8%, only nitrile rubber and the polythioether sealant show the potential to exhibit volume swell that is lower than the predicted range for Jet-A used in this study. For example, for the as-received nitrile rubber the overall overlap in the 90% prediction intervals between the 50% SPK/Jet-A fuel blends and the reference Jet-As were found to be 44%, and at the value of 8%

aromatics the overlap as 23%. This suggests that if SPK-1 was arbitrarily blended at 50% with any Jet-A there is a 44% chance that the volume swell of that fuel would be within the Jet-A range as predicted by the reference fuels used here. Furthermore, if the 50% fuel blend contained 8% aromatics, then there is a 23% chance that the volume swell of that fuel would be within the Jet-A range as predicted by the reference fuels used here. It is very important to note that this is not a statistical prediction of success or failure, but merely a statistical prediction as to whether the volume swell of a given blend would fall within the estimated behavior for Jet-A fuels used in this study.

Table 3-4 Overlap of the 90% Prediction Intervals for 50% SPK/Jet-A Fuel Blends And 50% SPK/Jet-A Fuel Blends with 8% Aromatic Content

Component	Sample ID	50% SPK	50% SPK 8% Aro.
O-Rings	N0602	44%	23%
	N0602e	51%	34%
	L1120	100%	100%
	V0835	100%	100%
Sealants	PR 1776	88%	100%
	PR 1828	57%	56%
Coatings	BMS 10-20	100%	100%
	BMS 10-123	96%	100%
Films	Nylon	80%	100%
	Kapton	100%	100%

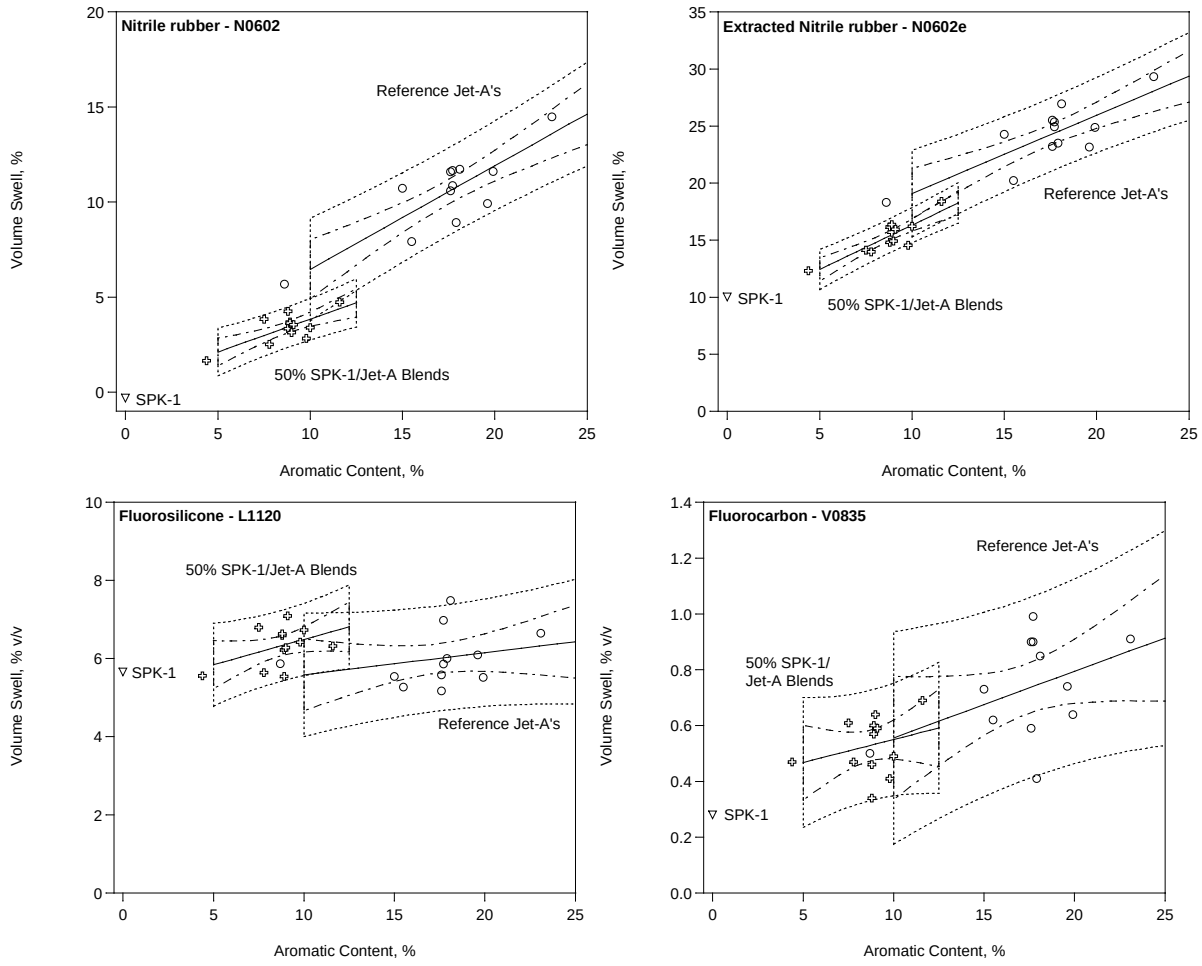

Figure 3-14. The volume swell of the O-ring materials after 40 hours at room temperature in the neat reference Jet-As and 50% SPK-/Jet-A blends.

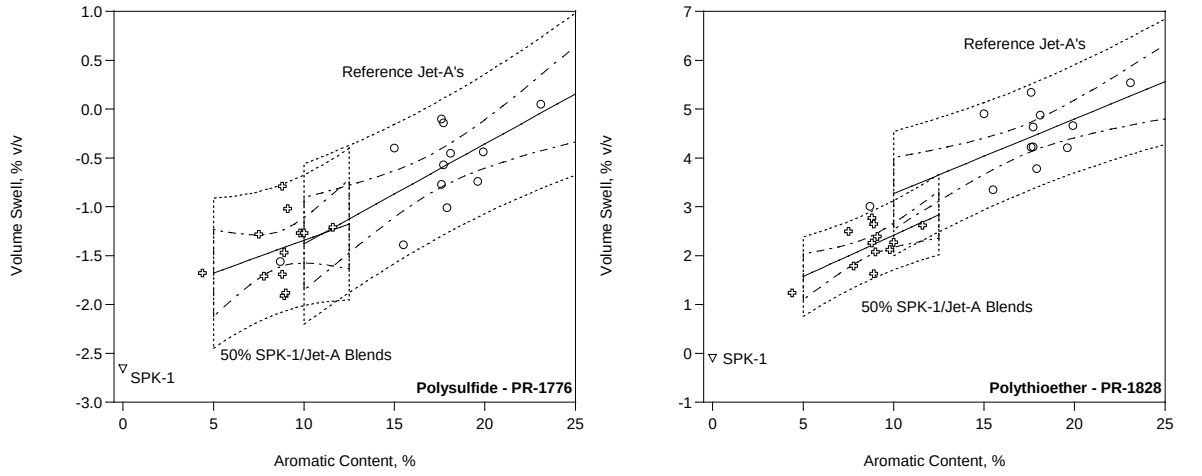

Figure 3-15. The volume swell of the sealant materials after 40 hours at room temperature in the neat reference Jet-As and 50% SPK-/Jet-A blends

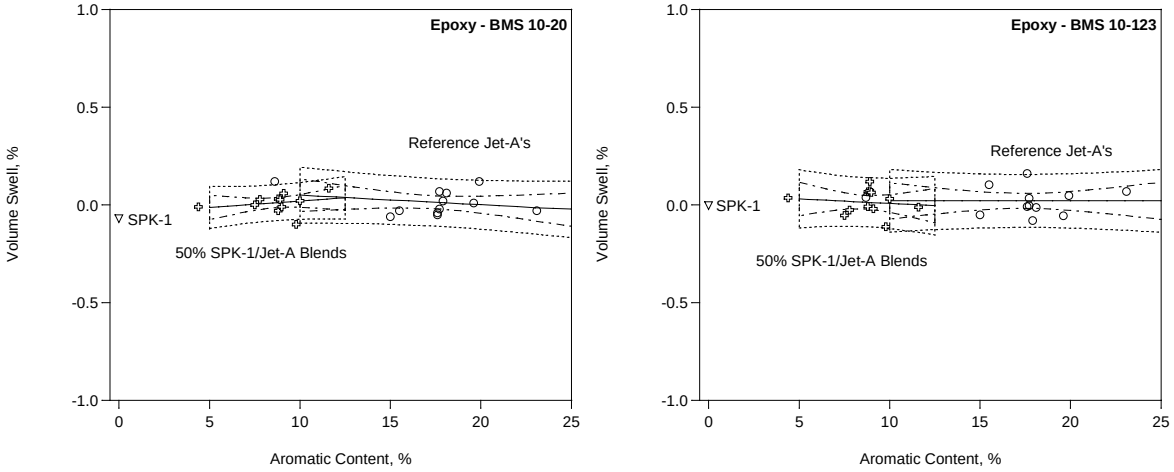

Figure 3-16. The volume swell of the coating materials after 40 hours at room temperature in the neat reference Jet-As and 50% SPK-/Jet-A blends

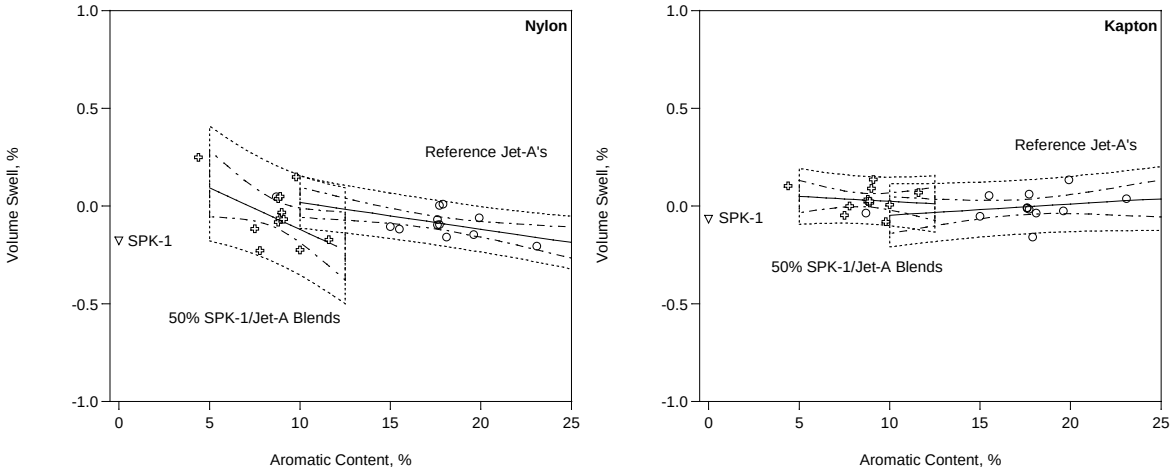

Figure 3-17. The volume swell of the film materials after 40 hours at room temperature in the neat reference Jet-As and 50% SPK-/Jet-A blends

3.5 The Behavior of SPK Blended with Selected Aromatics

The analysis of the fuel absorbed by each of the test materials is very informative with regard to the activity of the major class fractions that naturally occur in jet fuel. However, it is very challenging to isolate the activity of individual fuel components due to the complexity of the fuel and the fact that individual components are typically present at very low concentrations. To evaluate the activity of specific types of aromatics a set of aromatics was selected as listed in Table 3-5 and shown in Figure 3-18. These aromatics were selected in an effort to isolate the relative roles of molar volume (propyl-, butyl-, and pentylbenzene), polarity (1,3,5-, 1,2,4-, and 1,2,3-trimethylbenzene), and hydrogen bonding (tetrahydronaphthalene and naphthalene). Furthermore, indan was selected as a component that is common in jet fuel and is structurally similar to tetrahydronaphthalene. Methylindene was selected as an olefinic form of indan (indene was preferred, but proved to be unstable). The treatment level was set at 8% in SPK-1 to

determine if this level was sufficient to raise the volume swell of each material into the range for Jet-A fuels in this study. Note that 3% was selected for naphthalene as this is the maximum level allowed in jet fuel and the same level was selected for methylindene. The relative activity of each aromatic was measured in terms of the specific swell. Supporting data was obtained in the form of the polymer-fuel partition coefficients for each of the aromatics. This provided a measure of the solubility of each individual aromatic whereas the volume swell was a measure of the overall absorption of fuel by each material.

Table 3-5 Aromatics Used in this Study

Characteristic	ID	Aromatic	Conc. %v/v	HSPs, $MPa^{1/2}$			Density gm/mL	MV mL/mol
				Disp.	Polar	H-Bond		
Molar Volume	1	Propylbenzene*	8%	17.6	0.2	1.3	0.86	139
	2	Butylbenzene	8%	17.4	0.1	1.1	0.86	157
	3	Pentylbenzene*	8%	17.1	0.0	0.8	0.86	173
Polarity	4	1,3,5-Trimethylbenzene	8%	18.0	0.0	0.6	0.86	140
	5	1,2,4-Trimethylbenzene	8%	17.8	0.4	1.0	0.88	137
	6	1,2,3-Trimethylbenzene*	8%	17.6	0.8	1.4	0.89	134
Hydrogen Bonding	7	Tetrahydronaphthalene	8%	19.6	2.0	2.9	0.97	136
	8	Naphthalene	3%	19.2	2.0	5.9	1.03	112
Other	9	Indan*	8%	17.8	0.6	2.1	0.97	123
	10	Methylindene*	3%	20.1	1.0	7.2	0.97	134

*HSPs estimated from structural analogs.

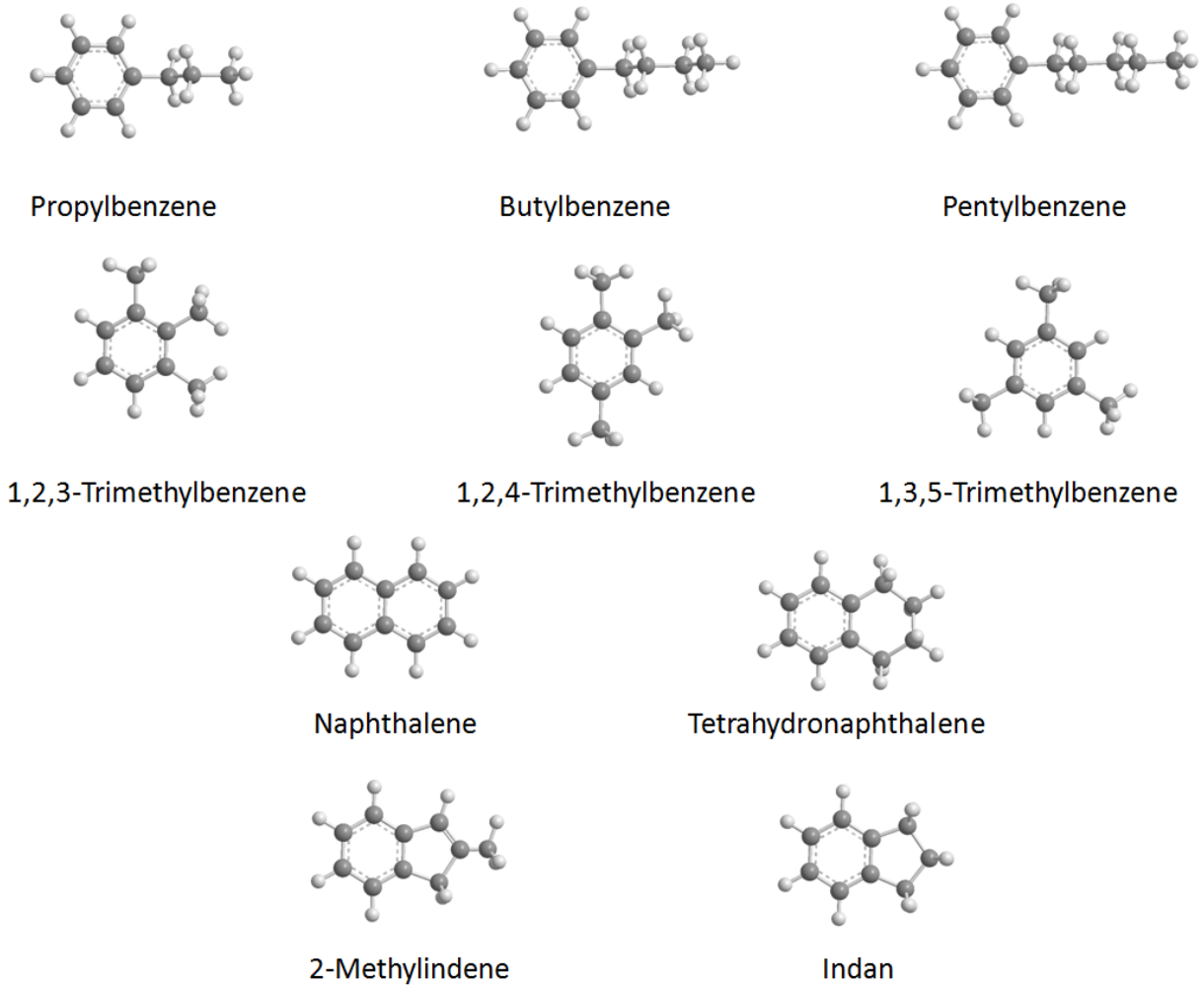

Figure 3-18. Molecular structures of the aromatic selected for this study.

The volume swell results are summarized in Table 3-6 (O-rings and sealants) and Table 3-7 (coatings and films). These tables also list the limits of the 90% prediction intervals for the reference Jet-As and the volume swell of the neat SPK-1. Values that are within the Jet-A range as predicted by the 90% prediction intervals are listed in bold type. Note that the volume swell of the fluorosilicone and fluorocarbon O-rings as well as all of the coatings and films aged in SPK-1 were all within the Jet-A range and no additional aromatics are needed for these materials based on this criterion. Of the remaining materials, the volume swell of the polysulfide sealant (PR-1776) in SPK-1 was near the lower bound of the 90% prediction interval and all of the aromatics used here promoted the volume swell of this material into the Jet-A range at their respective treatment levels. Similar results were found for the polythioether sealant (PR-1828) where most of the aromatics successfully promoted the volume swell of this materials into the Jet-A range with the exception of the two largest aromatics (butylbenzene and pentylbenzene) and the least polar aromatic (1,3,5-trimethylbenzene), in their respective series. The most impacted material was the nitrile rubber for which relatively few of the aromatics promoted sufficient volume swell to reach nominal swell found in the Jet-A range.

Table 3-6 Summary of Volume Swell Results for the O-ring and Sealants aged in SPK-1 Blended with Selected Aromatics

Characteristic	Aromatic	O-Rings*				Sealants*	
		N0602	N0602e	L1120	V0835	PR-1776	PR-1828
Jet-A Range	90% PI Upper Limit	17.4%	33.2%	8.0%	1.3%	1.0%	6.8%
	90% PI Lower Limit	3.7%	15.3%	4.0%	0.2%	-2.2%	2.0%
Molar Volume	Propylbenzene	2.4%	14.5%	**7.5%**	**0.9%**	**-1.4%**	**2.1%**
	Butylbenzene	2.0%	13.3%	**7.8%**	**0.6%**	**-1.9%**	1.6%
	Pentylbenzene	1.4%	12.2%	**6.0%**	**0.6%**	**-1.7%**	1.4%
Polarity	1,3,5-Trimethylbenzene	2.3%	14.2%	**6.8%**	**0.8%**	**-1.8%**	1.4%
	1,2,4-Trimethylbenzene	3.3%	**15.3%**	**5.4%**	**1.1%**	**-0.8%**	**2.9%**
	1,2,3-Trimethylbenzene	**4.3%**	**16.6%**	**7.5%**	**1.1%**	**-0.8%**	**3.6%**
H-Bonding	Tetrahydronaphthalene	**4.6%**	14.9%	**8.1%**	**0.4%**	**-0.4%**	**3.6%**
	Naphthalene	3.4%	**15.8%**	**6.7%**	**0.7%**	**-0.4%**	**4.4%**
Other	Indan	**4.1%**	**15.3%**	**6.5%**	**1.0%**	**0.3%**	**4.8%**
	Methylindene	2.1%	13.2%	**7.4%**	**0.8%**	**-1.9%**	**2.4%**
SPK-1	None	-0.3%	10.0%	**5.7%**	**0.3%**	-2.7%	-0.1%

*__Bold__ denotes volume swell that is within the predicted Jet-A range.

Table 3-7 Summary of Volume Swell Results for the Coatings and Films aged in SPK-1 Blended with Selected Aromatics

Characteristic	Aromatic	Coatings*		Films*	
		BMS 10-20	BMS 10-123	Nylon	Kapton
Jet-A Range	90% PI Upper Limit	0.2%	0.2%	0.2%	0.2%
	90% PI Lower Limit	-0.2%	-0.1%	-0.3%	-0.2%
Molar Volume	Propylbenzene	**0.0%**	**0.0%**	**-0.2%**	**0.1%**
	Butylbenzene	**0.0%**	**0.0%**	**-0.1%**	**0.1%**
	Pentylbenzene	**0.0%**	**0.0%**	**-0.2%**	**-0.1%**
Polarity	1,3,5-Trimethylbenzene	**0.0%**	**0.0%**	**-0.3%**	**-0.1%**
	1,2,4-Trimethylbenzene	**0.0%**	**0.1%**	**-0.3%**	**0.1%**
	1,2,3-Trimethylbenzene	**0.0%**	**0.1%**	**-0.2%**	**0.0%**
H-Bonding	Tetrahydronaphthalene	**0.0%**	**0.0%**	**-0.2%**	**-0.1%**
	Naphthalene	**0.0%**	**0.0%**	**-0.2%**	**0.0%**
Other	Indan	**0.2%**	**0.0%**	**-0.3%**	**0.0%**
	Methylindene	**-0.1%**	**0.0%**	**-0.2%**	**-0.1%**
SPK-1	None	**-0.1%**	**0.0%**	**-0.2%**	**-0.1%**

*__Bold__ denotes volume swell that is within the predicted Jet-A range.

The activity of each aromatic as expressed by the specific swell is summarized in Table 3-8 (O-rings and sealants) and Table 3-9 (coatings and films). These tables also list the average specific swell of the reference Jet-As which reflects the average activity of the aromatics that naturally occur in jet fuel. Values for the specific swell of the SPK-1 blended with the selected aromatics that are equal to or greater than the average Jet-As (used in this study) are shown in bold type.

These results illustrate that with the exception of nitrile rubber, the activity of most of the aromatics was equal to or greater than the average of those that naturally occur in jet fuel.

Table 3-8 Summary of Specific Swell Results for the O-ring and Sealants aged in SPK-1 Blended with Selected Aromatics at 8% (unless noted as 3%)

		O-Rings*				Sealants*	
Characteristic	**Aromatic**	N0602	N0602e	L1120	V0835	PR-1776	PR-1828
Average Jet-A	Naturally Occuring	0.55	0.69	0.06	0.02	0.10	0.15
Molar Volume	Propylbenzene	0.34	0.57	**0.26**	**0.08**	**0.16**	**0.28**
	Butylbenzene	0.29	0.41	**0.19**	**0.04**	**0.10**	**0.22**
	Pentylbenzene	0.21	0.28	**0.06**	**0.03**	**0.12**	**0.19**
Polarity	1,3,5-Trimethylbenzene	0.33	0.53	**0.08**	**0.07**	**0.10**	**0.19**
	1,2,4-Trimethylbenzene	0.45	0.66	0.04	**0.10**	**0.24**	**0.38**
	1,2,3-Trimethylbenzene	**0.57**	**0.82**	**0.16**	**0.10**	**0.24**	**0.46**
H-Bonding	Tetrahydronaphthalene	**0.61**	**0.61**	**0.12**	0.01	**0.28**	**0.46**
	Naphthalene (3%)	**1.22**	**1.92**	**0.29**	**0.15**	**0.74**	**1.51**
Other	Indan	0.55	0.66	**0.06**	**0.09**	**0.36**	**0.61**
	Methylindene (3%)	**0.81**	**1.07**	**0.61**	**0.18**	**0.27**	**0.84**

*__Bold__ denotes specific swell that is equal to or greater than the average measured for Jet-A.

Table 3-9 Summary of Specific Swell Results for the Coatings and Films aged in SPK-1 Blended with Selected Aromatics

		Coatings*		Films*	
Characteristic	**Aromatic**	BMS 10-20	BMS 10-123	Nylon	Kapton
Average Jet-A	Naturally Occuring	0.00	0.00	-0.01	0.01
Molar Volume	Propylbenzene	**0.01**	**0.01**	**-0.01**	**0.02**
	Butylbenzene	**0.01**	**0.00**	**0.01**	**0.02**
	Pentylbenzene	**0.01**	**0.00**	**0.00**	-0.01
Polarity	1,3,5-Trimethylbenzene	**0.01**	**0.00**	-0.01	**-0.01**
	1,2,4-Trimethylbenzene	**0.01**	**0.01**	**-0.01**	**0.02**
	1,2,3-Trimethylbenzene	**0.01**	**0.01**	**0.00**	**0.01**
H-Bonding	Tetrahydronaphthalene	**0.00**	**0.00**	**-0.01**	0.00
	Naphthalene	**0.02**	-0.01	-0.02	**0.01**
Other	Indan	**0.03**	**0.00**	**-0.01**	**0.01**
	Methylindene	-0.01	**0.00**	**0.00**	-0.01

*__Bold__ denotes specific swell that is equal to or greater than the average measured for Jet-A.

The trends in the activity of the selected aromatics are illustrated in Figure 3-19 through Figure 3-21 for molar volume, polarity, and hydrogen bonding, respectively. These show that for the soft materials (the O-rings and sealants) the volume swell tends to increase as the molar volume of the aromatic decreases, and as the polarity and hydrogen bonding increases. Amongst these three factors (molar volume, polarity, hydrogen bonding) molar volume had the least influence on the volume swell followed by polarity and hydrogen bonding. Furthermore, the influence of hydrogen bonding tended to be significantly higher than that of polarity. For the hard materials (coatings and films) the aromatics had little effect. This suggests that materials that are inert in Jet-A will also be inert in SPKs and SPKs blended with aromatics being used as swelling promoters.

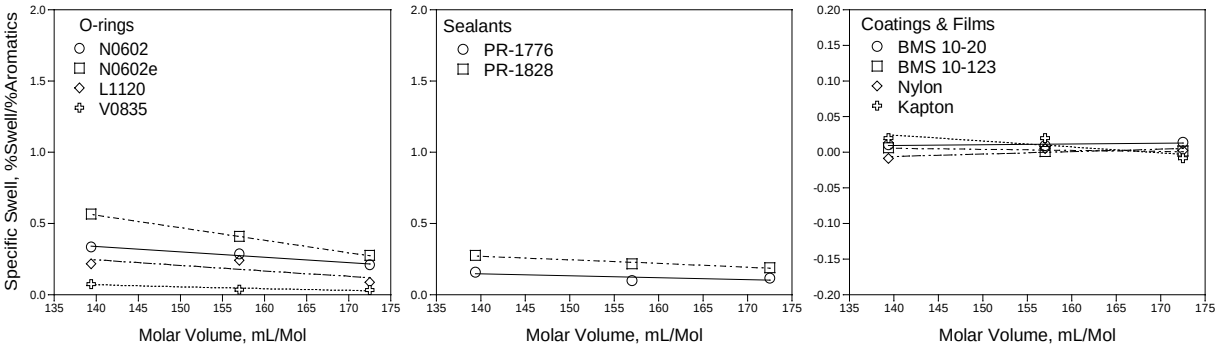

Figure 3-19. Specific swell as a function of the molar volume of the aromatic blended with SPK-1

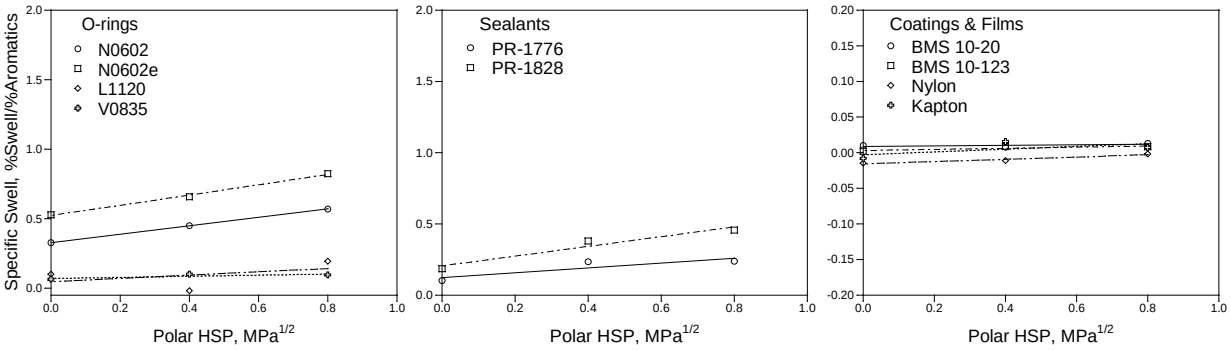

Figure 3-20. Specific swell as a function of the polar HSP of the aromatic blended with SPK-1

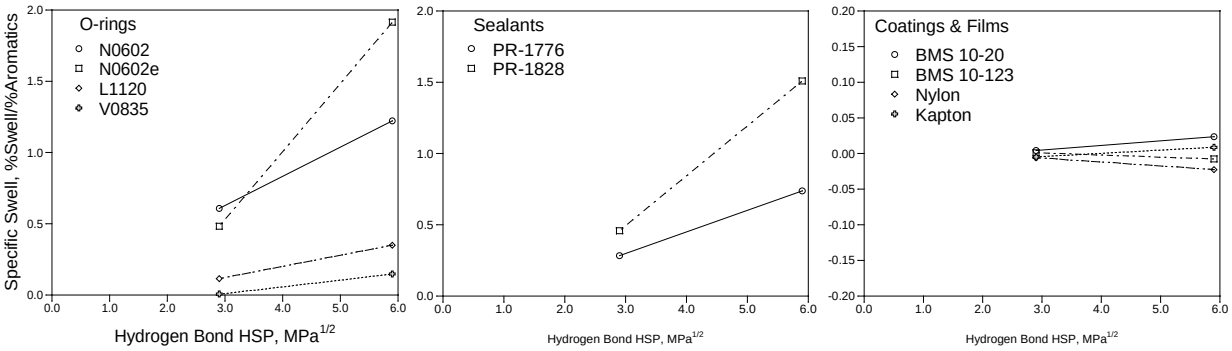

Figure 3-21. Specific swell as a function of the hydrogen bond HSP of the aromatic blended with SPK-1

The relative solubility of the specific aromatics in the O-rings and sealants are summarized in Table 3-10 and Figure 3-22 through Figure 3-24 for molar volume, polarity, and hydrogen bonding, respectively. (Note that the coatings and films did not absorb enough fuel to be analyzed by the methods used here.) The overall results are similar to that found for the volume swell, though more subtle. Specifically, solubility of the specific aromatics tended to increase as the molar volume of the aromatic decreases, and as the polarity and hydrogen bonding increases. Furthermore, over the range used in this study, the relative influence increased as molar volume, polarity, and hydrogen bonding.

Table 3-10 Summary of Partition Coefficient Results for the O-ring and Sealants aged in SPK-1 Blended with Selected Aromatics

		O-Rings*			**Sealants***	
Characteristic	**Aromatic**	N0602	L1120	V0835	PR-1776	PR-1828
Average Jet-A	Naturally Occuring	0.42	0.12	0.09	0.18	0.19
Molar Volume	Propylbenzene	**0.44**	**0.17**	0.08	**0.21**	**0.24**
	Butylbenzene	**0.49**	**0.18**	0.05	**0.20**	**0.23**
	Pentylbenzene	**0.46**	**0.15**	0.04	0.17	**0.20**
Polarity	1,3,5-Trimethylbenzene	**0.45**	**0.12**	**0.10**	0.17	**0.20**
	1,2,4-Trimethylbenzene	**0.50**	**0.17**	**0.12**	**0.23**	**0.24**
	1,2,3-Trimethylbenzene	**0.52**	**0.15**	**0.10**	**0.24**	**0.29**
H-Bonding	Tetrahydronaphthalene	**0.60**	**0.14**	0.07	**0.30**	**0.34**
	Naphthalene	**1.20**	**0.23**	**0.19**	**0.72**	**0.91**
Other	Indan	**0.48**	**0.14**	**0.10**	**0.31**	**0.20**
	Methylindene	**0.82**	**0.21**	**0.18**	**0.41**	**0.54**

*__Bold__ denotes partition coefficients that are equal to or greater than the average measured for Jet-A.

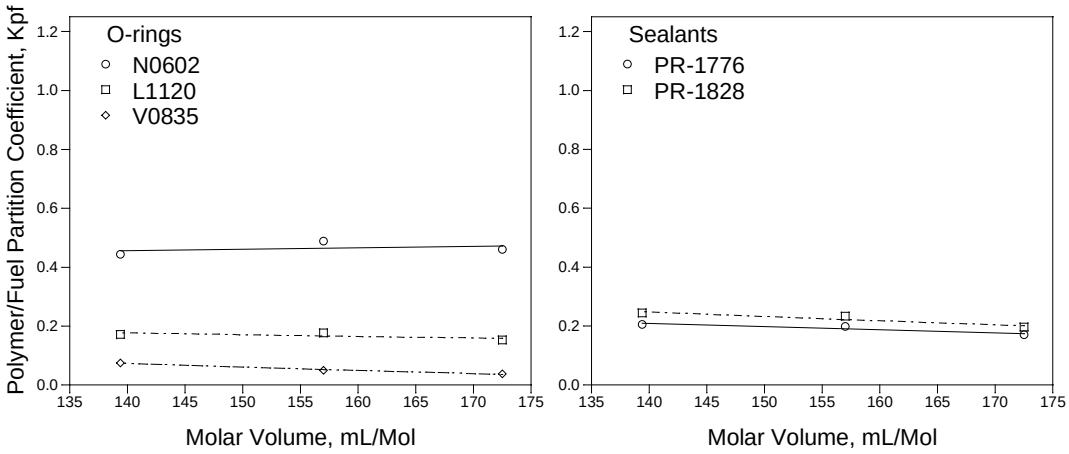

Figure 3-22. Polymer-fuel partition coefficients as a function of the molar volume of the aromatic blended with SPK-1

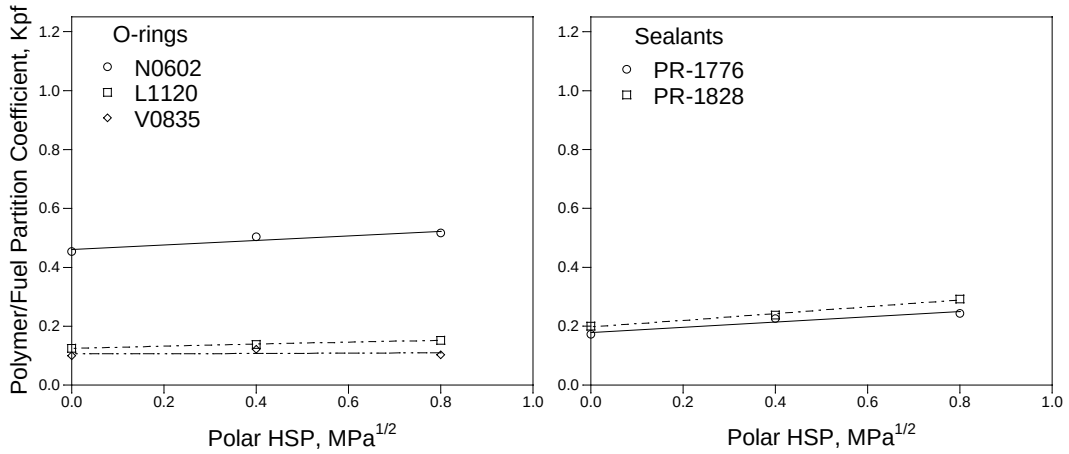

Figure 3-23. Polymer-fuel partition coefficients as a function of the polar HSP of the aromatic blended with SPK-1

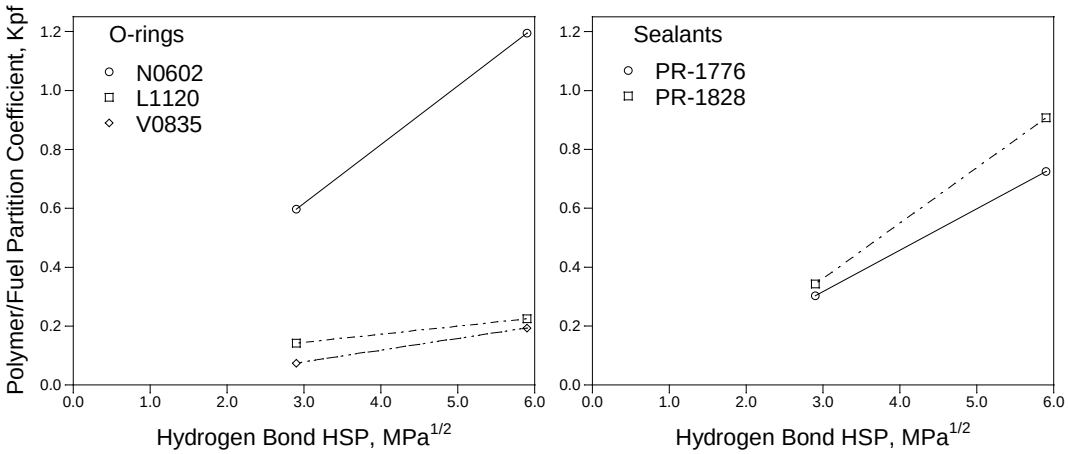

Figure 3-24. Polymer-fuel partition coefficients as a function of the hydrogen bond HSP of the aromatic blended with SPK-1

With respect to the indan and methylindene, for the materials that showed the greatest influence of the aromatic content of the fuel (the nitrile rubber and the polysulfide and polythioether sealants) the activity of the indan was slightly higher than tetrahydronaphthalene and the activity of the methylindene was intermediate between that of the tetrahydronaphthalene and naphthalene (see Table 3-8). This suggests that these two aromatics could serve as effective swelling promoters, though their performance is not exceptional.

4 Technical Summary

A study has been completed to examine the overall effect of SPK and SPK fuel blends on non-metallic materials used in commercial aircraft fuel systems. The primary measure of performance was the volume swell of dry source materials immersed in fuel for 40 hours at room temperature. Supporting data was obtained in the form of an analysis of the fuel absorbed by each test material using either thermogravimetric analysis as well as thermal desorption gas chromatography-mass spectrometry. The volume swell and fuel absorbed using a set of 12 Jet-As and 4 SPKs were used as the primary basis for comparison. The Jet-As were selected to span a broad range of aromatics (from 8.7% to 23.1%) while the SPKs were selected from a variety of sources, though they were processed into 4 very similar fuels with 0% aromatics. To evaluate the relative importance of the molecular structure of fuel components in general, and aromatics in particular, the activity of 10 aromatics selected to emphasize the relative roles of molar volume, polarity, and hydrogen bonding were measured and compared with the reference Jet-As. Furthermore, data was obtained on a set of fuels consisting of 50% SPK/Jet-A fuel blends to assess the performance of these fuels regardless of their aromatic content as well as those blends with 8% aromatics.

The overall response to the aromatic content of the fuel was found to be very material-dependent with the greatest effect being shown by a nitrile rubber O-ring material and a polythioether and -polysulfide sealant. A fluorocarbon O-ring material was found to be relatively inert while two epoxy coatings and a nylon and a Kapton® film were found to be essentially inert in all of the test fuels. A fluorosilicone O-ring material was found to show moderate volume swell behavior, however the volume swell of this material was a very weak function of the aromatic content. Although the volume swell of the test materials tended to increase with the aromatic of the fuel, only the nitrile rubber O-ring and polythioether and polysulfide sealant materials showed a volume swell character in the SPKs that was lower than the range predicted for Jet-A based on the reference fuels used here and only the nitrile rubber proved to be the most sensitive to aromatic content***. It is very important to note that this is not a statistical prediction of success or failure, but merely a statistical prediction as to whether the volume swell of a given blend would fall within the predicted 'normal' range for Jet-A.*** Based on recent testing (and ASTM D7566-11 approval of a minimum of 8% aromatics content) of up to 50% SPK blends, it is believed that fuel system materials can perform their intended functions when using fuel which provides volume swell that might be lower than present in-service conditions. Beyond these recent approvals, more complete operational and engineering data of low aromatic fuels will likely be needed to determine how far outside the statistical bounds our present day experience can be extended.

With respect to the influence of the molecular structure of the fuel; volume swell was found to increase as the molar volume of the fuel components decreases and as their polarity and hydrogen bonding increases. Amongst these three factors (molar volume, polarity, hydrogen bonding) molar volume had the least influence on the volume swell followed by polarity and hydrogen bonding. Furthermore, the influence of hydrogen bonding tended to be significantly higher than that of polarity. This suggests that the volume swell of jet fuel will increase as the boiling range skews towards lower temperatures (lower molecular weight) and as the overall

polarity and hydrogen bonding increases, and vice versa. Noting that the bulk of Jet-A and all of typical SPKs are paraffinic and therefore non-polar, the polarity and hydrogen bonding character of the fuel will be dominated by the aromatics. However, emphasizing that the bulk of the fuel is paraffinic, particularly as the aromatic content is lowered, the influence of the molecular weight distribution of the fuel must be considered. This emphasizes the importance of taking into account the composition of a fuel as a whole when considering how it interacts with non-metallic materials and not focusing on one class fraction of the fuel.

5 Appendices

5.1 Appendix A N0602 Nitrile Rubber O-Ring

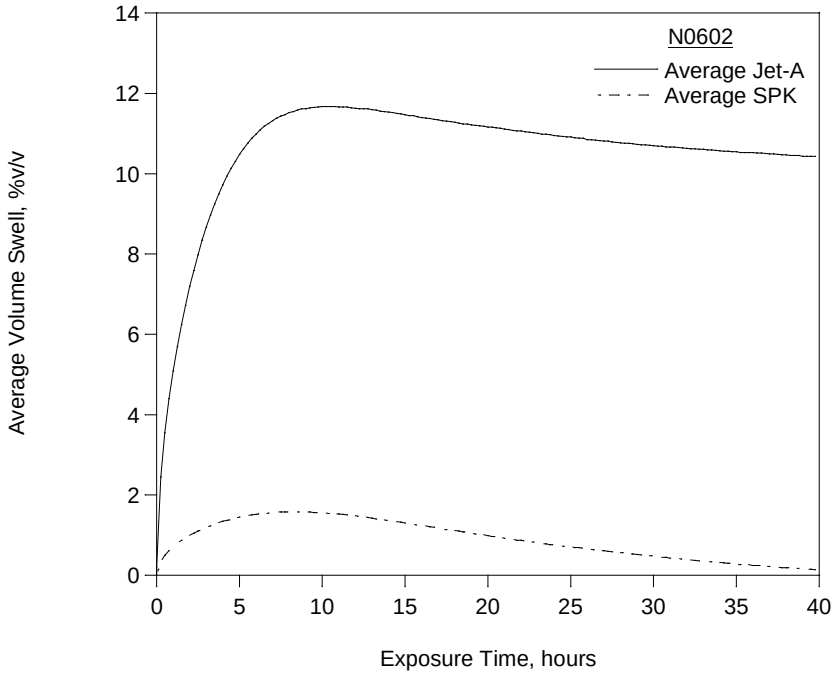

Figure A-1 Average volume swell as a function of time for N0602 at room temperature

Table A-1 Summary of Volume Swell and Mass Fraction of Fuel Absorbed by N0602

Fuel ID	Aromatics D6379	Naphs* D6379	Volume Swell	Mass Fraction
SRI-1	8.7%	0.2%	5.7%	11.2%
4597	15.0%	1.9%	10.7%	14.2%
5245	15.5%	0.2%	7.9%	12.5%
3166	17.6%	2.5%	11.6%	14.9%
4598	17.6%	1.4%	10.6%	14.3%
4600	17.7%	1.3%	11.7%	15.2%
4658	17.7%	1.3%	10.9%	14.5%
4626	17.9%	0.6%	8.9%	13.7%
5661	18.1%	0.6%	11.7%	14.9%
4877	19.6%	0.4%	9.9%	13.7%
4599	19.9%	1.4%	11.6%	14.7%
3602	23.1%	1.1%	14.5%	16.5%
SPK-1	0.0%	0.0%	-0.3%	6.2%
SPK-2	0.0%	0.0%	0.2%	6.5%
SPK-3	0.0%	0.0%	0.1%	6.5%
SPK-4	0.0%	0.0%	0.6%	6.6%

*Naphthalenes

Table A-2 Summary of Polymer-Fuel Partition Coefficients (Kpf) for N0602

Fuel ID	Aromatics D6379	Naphs* D6379	Kpf			
			Alkanes	Alkyl Bz	Naph	Naphs
SRI-1	8.7%	0.2%	0.129	0.405	**	**
4597	15.0%	1.9%	0.142	0.520	1.294	0.946
5245	15.5%	0.2%	0.114	0.409	**	**
3166	17.6%	2.5%	0.135	0.450	1.196	0.829
4598	17.6%	1.4%	0.122	0.418	1.117	0.576
4600	17.7%	1.3%	0.108	0.334	0.864	0.609
4658	17.7%	1.3%	0.117	0.400	1.059	0.668
4626	17.9%	0.6%	0.128	0.430	1.090	0.701
5661	18.1%	0.6%	0.134	0.455	1.035	0.680
4877	19.6%	0.4%	0.116	0.407	0.970	0.640
4599	19.9%	1.4%	0.123	0.403	1.027	0.679
3602	23.1%	1.1%	0.143	0.434	1.000	0.720
Average	17.4%	1.2%	0.126	0.422	1.065	0.705
90% CI	1.6%	0.3%	0.006	0.023	0.062	0.057
SPK-1	0.0%	0.0%	0.096	n.a.	n.a.	n.a.
SPK-2	0.0%	0.0%	0.098	n.a.	n.a.	n.a.
SPK-3	0.0%	0.0%	0.114	n.a.	n.a.	n.a.
SPK-4	0.0%	0.0%	0.103	n.a.	n.a.	n.a.

*Naphthalenes **Concentration too low in the fuel for accurate quantification.

Table A-3 Estimated Composition of the Bulk and Absorbed Fuels

Fuel	Bulk Fuel			Absorbed Fuel		
ID	Alkanes	Alkyl Bz	Naphs*	Alkanes	Alkyl Bz	Naphs*
SRI-1	91.3%	8.5%	0.2%	86.6%	13.4%	**
4597	85.0%	13.1%	1.9%	58.3%	33.0%	8.7%
5245	84.5%	15.3%	0.2%	60.7%	39.3%	**
3166	82.4%	15.1%	2.5%	55.6%	34.0%	10.4%
4598	82.4%	16.2%	1.4%	57.0%	38.4%	4.6%
4600	82.3%	16.4%	1.3%	58.6%	36.2%	5.2%
4658	82.3%	16.4%	1.3%	56.6%	38.4%	5.1%
4626	82.1%	17.3%	0.6%	57.2%	40.5%	2.3%
5661	81.9%	17.5%	0.6%	56.7%	41.2%	2.1%
4877	80.4%	19.2%	0.4%	53.6%	45.0%	1.5%
4599	80.1%	18.5%	1.4%	53.9%	40.9%	5.2%
3602	76.9%	22.0%	1.1%	51.5%	44.8%	3.7%
Average	82.6%	16.3%	1.1%	58.1%	37.9%	4.9%
90% CI	98.4%	1.3%	0.3%	0.6%	2.3%	6.2%
SPK-1	100.0%	0.0%	0.0%	100.0%	0.0%	0.0%
SPK-2	100.0%	0.0%	0.0%	100.0%	0.0%	0.0%
SPK-3	100.0%	0.0%	0.0%	100.0%	0.0%	0.0%
SPK-4	100.0%	0.0%	0.0%	100.0%	0.0%	0.0%

*Naphthalenes **Concentration too low in the fuel for accurate quantification.

5.2 Appendix B N0602e Extracted Nitrile Rubber O-Ring

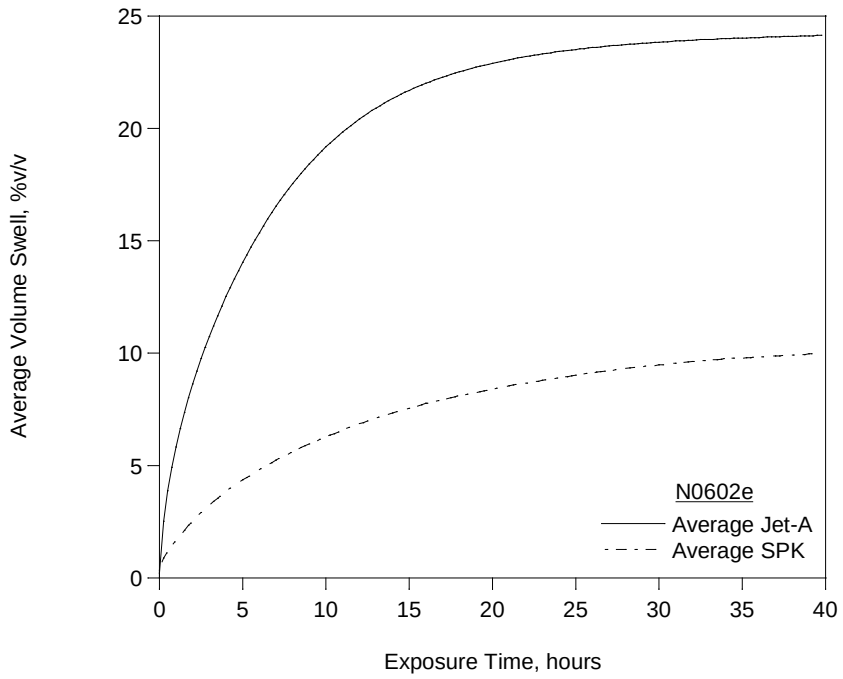

Figure B-1 Average volume swell as a function of time for N0602e at room temperature

Table B-1 Summary of Volume Swell and Mass Fraction of Fuel Absorbed by N0602e

Fuel ID	Aromatics D6379	Naphs* D6379	Volume Swell	Mass Fraction
SRI-1	8.7%	0.2%	18.3%	10.6%
4597	15.0%	1.9%	24.3%	14.0%
5245	15.5%	0.2%	20.2%	12.3%
3166	17.6%	2.5%	25.5%	14.9%
4598	17.6%	1.4%	23.2%	14.1%
4600	17.7%	1.3%	25.4%	15.3%
4658	17.7%	1.3%	25.0%	14.2%
4626	17.9%	0.6%	23.5%	13.4%
5661	18.1%	0.6%	26.9%	14.8%
4877	19.6%	0.4%	23.1%	13.6%
4599	19.9%	1.4%	24.9%	14.6%
3602	23.1%	1.1%	29.3%	16.2%
SPK-1	0.0%	0.0%	10.0%	6.1%
SPK-2	0.0%	0.0%	9.9%	6.4%
SPK-3	0.0%	0.0%	10.2%	6.3%
SPK-4	0.0%	0.0%	9.9%	6.4%

*Naphthalenes

5.3 Appendix C L1120 Fluorosilicone O-Ring

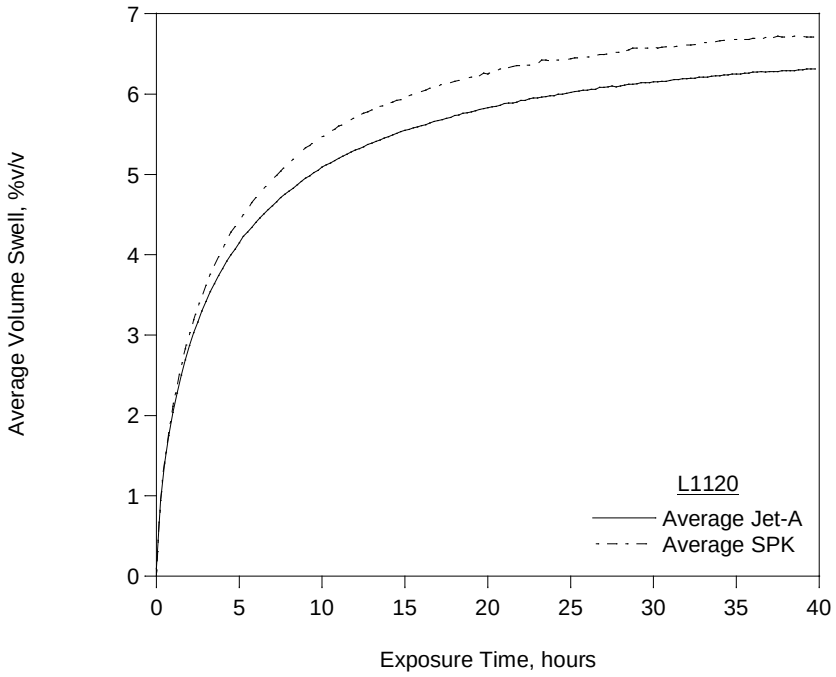

Figure C-1 Average volume swell as a function of time for L1120 at room temperature

Table C-1 Summary of Volume Swell and Mass Fraction of Fuel Absorbed by L1120

Fuel ID	Aromatics D6379	Naphs* D6379	Volume Swell	Mass Fraction
SRI-1	8.7%	0.2%	5.9%	3.5%
4597	15.0%	1.9%	5.5%	3.6%
5245	15.5%	0.2%	5.3%	3.4%
3166	17.6%	2.5%	5.6%	3.8%
4598	17.6%	1.4%	5.2%	3.5%
4600	17.7%	1.3%	7.0%	4.2%
4658	17.7%	1.3%	5.9%	3.7%
4626	17.9%	0.6%	6.0%	4.0%
5661	18.1%	0.6%	7.5%	3.9%
4877	19.6%	0.4%	6.1%	3.8%
4599	19.9%	1.4%	5.5%	3.8%
3602	23.1%	1.1%	6.6%	3.7%
SPK-1	0.0%	0.0%	5.7%	3.1%
SPK-2	0.0%	0.0%	6.6%	3.2%
SPK-3	0.0%	0.0%	6.6%	3.2%
SPK-4	0.0%	0.0%	6.9%	3.3%

*Naphthalenes

Table C-2 Summary of Polymer-Fuel Partition Coefficients (Kpf) for L1120

Fuel	Aromatics	Naphs*	Kpf			
ID	D6379	D6379	Alkanes	Alkyl Bz	Naph	Naphs*
SRI-1	8.7%	0.2%	0.068	0.112	**	**
4597	15.0%	1.9%	0.057	0.135	0.245	0.162
5245	15.5%	0.2%	0.059	0.123	**	**
3166	17.6%	2.5%	0.055	0.117	0.229	0.144
4598	17.6%	1.4%	0.045	0.097	0.193	0.092
4600	17.7%	1.3%	0.056	0.107	0.190	0.115
4658	17.7%	1.3%	0.059	0.123	0.233	0.131
4626	17.9%	0.6%	0.073	0.147	0.252	0.148
5661	18.1%	0.6%	0.065	0.136	0.225	0.138
4877	19.6%	0.4%	0.063	0.131	0.221	0.129
4599	19.9%	1.4%	0.062	0.125	0.229	0.132
3602	23.1%	1.1%	0.050	0.103	0.184	0.120
Average	18.2%	1.2%	0.059	0.121	0.220	0.131
90% CI	1.1%	0.3%	0.004	0.008	0.012	0.010
SPK-1	0.0%	0.0%	0.077	n.C.	n.C.	n.C.
SPK-2	0.0%	0.0%	0.081	n.C.	n.C.	n.C.
SPK-3	0.0%	0.0%	0.089	n.C.	n.C.	n.C.
SPK-4	0.0%	0.0%	0.060	n.C.	n.C.	n.C.

*Naphthalenes **Concentration too low in the fuel for accurate quantification.

Table C-3 Estimated Composition of the Bulk and Absorbed Fuels

Fuel	Bulk Fuel			Absorbed Fuel		
ID	Alkanes	Alkyl Bz	Naphs*	Alkanes	Alkyl Bz	Naphs*
SRI-1	91.3%	8.5%	0.2%	86.6%	13.4%	**
4597	85.0%	13.1%	1.9%	69.9%	25.6%	4.5%
5245	84.5%	15.3%	0.2%	72.5%	27.5%	**
3166	82.4%	15.1%	2.5%	67.9%	26.6%	5.4%
4598	82.4%	16.2%	1.4%	68.7%	28.9%	2.4%
4600	82.3%	16.4%	1.3%	70.6%	27.1%	2.3%
4658	82.3%	16.4%	1.3%	69.0%	28.6%	2.4%
4626	82.1%	17.3%	0.6%	69.6%	29.4%	1.0%
5661	81.9%	17.5%	0.6%	68.3%	30.6%	1.1%
4877	80.4%	19.2%	0.4%	66.3%	33.0%	0.7%
4599	80.1%	18.5%	1.4%	66.5%	31.0%	2.5%
3602	76.9%	22.0%	1.1%	61.4%	36.5%	2.1%
Average	82.6%	16.3%	1.1%	69.8%	28.2%	2.4%
90% CI	98.9%	0.7%	0.3%	0.4%	0.8%	1.2%
SPK-1	100.0%	0.0%	0.0%	100.0%	0.0%	0.0%
SPK-2	100.0%	0.0%	0.0%	100.0%	0.0%	0.0%
SPK-3	100.0%	0.0%	0.0%	100.0%	0.0%	0.0%
SPK-4	100.0%	0.0%	0.0%	100.0%	0.0%	0.0%

*Naphthalenes **Concentration too low in the fuel for accurate quantification.

5.4 Appendix D V0835 Fluorocarbon O-ring

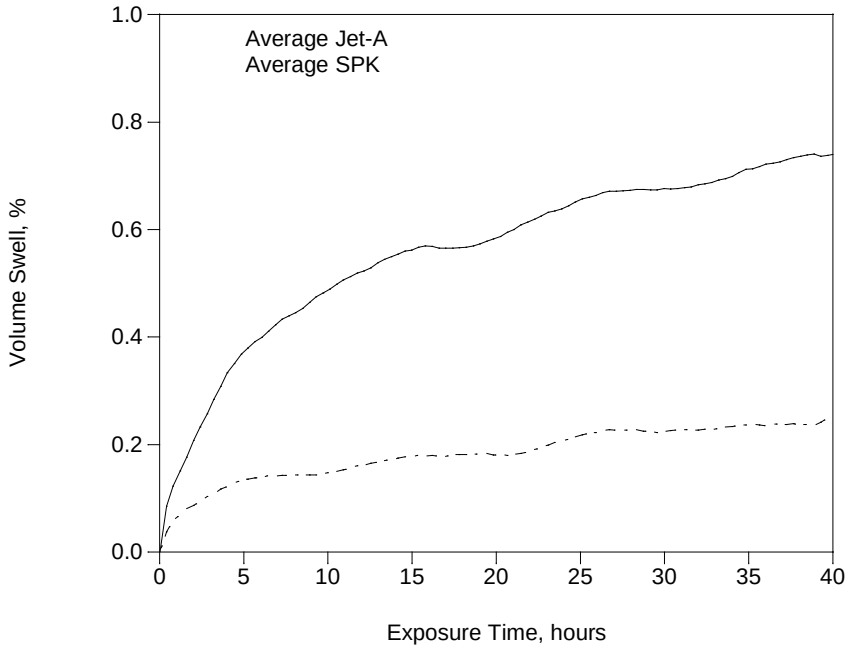

Figure D-1 Average volume swell as a function of time for V0835 at room temperature

Table D-1 Summary of Volume Swell and Mass Fraction of Fuel Absorbed by V0835

Fuel ID	Aromatics D6379	Naphs* D6379	Volume Swell	Mass Fraction
SRI-1	8.7%	0.2%	0.5%	0.3%
4597	15.0%	1.9%	0.7%	0.6%
5245	15.5%	0.2%	0.6%	0.7%
3166	17.6%	2.5%	0.9%	0.6%
4598	17.6%	1.4%	0.6%	0.7%
4600	17.7%	1.3%	1.0%	0.6%
4658	17.7%	1.3%	0.9%	0.7%
4626	17.9%	0.6%	0.4%	0.6%
5661	18.1%	0.6%	0.9%	0.3%
4877	19.6%	0.4%	0.7%	0.5%
4599	19.9%	1.4%	0.6%	0.6%
3602	23.1%	1.1%	0.9%	0.7%
SPK-1	0.0%	0.0%	0.3%	bdl
SPK-2	0.0%	0.0%	0.3%	bdl
SPK-3	0.0%	0.0%	0.3%	0.3%
SPK-4	0.0%	0.0%	0.2%	0.2%

*Naphthalenes

Table D-2 Summary of Polymer-Fuel Partition Coefficients (Kpf) for V0835

Fuel ID	Aromatics D6379	Naphs* D6379	Kpf			
			Alkanes	Alkyl Bz	Naph	Naphs*
SRI-1	8.7%	0.2%	0.013	0.094	0.279	**
4597	15.0%	1.9%	0.011	0.091	0.255	0.151
5245	15.5%	0.2%	0.011	0.084	0.163	0.060
3166	17.6%	2.5%	0.010	0.071	0.199	0.168
4598	17.6%	1.4%	0.010	0.079	0.160	0.104
4600	17.7%	1.3%	0.012	0.091	0.272	0.156
4658	17.7%	1.3%	0.011	0.086	0.248	0.118
4626	17.9%	0.6%	0.010	0.079	0.209	0.095
5661	18.1%	0.6%	0.009	0.074	0.182	0.107
4877	19.6%	0.4%	0.011	0.076	0.218	0.116
4599	19.9%	1.4%	0.013	0.107	0.327	0.160
3602	23.1%	1.1%	0.014	0.086	0.248	0.125
Average	18.2%	1.2%	0.011	0.085	0.230	0.124
90% CI	1.1%	0.3%	0.001	0.005	0.024	0.016
SPK-1	0.0%	0.0%	0.012	n.a.	n.a.	n.a.
SPK-2	0.0%	0.0%	0.007	n.a.	n.a.	n.a.
SPK-3	0.0%	0.0%	0.012	n.a.	n.a.	n.a.
SPK-4	0.0%	0.0%	0.011	n.a.	n.a.	n.a.

*Naphthalenes **Concentration too low in the fuel for accurate quantification.
***Analysis pending.

Table D-3 Estimated Composition of the Bulk and Absorbed Fuels

Fuel ID	Bulk Fuel			Absorbed Fuel		
	Alkanes	Alkyl Bz	Naphs*	Alkanes	Alkyl Bz	Naphs*
SRI-1	91.3%	8.5%	0.2%	59.3%	40.7%	**
4597	85.0%	13.1%	1.9%	39.2%	49.0%	11.8%
5245	84.5%	15.3%	0.2%	40.7%	58.8%	**
3166	82.4%	15.1%	2.5%	35.5%	46.3%	18.2%
4598	82.4%	16.2%	1.4%	35.8%	57.7%	6.5%
4600	82.3%	16.4%	1.3%	35.9%	56.4%	7.7%
4658	82.3%	16.4%	1.3%	36.3%	57.5%	6.2%
4626	82.1%	17.3%	0.6%	35.4%	62.0%	2.6%
5661	81.9%	17.5%	0.6%	35.5%	61.5%	3.0%
4877	80.4%	19.2%	0.4%	37.1%	61.0%	1.9%
4599	80.1%	18.5%	1.4%	32.2%	60.9%	6.9%
3602	76.9%	22.0%	1.1%	34.2%	61.3%	4.5%
Average	82.6%	16.3%	1.1%	38.1%	56.1%	6.9%
90% CI	98.9%	0.7%	0.3%	0.1%	0.5%	2.4%
SPK-1	100.0%	0.0%	0.0%	100%	0%	0%
SPK-2	100.0%	0.0%	0.0%	100%	0%	0%
SPK-3	100.0%	0.0%	0.0%	100%	0%	0%
SPK-4	100.0%	0.0%	0.0%	100%	0%	0%

*Naphthalenes **Concentration too low in the fuel for accurate quantification.
***Analysis pending.

5.5 Appendix E PR-1776 Polysulfide Sealant

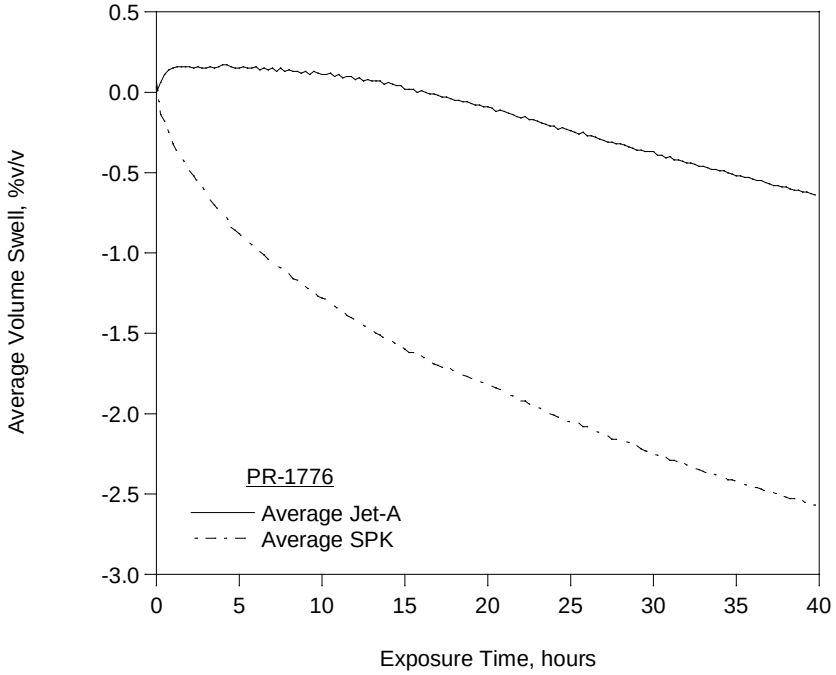

Figure E-1 Average volume swell as a function of time for PR-1776 at room temperature

Table E-1 Summary of Volume Swell and Mass Fraction of Fuel Absorbed by PR-1776

Fuel ID	Aromatics D6379	Naphs* D6379	Volume Swell	Mass Fraction
SRI-1	8.7%	0.2%	-1.6%	3.3%
4597	15.0%	1.9%	-0.4%	3.7%
5245	15.5%	0.2%	-1.4%	3.7%
3166	17.6%	2.5%	-0.1%	4.7%
4598	17.6%	1.4%	-0.8%	3.8%
4600	17.7%	1.3%	-0.1%	4.4%
4658	17.7%	1.3%	-0.6%	4.4%
4626	17.9%	0.6%	-1.0%	4.2%
5661	18.1%	0.6%	-0.5%	4.3%
4877	19.6%	0.4%	-0.7%	4.2%
4599	19.9%	1.4%	-0.4%	4.6%
3602	23.1%	1.1%	0.1%	4.6%
SPK-1	0.0%	0.0%	-2.7%	2.0%
SPK-2	0.0%	0.0%	-3.0%	2.0%
SPK-3	0.0%	0.0%	-2.5%	2.2%
SPK-4	0.0%	0.0%	-2.1%	1.8%

*Naphthalenes

Table E-2 Summary of Polymer-Fuel Partition Coefficients (Kpf) for PR-1776

Fuel ID	Aromatics D6379	Naphs* D6379	Kpf			
			Alkanes	Alkyl Bz	Naph	Naphs*
SRI-1	8.7%	0.2%	0.039	0.143	**	**
4597	15.0%	1.9%	0.053	0.228	1.020	0.557
5245	15.5%	0.2%	0.043	0.165	**	**
3166	17.6%	2.5%	0.051	0.200	0.931	0.484
4598	17.6%	1.4%	0.042	0.178	0.808	0.289
4600	17.7%	1.3%	0.042	0.165	0.660	0.341
4658	17.7%	1.3%	0.045	0.169	0.761	0.356
4626	17.9%	0.6%	0.046	0.201	0.820	0.401
5661	18.1%	0.6%	0.038	0.189	0.715	0.350
4877	19.6%	0.4%	0.041	0.169	0.688	0.344
4599	19.9%	1.4%	0.038	0.174	0.757	0.356
3602	23.1%	1.1%	0.043	0.183	0.771	0.403
Average	18.2%	1.2%	0.044	0.181	0.796	0.389
90% CI	1.1%	0.3%	0.002	0.011	0.061	0.042
SPK-1	0.0%	0.0%	0.032	n.a.	n.a.	n.a.
SPK-2	0.0%	0.0%	0.038	n.a.	n.a.	n.a.
SPK-3	0.0%	0.0%	0.040	n.a.	n.a.	n.a.
SPK-4	0.0%	0.0%	0.029	n.a.	n.a.	n.a.

*Naphthalenes **Concentration too low in the fuel for accurate quantification.

Table E-3 Estimated Composition of the Bulk and Absorbed Fuels

Fuel ID	Bulk Fuel			Absorbed Fuel		
	Alkanes	Alkyl Bz	Naphs*	Alkanes	Alkyl Bz	Naphs*
SRI-1	91.3%	8.5%	0.2%	74.5%	25.5%	**
4597	85.0%	13.1%	1.9%	52.6%	35.0%	12.4%
5245	84.5%	15.3%	0.2%	58.9%	41.1%	**
3166	82.4%	15.1%	2.5%	50.0%	35.7%	14.3%
4598	82.4%	16.2%	1.4%	51.2%	42.8%	6.0%
4600	82.3%	16.4%	1.3%	52.2%	41.1%	6.7%
4658	82.3%	16.4%	1.3%	53.4%	39.9%	6.7%
4626	82.1%	17.3%	0.6%	50.5%	46.3%	3.2%
5661	81.9%	17.5%	0.6%	47.2%	49.7%	3.2%
4877	80.4%	19.2%	0.4%	49.1%	48.9%	2.1%
4599	80.1%	18.5%	1.4%	45.3%	47.4%	7.3%
3602	76.9%	22.0%	1.1%	42.7%	51.6%	5.7%
Average	82.6%	16.3%	1.1%	52.3%	42.1%	6.8%
90% CI	98.9%	0.7%	0.3%	0.2%	1.1%	5.7%
SPK-1	100.0%	0.0%	0.0%	100.0%	0.0%	0.0%
SPK-2	100.0%	0.0%	0.0%	100.0%	0.0%	0.0%
SPK-3	100.0%	0.0%	0.0%	100.0%	0.0%	0.0%
SPK-4	100.0%	0.0%	0.0%	100.0%	0.0%	0.0%

*Naphthalenes **Concentration too low in the fuel for accurate quantification.

5.6 Appendix F PR-1828 Polythioether Sealant

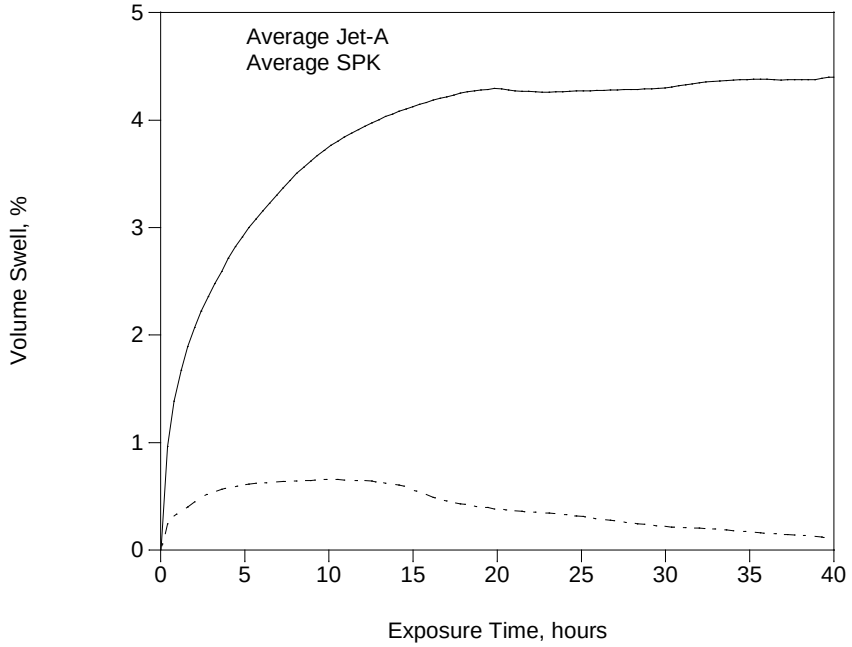

Figure F-1 Average volume swell as a function of time for PR-1828 at room temperature

Table F-1 Summary of Volume Swell and Mass Fraction of Fuel Absorbed by PR-1828

Fuel ID	Aromatics D6379	Naphs* D6379	Volume Swell	Mass Fraction
SRI-1	8.7%	0.2%	3.0%	2.8%
4597	15.0%	1.9%	4.9%	4.3%
5245	15.5%	0.2%	3.3%	3.7%
3166	17.6%	2.5%	5.3%	4.7%
4598	17.6%	1.4%	4.2%	3.6%
4600	17.7%	1.3%	4.6%	4.2%
4658	17.7%	1.3%	4.2%	4.1%
4626	17.9%	0.6%	3.8%	3.7%
5661	18.1%	0.6%	4.9%	4.4%
4877	19.6%	0.4%	4.2%	3.8%
4599	19.9%	1.4%	4.7%	4.0%
3602	23.1%	1.1%	5.5%	4.9%
SPK-1	0.0%	0.0%	-0.1%	1.2%
SPK-2	0.0%	0.0%	0.3%	1.4%
SPK-3	0.0%	0.0%	0.3%	1.4%
SPK-4	0.0%	0.0%	0.2%	1.3%

*Naphthalenes

Table F-2 Summary of Polymer-Fuel Partition Coefficients (Kpf) for PR-1828

Fuel ID	Aromatics D6379	Naphs* D6379	Kpf			
			Alkanes	Alkyl Bz	Naph	Naphs*
SRI-1	8.7%	0.2%	0.023	0.164	**	**
4597	15.0%	1.9%	0.027	0.188	0.674	0.447
5245	15.5%	0.2%	0.032	0.217	**	**
3166	17.6%	2.5%	0.030	0.201	0.741	0.416
4598	17.6%	1.4%	0.027	0.196	0.919	0.372
4600	17.7%	1.3%	0.029	0.181	0.758	0.408
4658	17.7%	1.3%	0.026	0.176	0.703	0.376
4626	17.9%	0.6%	0.030	0.185	0.882	0.456
5661	18.1%	0.6%	0.036	0.219	0.844	0.457
4877	19.6%	0.4%	0.029	0.176	0.707	0.434
4599	19.9%	1.4%	0.026	0.174	0.758	0.391
3602	23.1%	1.1%	0.034	0.190	0.767	0.439
Average	18.2%	1.2%	0.029	0.189	0.775	0.419
90% CI	1.1%	0.3%	0.002	0.008	0.042	0.017
SPK-1	0.0%	0.0%	0.025	n.a.	n.a.	n.a.
SPK-2	0.0%	0.0%	0.027	n.a.	n.a.	n.a.
SPK-3	0.0%	0.0%	0.025	n.a.	n.a.	n.a.
SPK-4	0.0%	0.0%	0.032	n.a.	n.a.	n.a.

*Naphthalenes **Concentration too low in the fuel for accurate quantification.

Table F-3 Estimated Composition of the Bulk and Absorbed Fuels

Fuel ID	Bulk Fuel			Absorbed Fuel		
	Alkanes	Alkyl Bz	Naphs*	Alkanes	Alkyl Bz	Naphs*
SRI-1	91.3%	8.5%	0.2%	74.5%	25.5%	**
4597	85.0%	13.1%	1.9%	52.6%	35.0%	12.4%
5245	84.5%	15.3%	0.2%	58.9%	41.1%	**
3166	82.4%	15.1%	2.5%	50.0%	35.7%	14.3%
4598	82.4%	16.2%	1.4%	51.2%	42.8%	6.0%
4600	82.3%	16.4%	1.3%	52.2%	41.1%	6.7%
4658	82.3%	16.4%	1.3%	53.4%	39.9%	6.7%
4626	82.1%	17.3%	0.6%	50.5%	46.3%	3.2%
5661	81.9%	17.5%	0.6%	47.2%	49.7%	3.2%
4877	80.4%	19.2%	0.4%	49.1%	48.9%	2.1%
4599	80.1%	18.5%	1.4%	45.3%	47.4%	7.3%
3602	76.9%	22.0%	1.1%	42.7%	51.6%	5.7%
Average	82.6%	16.3%	1.1%	52.3%	42.1%	6.8%
90% CI	98.9%	0.7%	0.3%	0.2%	1.1%	5.7%
SPK-1	100.0%	0.0%	0.0%	100.0%	0.0%	0.0%
SPK-2	100.0%	0.0%	0.0%	100.0%	0.0%	0.0%
SPK-3	100.0%	0.0%	0.0%	100.0%	0.0%	0.0%
SPK-4	100.0%	0.0%	0.0%	100.0%	0.0%	0.0%

*Naphthalenes **Concentration too low in the fuel for accurate quantification.

5.7 Appendix G BMS 10-20 Epoxy Fuel Tank Coating

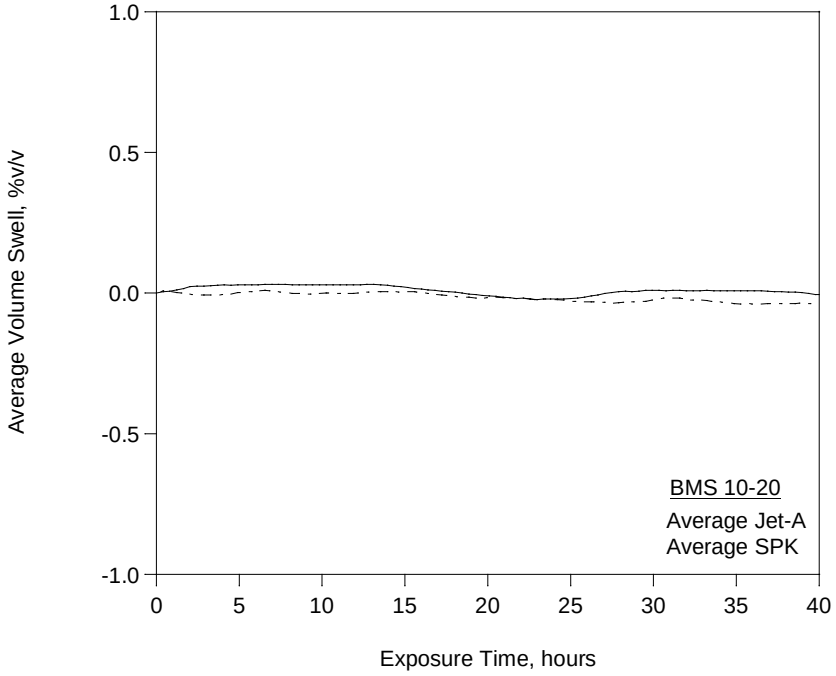

Figure G-1 Average volume swell as a function of time for BMS 10-20 at room temperature

Table G-1 Summary of Volume Swell and Mass Fraction of Fuel Absorbed by BMS 10-20

Fuel ID	Aromatics D6379	Naphs D6379	Volume Swell	Mass Fraction
SRI-1	8.7%	0.2%	0.1%	*
4597	15.0%	1.9%	-0.1%	*
5245	15.5%	0.2%	0.0%	*
3166	17.6%	2.5%	0.0%	*
4598	17.6%	1.4%	0.0%	*
4600	17.7%	1.3%	0.0%	*
4658	17.7%	1.3%	0.1%	*
4626	17.9%	0.6%	0.0%	*
5661	18.1%	0.6%	0.1%	*
4877	19.6%	0.4%	0.0%	*
4599	19.9%	1.4%	0.1%	*
3602	23.1%	1.1%	-0.1%	*
SPK-1	0.0%	0.0%	-0.1%	*
SPK-2	0.0%	0.0%	-0.1%	*
SPK-3	0.0%	0.0%	0.0%	*
SPK-4	0.0%	0.0%	0.0%	*

*The mass of fuel absorbed was too small to be accurately measured by TGA

5.8 Appendix H BMS 10-123 Epoxy Fuel Tank Coating

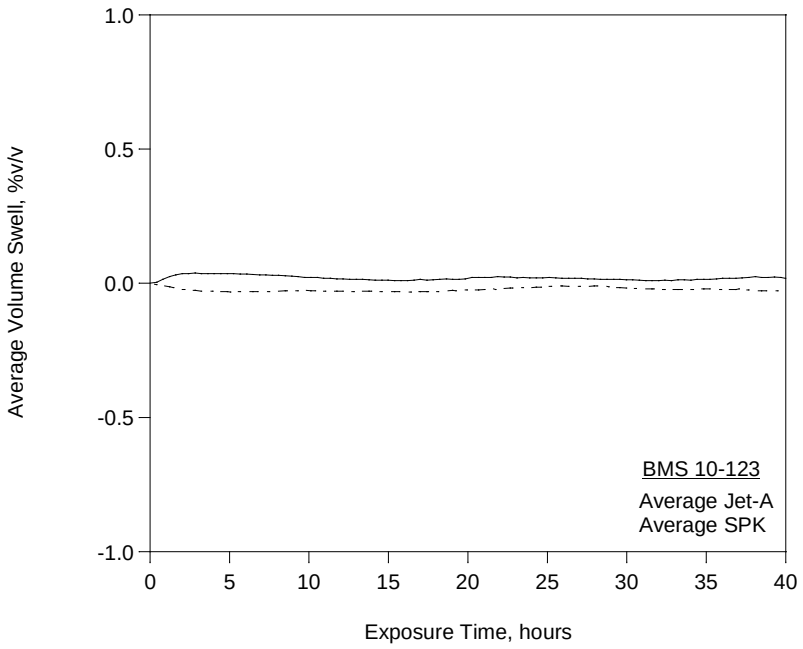

Figure H-1 Average volume swell as a function of time for BMS 10-123 at room temperature

Table H-1 Summary of Volume Swell and Mass Fraction of Fuel Absorbed by BMS 10-123

Fuel ID	Aromatics D6379	Naphs D6379	Volume Swell	Mass Fraction
SRI-1	8.7%	0.2%	0.0%	*
4597	15.0%	1.9%	0.0%	*
5245	15.5%	0.2%	0.1%	*
3166	17.6%	2.5%	0.2%	*
4598	17.6%	1.4%	0.0%	*
4600	17.7%	1.3%	0.0%	*
4658	17.7%	1.3%	0.0%	*
4626	17.9%	0.6%	-0.1%	*
5661	18.1%	0.6%	0.0%	*
4877	19.6%	0.4%	-0.1%	*
4599	19.9%	1.4%	0.0%	*
3602	23.1%	1.1%	0.1%	*
SPK-1	0.0%	0.0%	0.0%	*
SPK-2	0.0%	0.0%	0.0%	*
SPK-3	0.0%	0.0%	-0.1%	*
SPK-4	0.0%	0.0%	0.0%	*

*The mass of fuel absorbed was too small to be accurately measured by TGA

5.9 Appendix I Nylon (6,6) Film

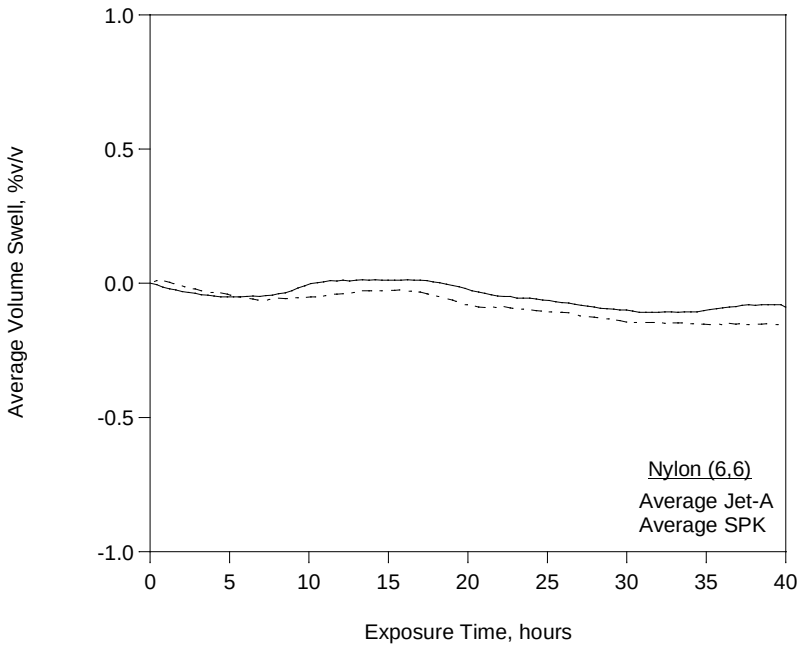

Figure I-1 Average volume swell as a function of time for Nylon (6,6) at room temperature

Table I-1 Summary of Volume Swell and Mass Fraction of Fuel Absorbed by Nylon (6,6)

Fuel ID	Aromatics D6379	Naphs D6379	Volume Swell	Mass Fraction
SRI-1	8.7%	0.2%	0.0%	*
4597	15.0%	1.9%	-0.1%	*
5245	15.5%	0.2%	-0.1%	*
3166	17.6%	2.5%	-0.1%	*
4598	17.6%	1.4%	-0.1%	*
4600	17.7%	1.3%	-0.1%	*
4658	17.7%	1.3%	0.0%	*
4626	17.9%	0.6%	0.0%	*
5661	18.1%	0.6%	-0.2%	*
4877	19.6%	0.4%	-0.1%	*
4599	19.9%	1.4%	-0.1%	*
3602	23.1%	1.1%	-0.2%	*
SPK-1	0.0%	0.0%	-0.2%	*
SPK-2	0.0%	0.0%	-0.1%	*
SPK-3	0.0%	0.0%	-0.2%	*
SPK-4	0.0%	0.0%	-0.1%	*

*The mass of fuel absorbed was too small to be accurately measured by TGA

5.10 Appendix J Kapton® Film

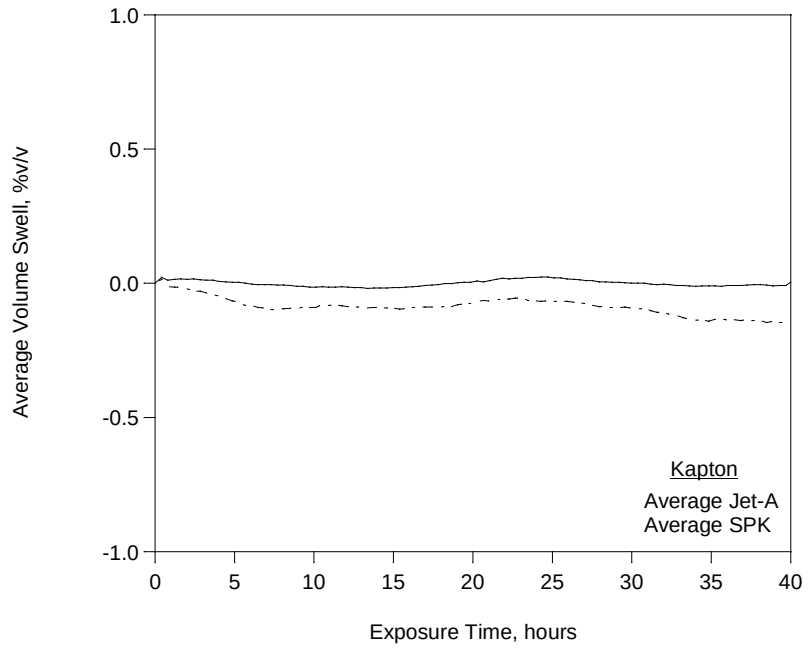

Figure J-1 Average volume swell as a function of time for Kapton® at room temperature

Table J-1 Summary of Volume Swell and Mass Fraction of Fuel Absorbed by Kapton

Fuel ID	Aromatics D6379	Naphs D6379	Volume Swell	Mass Fraction
SRI-1	8.7%	0.2%	0.0%	*
4597	15.0%	1.9%	-0.1%	*
5245	15.5%	0.2%	0.1%	*
3166	17.6%	2.5%	0.0%	*
4598	17.6%	1.4%	0.0%	*
4600	17.7%	1.3%	0.0%	*
4658	17.7%	1.3%	0.1%	*
4626	17.9%	0.6%	-0.2%	*
5661	18.1%	0.6%	0.0%	*
4877	19.6%	0.4%	0.0%	*
4599	19.9%	1.4%	0.1%	*
3602	23.1%	1.1%	0.0%	*
SPK-1	0.0%	0.0%	-0.1%	*
SPK-2	0.0%	0.0%	-0.1%	*
SPK-3	0.0%	0.0%	-0.3%	*
SPK-4	0.0%	0.0%	-0.1%	*

*The mass of fuel absorbed was too small to be accurately measured by TGA

5.11 Appendix K JP-8 to FT Transition

Prior, related studies were conducted by UDRI, using JP-8 for similar materials as used in this study. As shown in Figure K-1, nitrile rubber, fluorosilicone, and fluorocarbon were tested out to over 150 hours from dry to JP-8, after which they were transitioned to 100% FT fuel, and examined to over 300 hours. These results indicate that the aromatics' impact on nitrile rubber in a fuel-switching scenario should be considered for further evaluation. Note that these tests were conducted using approximately 1/3rd sections of whole O-rings as compared to the 1mm slices of O-rings used in this study. Earlier work has shown that using the 1mm slices increased the rate of volume swell (by virtue of a higher surface to volume ratio), but did not affect the extent of volume swell. This permitted the exposure time to be shortened from 150 hours to 40 hours in the present study where the temporal behavior was not considered as a primary factor.

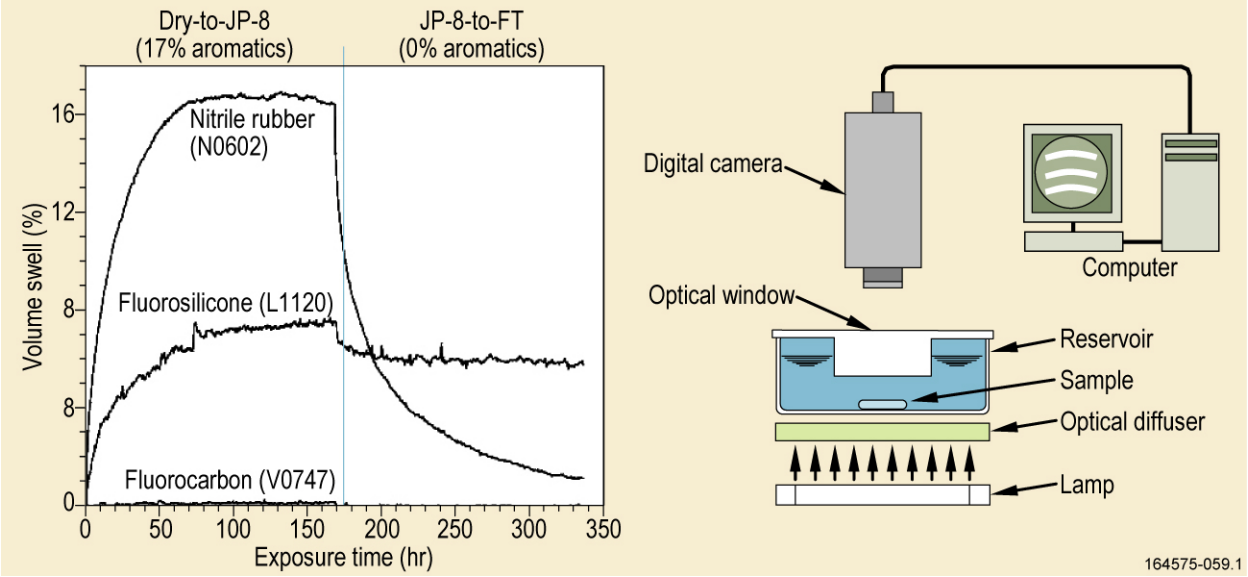

Figure K-1 Volume swell for JP-8 to FT Transition

5.12 Appendix L Cycloparaffins

5.12.1 Introduction

In this and similar studies, it has been observed that SPKs tend to under-swell the value predicted by extrapolating the data from the Jet-A reference populations to 0% aromatics. For example, consider the results in Table L-1 which summarizes the expected value (the volume swell of the reference Jet-As extrapolated to 0% aromatics using a linear model) with the measured values for the SPKs and materials used in this study. This shows that the materials that showed the greatest sensitivity to the composition of the test fuels (for example the sealants and nitrile rubber O-rings) typically under-swell the expected values. The impact of this phenomenon is illustrated in Figure L-1 which summarizes the volume swell of the N0602 nitrile rubber O-ring material in the reference Jet-As, SPK-1, and 50% Jet-A/SPK-1 fuel blends. This shows how the lower than expected volume swell of the SPK-1 also lowers the volume swell of the 50% fuel blends prepared with this fuel. This behavior has been frequently observed in other studies with a variety of paraffinic alternative fuels. Figure L-2 shows the estimated behavior of 50% fuel blends prepared with a model SPK that exhibits a volume swell that matches the expected value at 0% aromatics. This suggests that if SPKs can be made with a volume swell character that is equal to or greater than the expected value at 0% aromatics, the fuel blends prepared from these SPKs would have a far greater probability of being compatible with conventional Jet-A fuels.

Table L-1. Summary of the Volume Swell of the Test Materials in the SPKs and the Expected Values*

Component	Sample ID	SPK-1	SPK-2	SPK-3	SPK-4	Average	Expected Value*	Difference
O-Rings	N0602	-0.3%	0.2%	0.1%	0.6%	0.2%	0.9%	-0.8%
	N0602e	10.0%	9.9%	10.2%	9.9%	10.0%	12.1%	-2.1%
	L1120	5.7%	6.8%	5.8%	6.3%	6.1%	5.0%	1.1%
	V0835	0.3%	0.3%	0.3%	0.2%	0.3%	0.3%	0.0%
Sealants	PR 1776	-2.7%	-3.0%	-2.5%	-2.1%	-2.6%	-2.4%	-0.2%
	PR 1828	-0.1%	0.3%	0.3%	0.2%	0.2%	1.7%	-1.5%
Coatings	BMS 10-20	-0.1%	-0.1%	0.0%	0.0%	0.0%	0.1%	-0.1%
	BMS 10-123	0.0%	0.0%	-0.1%	0.0%	0.0%	0.0%	0.0%
Films	Nylon	-0.2%	-0.1%	-0.2%	-0.1%	-0.1%	0.2%	-0.3%
	Kapton	-0.1%	-0.1%	-0.3%	-0.1%	-0.1%	-0.1%	0.0%

*Expected value for a Jet-A with 0% aromatics based on extrapolating the swell results reported in the core study for each material in a set of reference Jet-A fuels.

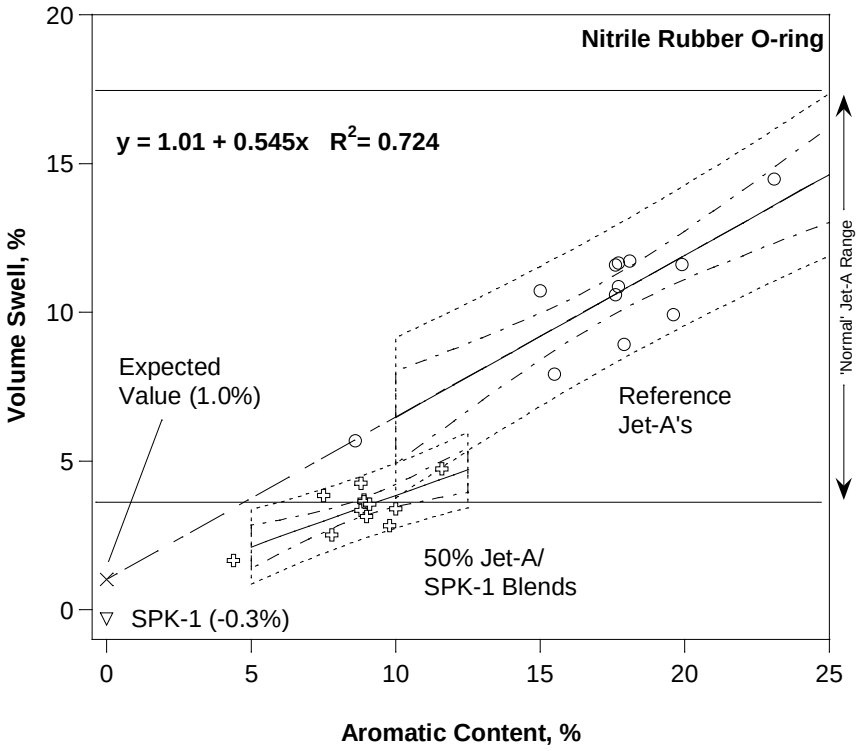

Figure L- 1. Volume swell of nitrile rubber (N0602) in the reference Jet-As, SPK-1, and 50% Jet-A/SPK-1 fuel blends showing the expected versus measured values at 0% aromatics.

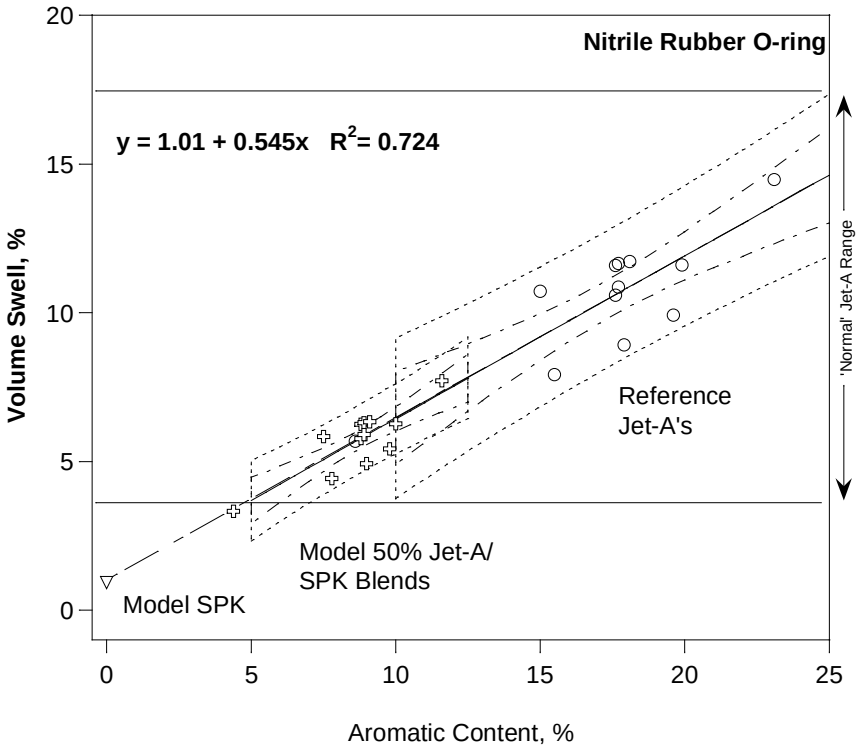

Figure L-2. Volume swell of nitrile rubber (N0602) in the reference Jet-As, a model SPK that exhibits a volume swell at the expected value, and the estimated volume swell of 50% Jet-A/Model SPK fuel blends.

The 2011 study concluded that volume swell increases as the polarity and hydrogen bonding characteristics of the fuel components increase, and as their molar decreases. This suggests that the SPKs used in this, and similar studies, include factors that decrease their volume swell character either through the lack of components that impart polarity and hydrogen bonding to the fuel and/or that the molar volume of these fuels is biased towards a value that is higher than expected as compared to Jet-A fuels. Noting that there is no mechanism to impart hydrogen bonding character in the paraffinic components of jet fuel, the relevant factors are likely to be primarily related to molar volume and polarity.

With respect to molar volume, Figure L-3 shows chromatograms of a typical Jet-A and the SPK (SPK-1) used in this study. Noting that molecular weight and molar volume increase from left to right in this figure, the overall distribution of SPK-1 is biased towards the light end of the boiling range, which would tend to increase its volume swell character, although, the distribution of components in SPK-1 is wide enough that it includes components that are heavier than those in the Jet-A, which would tend to decrease the volume swell character of this fuel. However, these components comprise a relatively small fraction of the fuel, suggesting that the lower than expected volume swell character of SPK-1 cannot be explained solely on the basis of molar volume. This indicates that there is a compositional component contributing to the volume swell behavior of this fuel.

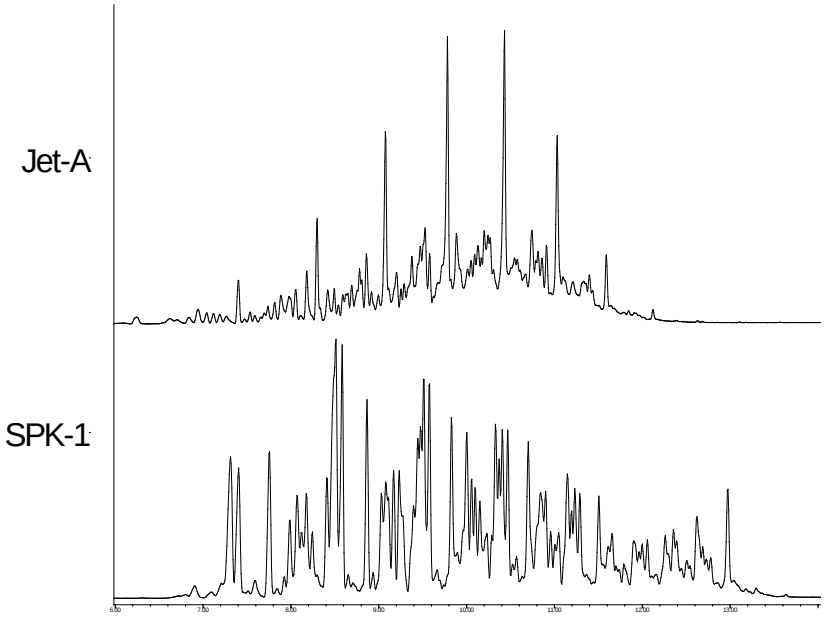

Figure L-3. Example chromatograms of a typical Jet-A and SPK-1. Note that molecular weight and molar volume increases from left to right.

With respect to its composition, SPK-1 is almost completely composed of linear and branched paraffins whereas conventional jet fuels contain these components plus 15%-45% cycloparaffins (based on communications with fuel analysts at Wright-Patterson Air Force Base), suggesting that the missing component in the SPK-1 may be related to the cycloparaffins. Furthermore,

analysis of the fuel absorbed by polymeric materials aged in jet fuel, such as reported in the core study described here, has shown that the solubility of the cycloparaffins that naturally occur in jet fuels tends to be about 10% higher than the linear and branched paraffins in these fuels. Interestingly, as shown in Figure L-4, an analysis of the volume swell of nitrile rubber in JP-900, a coal-derived cycloparaffinic fuel with 0%, exhibited a volume swell character that is comparable to a typical jet fuel with 17% aromatics. (Balster, L.M., et al., "Development of an Advanced, Thermally Stable, Coal-based Jet Fuel," Fuel Processing Technology, 2007.) This suggests that cycloparaffins can have a positive influence on the volume swell character of jet turbine fuels and that the absence of cycloparaffins from SPKs could be an important contributing factor to their volume swell behavior.

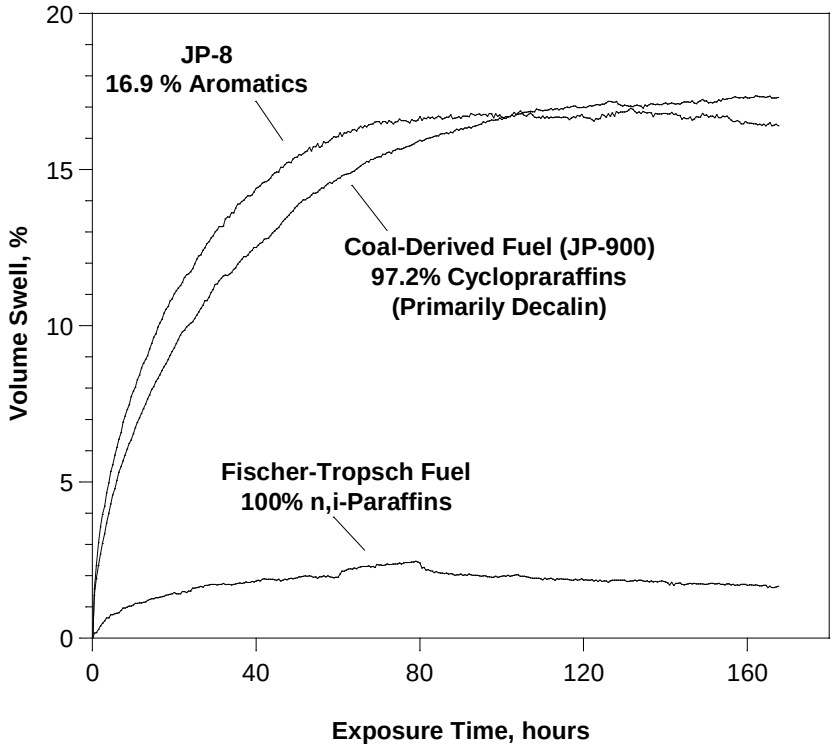

Figure L-4. The volume swell of nitrile rubber (N0602) in a Fischer-Tropsch fuel, JP-8, and JP-900.

In the context of the guidelines described in the core study of the factors that contribute to the volume swell character of fuel components it is informative to consider the molar volume, polarity, and hydrogen bonding of cycloparaffins. Noting that it is very unlikely that cycloparaffins can exhibit any significant hydrogen bonding character, the emphasis should be placed on evaluating molecular characteristics that can influence molar volume and polarity. For this study, the primary molecular characteristics of interest include the size of the cycloparaffinic ring (the number of carbons in the ring), molar volume, substitution position of pendant groups, and the number of rings.

To investigate the influence of these factors on the volume swell character of alternative jet fuels a study was conducted in the same manner as described in the core study, however here the subject of the study was the relative activity of selected cycloparaffins rather than the relative

activity of aromatics. A synthetic paraffinic kerosene (SPK-1) from the core study was blended with a set of cycloparaffins selected to isolate each of the molecular characteristics of interest. The volume swell of the test materials used in the core study was measured in the neat SPK and the SPK blended with the cycloparaffins and compared against the volume swell of the materials aged in a reference set of Jet-As. Supporting data was obtained in the form of polymer-fuel partition coefficients for each of the cycloparaffins in each of the test materials. Finally, to demonstrate the influence of at least one cycloparaffin on the performance of fuel blends, the volume swell of 50% Jet-A fuel blends prepared with the SPK-1 that included a selected cycloparaffin was compared with similar data from the core study where the blends were prepared with the neat SPK-1. For completeness, the mass fraction of absorbed fuel was measured using thermogravimetric analysis (TGA) as was done in the core study.

5.12.2 Source Materials

The specific cycloparaffins selected for this study are listed in Table L-2 and shown in Figure L-5 to Figure L-9. A series of cycloparaffins with 6-12 carbons in the ring were selected as shown in Figure L-5. Although the molar volume increases with the ring size, a separate set of cycloparaffins were selected in an effort to isolate the effect of increasing the molar volume from any changes that the ring size would have on the activity of the molecular probe. For this purpose, a set of substituted cyclohexanes were selected as shown in Figure L-6. To evaluate the influence of the substitution position a set of 3 dimethylcyclohexanes were selected as shown in Figure L-7. To evaluate the number of rings in the probe molecules decalin (decahydronaphthalene) and Adamantane were selected as shown in Figure L-8. Note that while both of these molecules are comprised of 10 carbon atoms, decalin is composed of two relatively planar rings and Adamantane is a complex non-planar structure of 4 rings. Finally, interest has been expressed in the activity of Farnesane (2,6,10-trimethyldodecane), so this component was included as an example of a branched alkane, Figure L-9.

Table L- 2. Cycloparaffins Used in this Study with Selected Linear Paraffins for Comparison

Class	Component	MW g/mol	Density g/mL	MV mL/mol	$T_{boiling}$ °C	Notes
Linear Alkane (Comparison)	n-Hexane	86.2	0.659	130.7	69	C6
	n-Octane	114.2	0.703	162.6	126	C8
	n-Decane	142.3	0.730	194.9	174	C10
	n-Dodecane	170.4	0.749	227.5	216	C12
	n-Tetradecane	198.4	0.763	260.1	254	C14
	n-Hexadecane	226.5	0.773	292.8	281	C16
Ring Size	Cyclohexane	84.2	0.779	108.1	81	C6
	Cyclooctane	112.2	0.834	134.6	151	C8
	Cyclodecane	140.3	0.871	161.0	201	C10
	Cyclododecane	168.3	0.790	213.1	243	C12
Molar Volume	Methylcyclohexane	98.2	0.769	127.6	101	C6 + C1
	Butylcyclohexane	140.3	0.818	171.5	181	C6 + C4
	Heptylcyclohexane	182.4	0.810	225.1	237	C6 + C7
Substitution Pattern	1,2-Dimethylcyclohexane	122.2	0.773	158.1	127	Mix of cis and trans
	1,3-Dimethylcyclohexane	122.2	0.775	157.7	122	Mix of cis and trans
	1,4-Dimethylcyclohexane	122.2	0.773	158.2	120	Mix of cis and trans
Multiple Rings	Decalin	138.3	0.883	156.6	192	Mix of cis and trans
	Adamantane	136.2	1.090	125.0	205*	4-Ring C10 Complex
iso-Alkane	Farnesane	212.4	0.770	275.9	249	2,6,10-Trimethyldodecane

*Sublimes

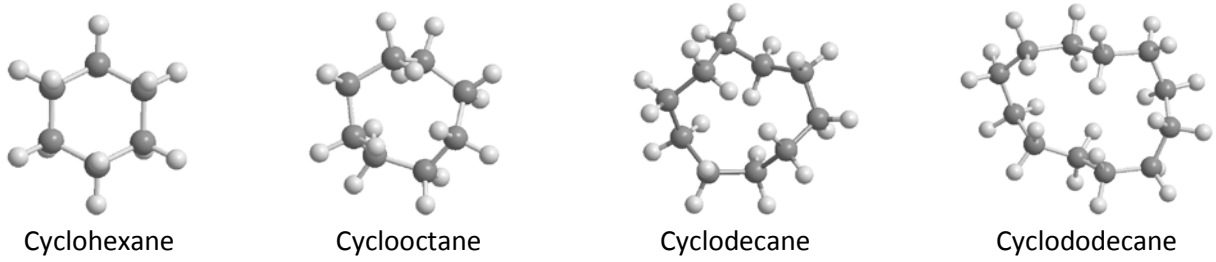

Figure L-5. Molecular structures of the cycloparaffins selected to examine the effect of ring size.

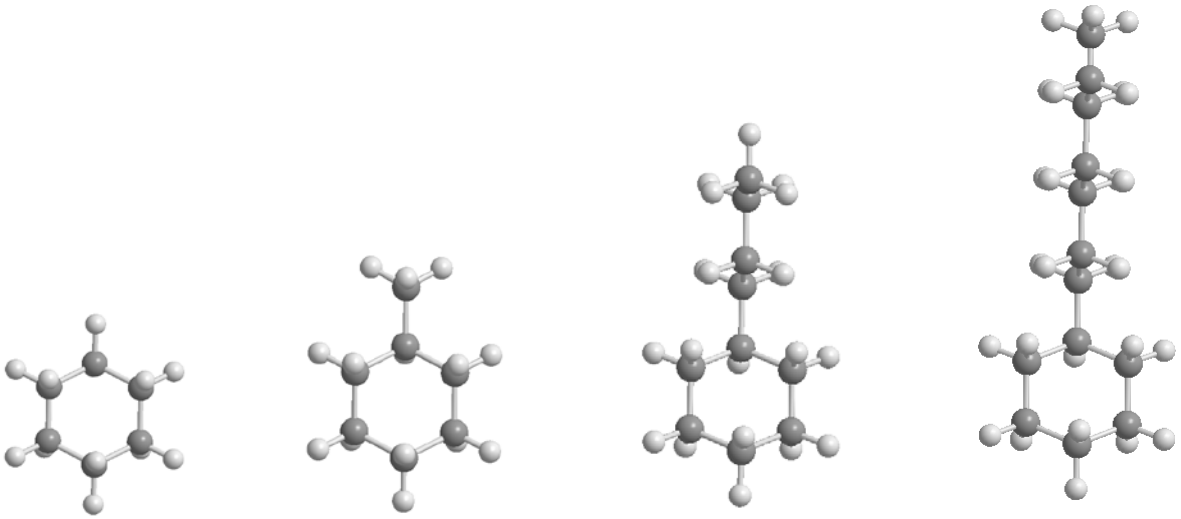

Figure L-6. Molecular structures of the cycloparaffins selected to examine the effect of molar volume.

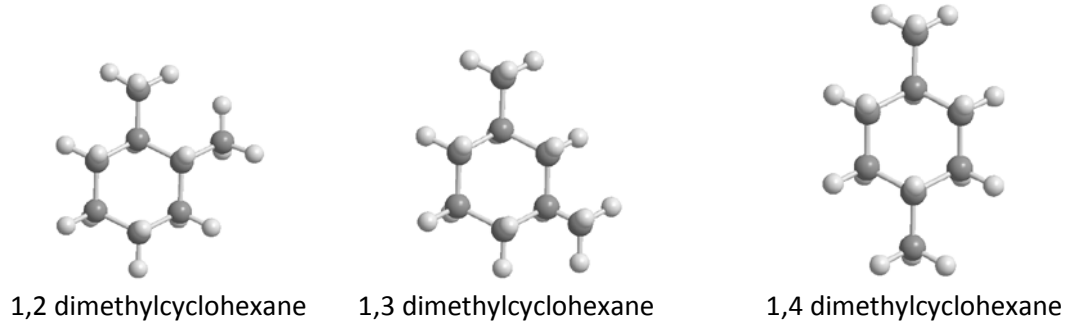

Figure L-7. Molecular structures of the cycloparaffins selected to examine the effect of substitution pattern.

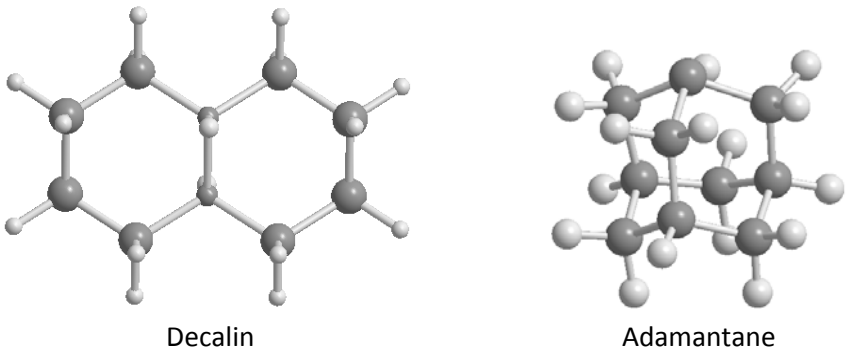

Figure L-8. Molecular structures of the cycloparaffins selected to examine the effect of the number of rings.

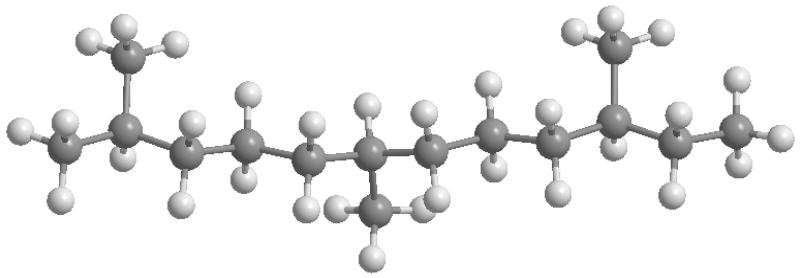

Farnesane

Figure L-9. Molecular structures of the cycloparaffins selected to examine the effect of a branched paraffin.

To establish a representative concentration for the cycloparaffin probes species in the test fuels the cycloparaffins content of the reference Jet-A fuels used in the core program was measured as summarized in Table L-3. This shows that the average cycloparaffin content of the reference Jet-A fuels was 31% v/v. Therefore, for the purposes of this study the cycloparaffins were blended with the SPK-1 at 30% v/v. Note that the solubility limit of Adamantane was found to be on the order of 10% v/v in SPK-1, so the blending level for this component was limited to 5% v/v.

Table L-3 . Fuels used in the Study

Fuel	ID	Aromatics	Naphthalenes	Cycloparaffins	Notes
Jet-A	SRI-1	8.7%	0.2%	n.a.	Clay-treated JP-8
	4597	15.0%	1.9%	28%	Jet-A
	5245	15.5%	0.2%	30%	Jet-A
	3166	17.6%	2.5%	38%	Jet-A
	4598	17.6%	1.4%	n.a.	Jet-A
	4600	17.7%	1.3%	29%	Jet-A
	4658	17.7%	1.3%	30%	Jet-A
	4626	17.9%	0.6%	23%	Jet-A
	5661	18.1%	0.6%	40%	Jet-A
	4877	19.6%	0.4%	25%	Jet-A
	4599	19.9%	1.4%	29%	Jet-A
	3602	23.1%	1.1%	38%	Jet-A
Average		17.4%	1.1%	31%	Average Jet-A
SPK	SPK-1	0.0%	0.0%	2%	Jatropha

The materials used in this study are the same as those used in the core study. These are listed in Table 2-2.

5.12.3 Experimental Procedures

The experimental procedures used in this study are identical to those used in the core study (Section 2). The volume swell of each material in each test fuel was measured at room temperature over a period of 40 hours using optical dilatometry. These results were evaluated in terms of the absolute volume swell and the specific swell; the change in volume (% v/v) normalized by the change in concentration (% v/v) of the component of interest. Supporting data in the form of polymer-fuel partition coefficients (Kpf, the ratio of the concentration of the component of interest in the test material to its concentration in the fuel in which the material was aged) were measured using GC-MS to analyze the composition of the fuel in which each was aged and the fuel absorbed by each material. Supplemental data was also obtained on the mass fraction of fuel absorbed using TGA to assess whether this technique could be used under circumstances where measuring the volume swell would be problematic.

5.12.4 Results and Discussion

5.12.4.1 Analysis of Polarity by GCxGC

Although paraffins in general are considered to be non-polar, theoretical considerations suggest that cycloparaffins may exhibit some polar character. Specifically, the weak charge distributions and freedom of rotation about the single bonds that make up linear and branched paraffins render then essentially non-polar. In contrast, the more rigid ring structure of the cycloparaffins limits the conformations of these molecules, often to asymmetric geometries that may exhibit a small amount of polarity. To demonstrate this, the SPK-1 fuel was blended with each of the cycloparaffins selected for this study and analyzed by GCxGC as shown in Figure L-10. In GCxGC the sample is separated in order of increasing boiling point (increasing molecular weight) using a chromatographic column with a non-polar stationary phase as shown along the x-axis in Figure L-10. The sample is simultaneously separated in order of increasing polarity using a second column with a polar stationary phase as shown on the y-axis in Figure L-10. The top of Figure L-10 gives the actual GCxGC data showing the n,i-paraffins in the SPK-1 fuel forming a band along the bottom of the graph indicating that these components have no significant polarity. Above this band are several vertically elongated spots that are the various cycloparaffins, illustrating that each of these exhibits at least a small degree of polarity. The bottom of Figure L-10 shows the non-polar band, represented by the SPK-1 fuel itself, and the individual cycloparaffins from the source data. This shows that the cycloparaffins fall into two groups with the non-substituted rings having greater polarity than the substituted rings. This data also shows that the polarity of the multi-ring decalin and Adamantane are comparable to cyclodecane. This suggests that the polar character of cycloparaffins can be strongly influenced by substitutions on the ring, but not by the number of rings.

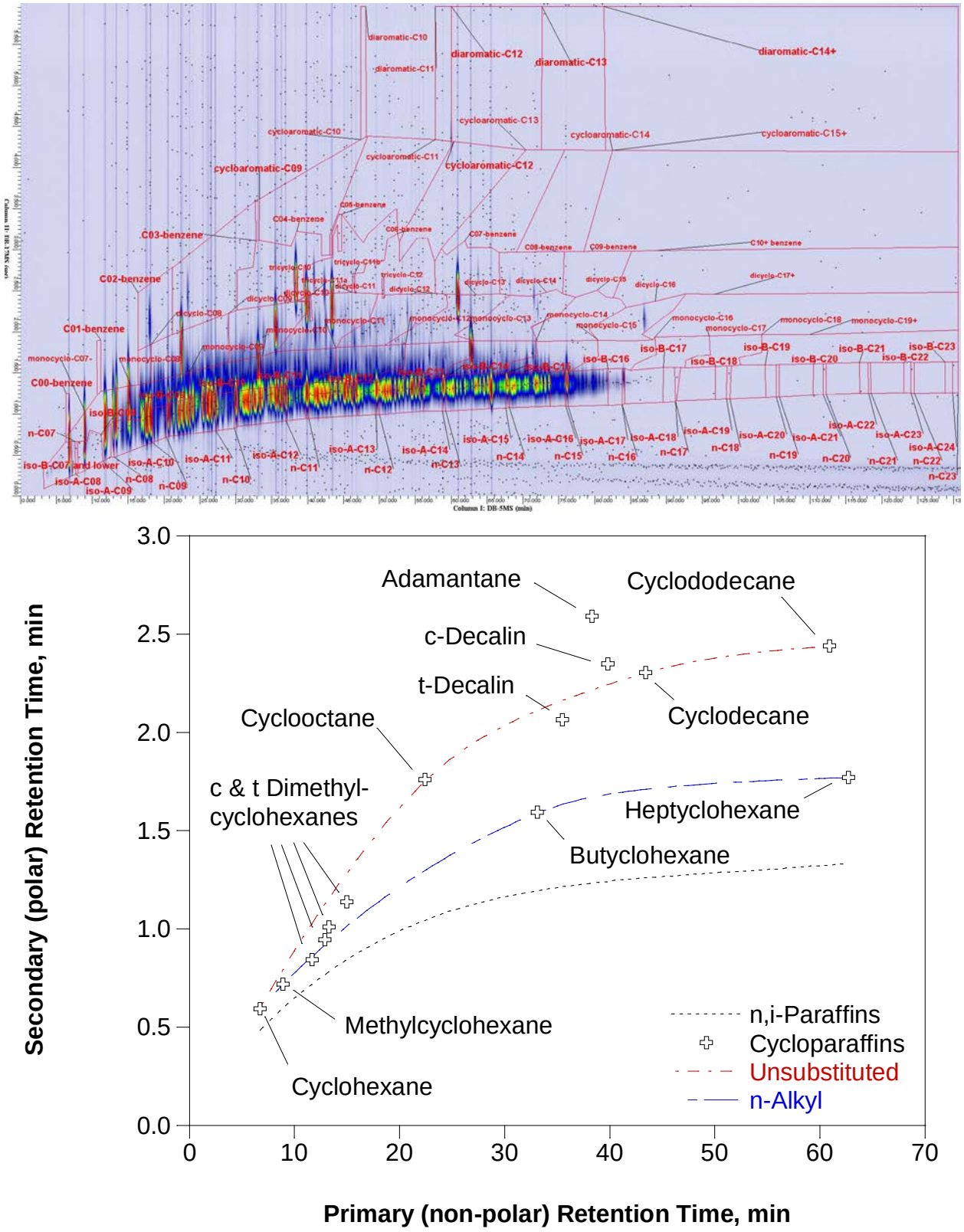

Figure L- 10. Source (top) and simplified (bottom) GCxGC analysis of the SPK-1 blended with the selected

5.12.4.2 Volume Swell and Solubility

The volume swell, specific swell, and polymer-fuel partition coefficient results are summarized in Table L-4 through Table L-8, and Figure L-11 through Figure L-20. Note that the top four panels in each figure summarizes the volume swell data grouped by ring size, molar volume, substitution pattern, and number of rings as well as the Farnesane (grouped together as 'other'). Each of these panes summarizes the region for the reference Jet-As as a function of their aromatic content, the upper and lower bounds for the normal volume swell behavior, and the expected value for a Jet-A with 0% aromatics. Note that comparing the slope of the reference fuels with the cycloparaffins gives a visual indication of the relative activity of the cycloparaffins and the aromatics that naturally occur in Jet-A. The expected value is a visual indication of the target value for the volume swell character of the SPK, while the lower limit of the normal volume swell range gives a visual indication of the ideal blending stock; an SPK that swells within the normal range as would all of the blends prepared with this fuel (Note that these fuels are shown in bold type in Table L-4 and Table L-5). The bottom left pane summarizes the volume swell results in terms of the specific swell as a function of the molar volume of each cycloparaffin. This summarizes the relative activity of each cycloparaffin and its influence on the overall absorption of fuel (Note that Adamantane is not shown in this summary since it was blended at only 5% in each fuel). The bottom right pane summarizes the polymer-fuel partition coefficients (Kpf) as a function of the molar volume of each cycloparaffin. This summarizes the specific activity of each individual cycloparaffin in terms of its solubility in each material. Note that the Kpf values for the n,i-paraffins in the SPK-1 as well as the values for the average aromatics in Jet-A are also shown. Also note that the coatings and films did not absorb enough fuel for the Kpf values to be measured.

Table L- 4.Volume Swell Results O-rings and Sealants aged in SPK-1 Blended with Selected Cycloparaffins at 30% v/v (unless noted at 5%)*

Characteristic	Component	O-rings				Sealants	
		N0602e	N0602	L1120	V0835	PR-1776	PR-1828
Average Jet-A	Estimated 0% Aromatic	12.1%	0.9%	5.0%	0.3%	-2.4%	1.7%
	Lower Limit	15.3%	3.7%	4.0%	0.2%	-2.2%	2.0%
	Upper Limit	33.2%	17.4%	8.0%	1.3%	1.0%	6.9%
Example SPK	SPK-1	9.6%	-0.8%	**7.0%**	**0.2%**	-2.6%	0.4%
Ring Size	Cyclohexane	**16.9%**	3.7%	**7.9%**	**0.6%**	**-1.4%**	**2.6%**
	Cyclooctane	**15.4%**	**3.8%**	**7.7%**	**0.7%**	**-1.3%**	**2.5%**
	Cyclodecane	15.0%	**3.8%**	**6.3%**	**0.4%**	**-1.2%**	**2.4%**
	Cyclododecane	13.8%	2.7%	**5.5%**	**0.6%**	**-2.5%**	0.9%
Molar Volume	Cyclohexane	**16.9%**	3.7%	**7.9%**	**0.6%**	**-1.4%**	**2.6%**
	Methylcyclohexane	13.7%	2.3%	**6.6%**	**0.8%**	**-1.6%**	1.8%
	Butylcyclohexane	13.0%	1.2%	**5.3%**	**0.3%**	**-2.0%**	0.7%
	Heptylcyclohexane	11.4%	-0.3%	**5.2%**	**0.3%**	-2.3%	0.7%
Substitution Pattern	1,2 Dimethylcyclohexane	13.9%	2.3%	**7.4%**	**0.5%**	**-1.4%**	**2.5%**
	1,3 Dimethylcyclohexane	11.8%	0.9%	**7.0%**	**0.6%**	**-1.3%**	1.4%
	1,4 Dimethylcyclohexane	12.7%	1.3%	**8.3%**	**0.6%**	**-1.7%**	1.3%
Number of Rings	Cyclodecane	15.0%	**3.8%**	**6.3%**	**0.4%**	**-1.2%**	**2.4%**
	Decalin	**16.3%**	3.4%	**6.4%**	**0.3%**	**-1.7%**	1.9%
	Adamantane (5%)	10.9%	-0.2%	**6.1%**	**0.4%**	-2.3%	0.7%
Branched Alkane	Farnesane	8.6%	-1.3%	**4.2%**	**0.4%**	-2.9%	0.0%

*Entries in **bold** are within the predicted Jet-A range.

Table L- 5. Volume Swell Results Coatings and Films aged in SPK-1 Blended with Selected Cycloparaffins at 30% v/v (unless noted at 5%)*

Characteristic	Component	Coatings		Films	
		BMS 10-20	BMS 10-123	Nylon	Kapton
Average Jet-A	Estimated 0% Aromatic	0.1%	0.0%	0.2%	-0.1%
	Lower Limit	-0.2%	-0.1%	-0.3%	-0.2%
	Upper Limit	0.2%	0.2%	0.2%	0.2%
Example SPK	SPK-1	**0.1%**	**0.0%**	**-0.1%**	**-0.1%**
Ring Size	Cyclohexane	**0.1%**	**-0.1%**	**-0.2%**	-0.2%
	Cyclooctane	**0.1%**	**0.1%**	**0.3%**	**0.1%**
	Cyclodecane	**0.2%**	**0.1%**	**0.4%**	**0.0%**
	Cyclododecane	**0.3%**	**0.0%**	**0.1%**	**0.1%**
Molar Volume	Cyclohexane	**0.1%**	**-0.1%**	**-0.2%**	-0.2%
	Methylcyclohexane	**0.3%**	**-0.1%**	**0.4%**	-0.2%
	Butylcyclohexane	**0.1%**	**0.0%**	**0.2%**	**0.0%**
	Heptylcyclohexane	**0.2%**	**0.0%**	**0.1%**	**0.1%**
Substitution Pattern	1,2 Dimethylcyclohexane	**0.2%**	**0.1%**	**0.2%**	**0.0%**
	1,3 Dimethylcyclohexane	**0.2%**	**0.0%**	**0.2%**	**0.0%**
	1,4 Dimethylcyclohexane	**0.3%**	**0.0%**	**0.3%**	**0.1%**
Number of Rings	Cyclodecane	**0.2%**	**0.1%**	**0.4%**	**0.0%**
	Decalin	**0.2%**	**0.1%**	**0.7%**	**0.1%**
	Adamantane (5%)	**0.2%**	**0.1%**	**0.3%**	**0.1%**
Branched Alkane	Farnesane	**0.1%**	**0.8%**	**0.2%**	**0.0%**

*Entries in **bold** are within the predicted Jet-A range.

Table L- 6. Specific Swell Results O-rings and Sealants aged in SPK-1 Blended with Selected Cycloparaffins at 30% v/v (unless noted at 5%)

Characteristic	Component	O-rings				Sealants	
		N0602e	N0602	L1120	V0835	PR 1776	PR 1828
Average Jet-A	Jet-A Aromatics	0.69	0.55	0.06	0.02	0.10	0.15
Ring Size	Cyclohexane	0.24	0.15	0.03	0.01	0.04	0.07
	Cyclooctane	0.21	0.16	0.03	0.02	0.04	0.07
	Cyclodecane	0.18	0.15	-0.02	0.01	0.05	0.06
	Cyclododecane	0.14	0.12	-0.05	0.01	0.02	0.02
Molar Volume	Cyclohexane	0.24	0.15	0.03	0.01	0.04	0.07
	Methylcyclohexane	0.14	0.10	-0.01	0.02	0.03	0.05
	Butylcyclohexane	0.12	0.07	-0.05	0.00	0.02	0.01
	Heptylcyclohexane	0.06	0.02	-0.06	0.00	0.01	0.01
Substitution Pattern	1,2 Dimethylcyclohexane	0.15	0.11	0.01	0.01	0.05	0.07
	1,3 Dimethylcyclohexane	0.07	0.06	0.00	0.01	0.04	0.03
	1,4 Dimethylcyclohexane	0.11	0.07	0.05	0.01	0.03	0.03
Number of Rings	Cyclodecane	0.18	0.15	-0.02	0.01	0.05	0.06
	Decalin	0.23	0.14	-0.02	0.00	0.03	0.05
	Adamantane (5%)	0.27	0.13	-0.16	0.03	0.06	0.06
Branched Alkane	Farnesane	-0.03	-0.01	-0.09	0.01	-0.01	-0.01

Table L- 7. Specific Swell Results Coatings and Films aged in SPK-1 Blended with Selected Cycloparaffins at 30% v/v (unless noted at 5%)

Characteristic	Component	Coatings		Films	
		BMS 10-20	BMS 10-123	Nylon	Kapton
Average Jet-A	Jet-A Aromatics	-0.01	0.00	-0.01	0.01
Ring Size	Cyclohexane	0.00	0.00	0.00	-0.01
	Cyclooctane	0.00	0.00	0.01	0.01
	Cyclodecane	0.01	0.00	0.01	0.00
	Cyclododecane	0.01	0.00	0.01	0.00
Molar Volume	Cyclohexane	0.00	0.00	0.00	-0.01
	Methylcyclohexane	0.01	0.00	0.02	-0.01
	Butylcyclohexane	0.00	0.00	0.01	0.00
	Heptylcyclohexane	0.00	0.00	0.01	0.01
Substitution	1,2 Dimethylcyclohexane	0.00	0.00	0.01	0.00
Pattern	1,3 Dimethylcyclohexane	0.00	0.00	0.01	0.00
	1,4 Dimethylcyclohexane	0.01	0.00	0.01	0.01
Number of Rings	Cyclodecane	0.01	0.00	0.01	0.00
	Decalin	0.01	0.00	0.02	0.01
	Adamantane (5%)	0.03	0.02	0.07	0.04
Branched Alkane	Farnesane	0.00	0.03	0.01	0.00

Table L- 8. Polymer-Fuel Partition Coefficients for the O-rings and Sealants aged in SPK-1 Blended with Selected Cycloparaffins at 30% v/v (unless noted at 5%)*

Class	Component	O-rings			Sealants	
		N0602**	L1120	V0835	PR 1776	PR 1828
Jet-A	Aromatics	0.422	0.121	0.085	0.181	0.189
	n,i-Paraffins	0.126	0.059	0.011	0.044	0.029
SPK-1	n,i-Paraffins	0.105	0.057	0.006	0.024	0.017
Ring Size	Cyclohexane	0.244	0.126	0.037	0.088	0.098
	Cyclooctane	0.238	0.126	0.017	0.093	0.101
	Cyclodecane	0.233	0.097	0.007	0.084	0.078
	Cyclododecane	0.188	0.089	0.011	0.060	0.056
Molar Volume	Cyclohexane	0.244	0.126	0.037	0.088	0.098
	Methylcyclohexane	0.218	0.139	0.032	0.075	0.072
	Butylcyclohexane	0.166	0.094	0.014	0.060	0.042
	Heptylcyclohexane	0.135	0.079	0.008	0.046	0.029
Substitution Pattern	1,2 Dimethylcyclohexane	0.202	0.119	0.018		
	1,3 Dimethylcyclohexane	0.188	0.101	0.021	0.045	0.059
	1,4 Dimethylcyclohexane	0.166	0.103	0.025	0.046	0.061
Number of Rings	Cyclodecane	0.233	0.097	0.007	0.084	0.078
	Decalin	0.240	0.090	0.014	0.072	0.072
	Adamantane (5%)	0.249	0.106	0.012	0.095	0.095
Branched Alkane	Farnesane	0.104	0.059	0.004	0.041	0.011

*The coatings and films did not abosrb enough fuel for this analysis
**The Kpf values for N0602e are the same as those for N0602

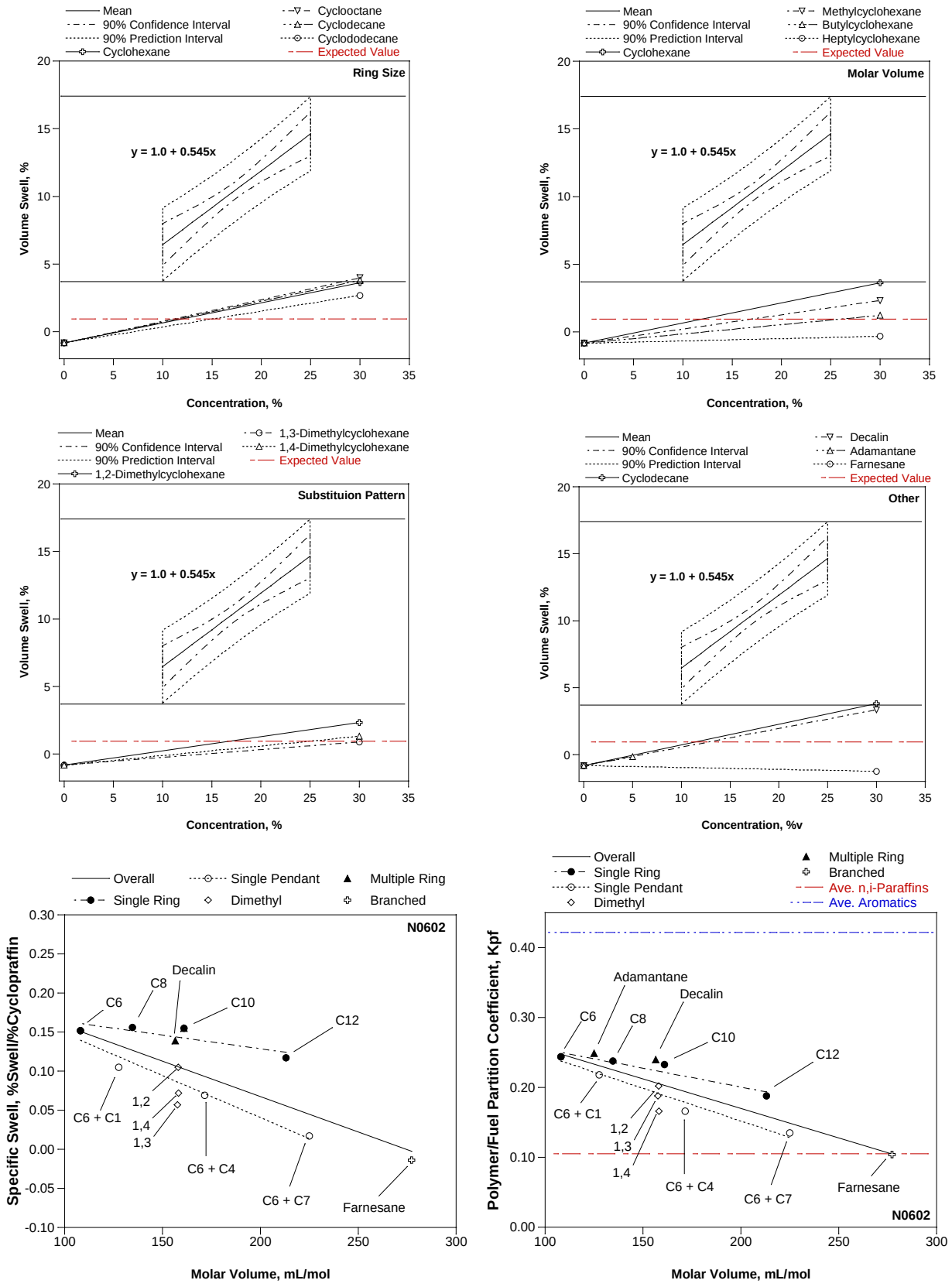

Figure L-11. As-received nitrile rubber O-ring (N0602).

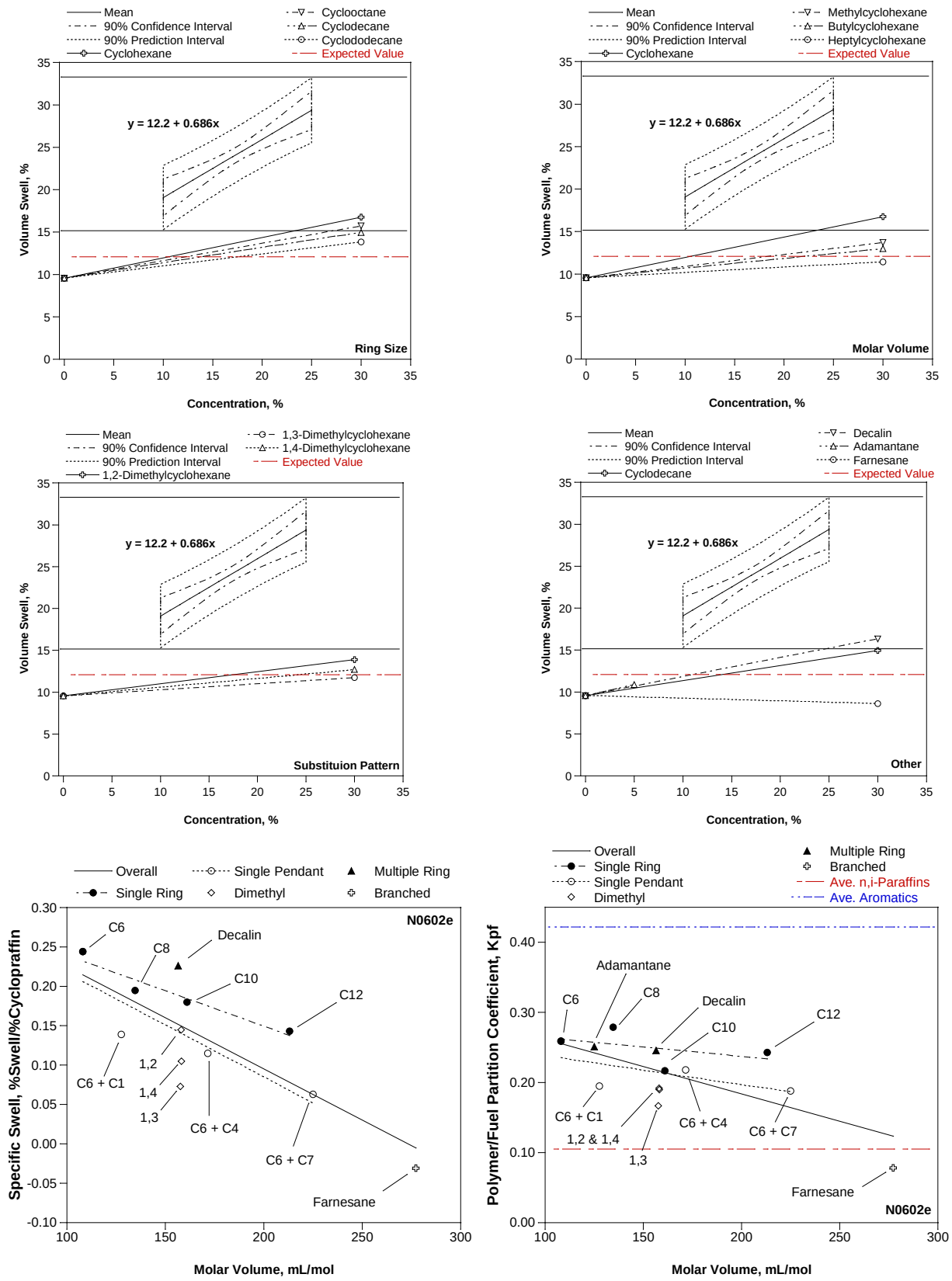

Figure L-12. Extracted nitrile rubber O-ring (N0602e).

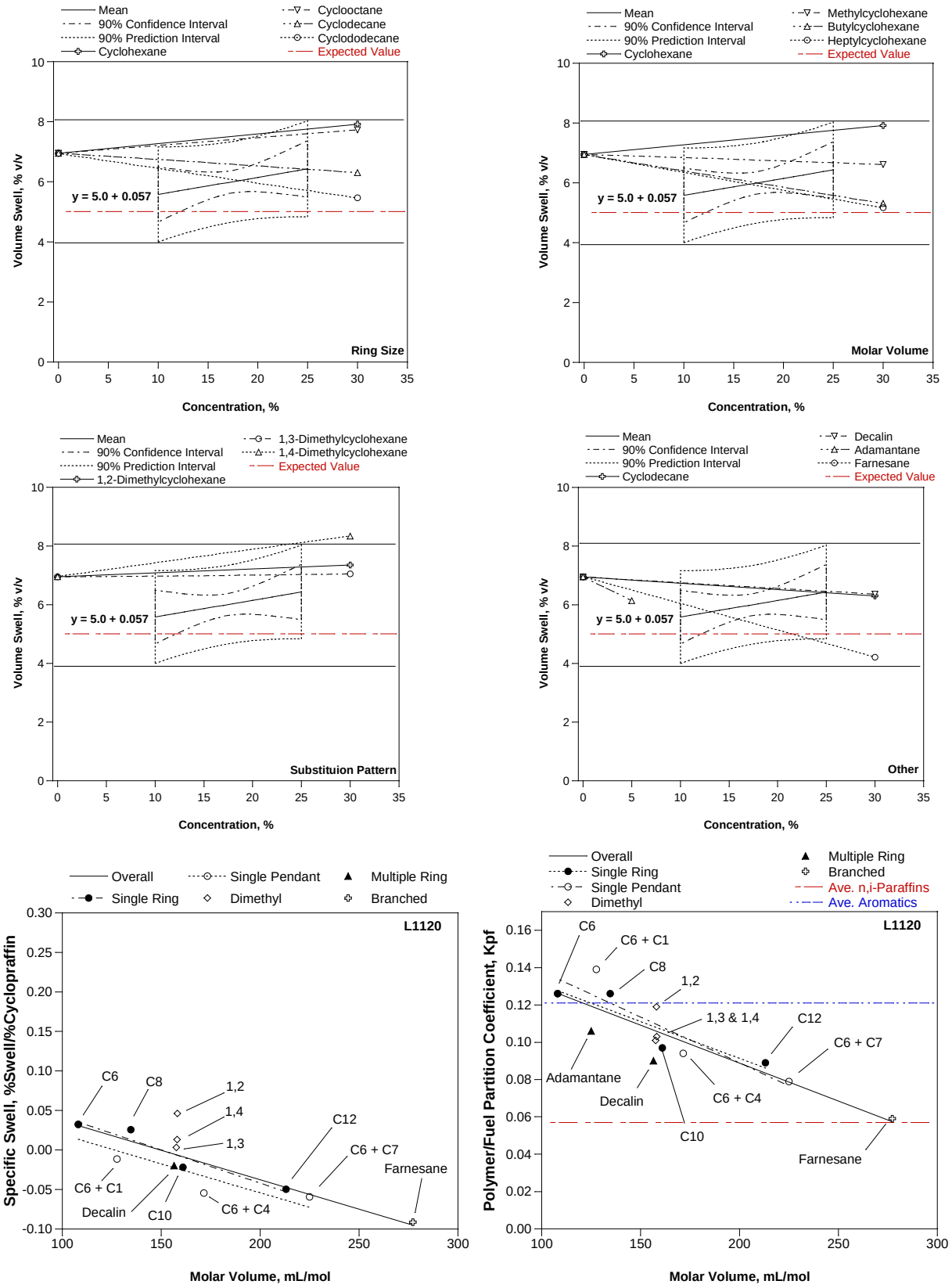

Figure L-13. Fluorosilicone O-ring (L1120).

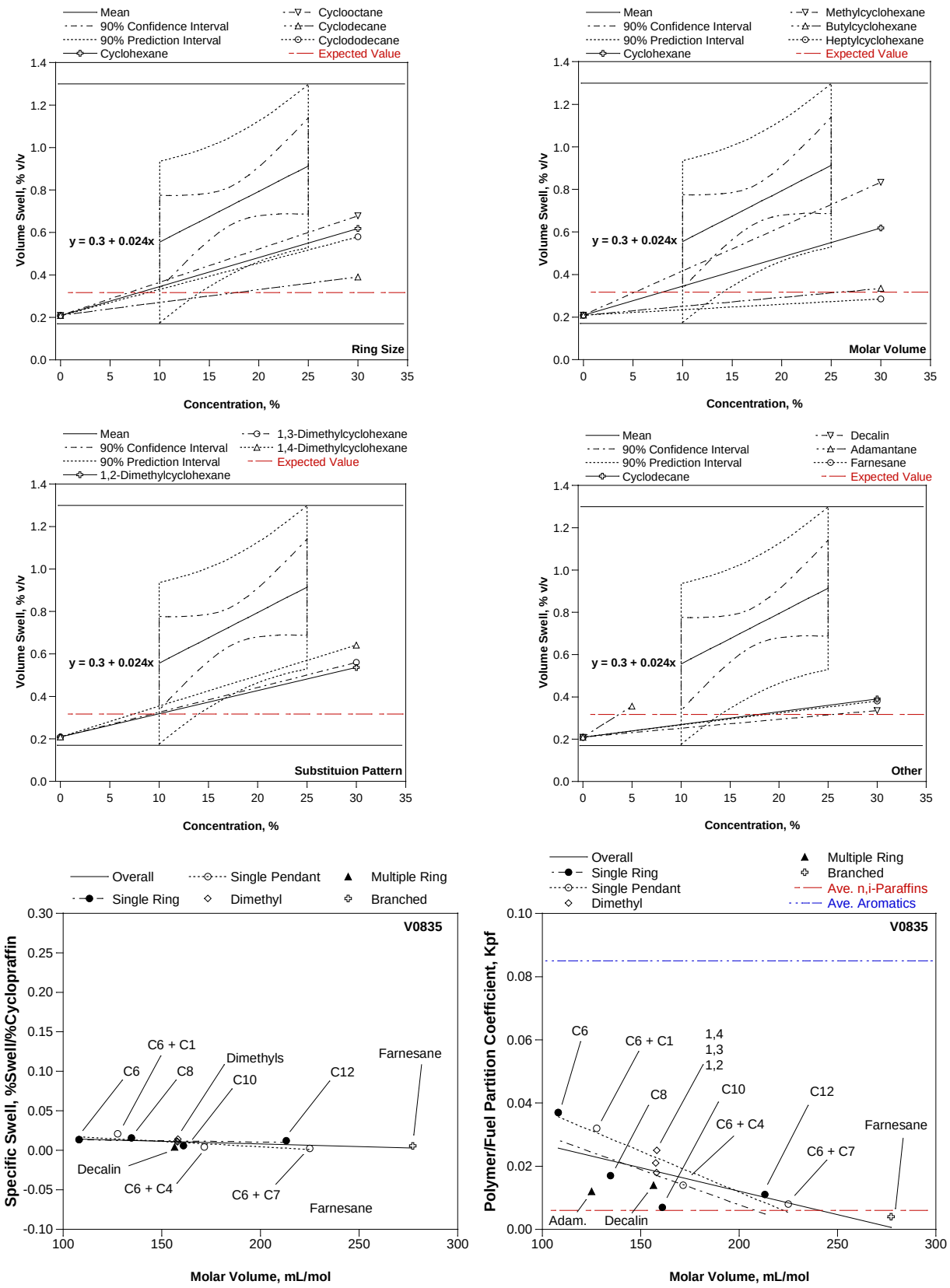

Figure L-14. Fluorocarbon O-ring (V0835).

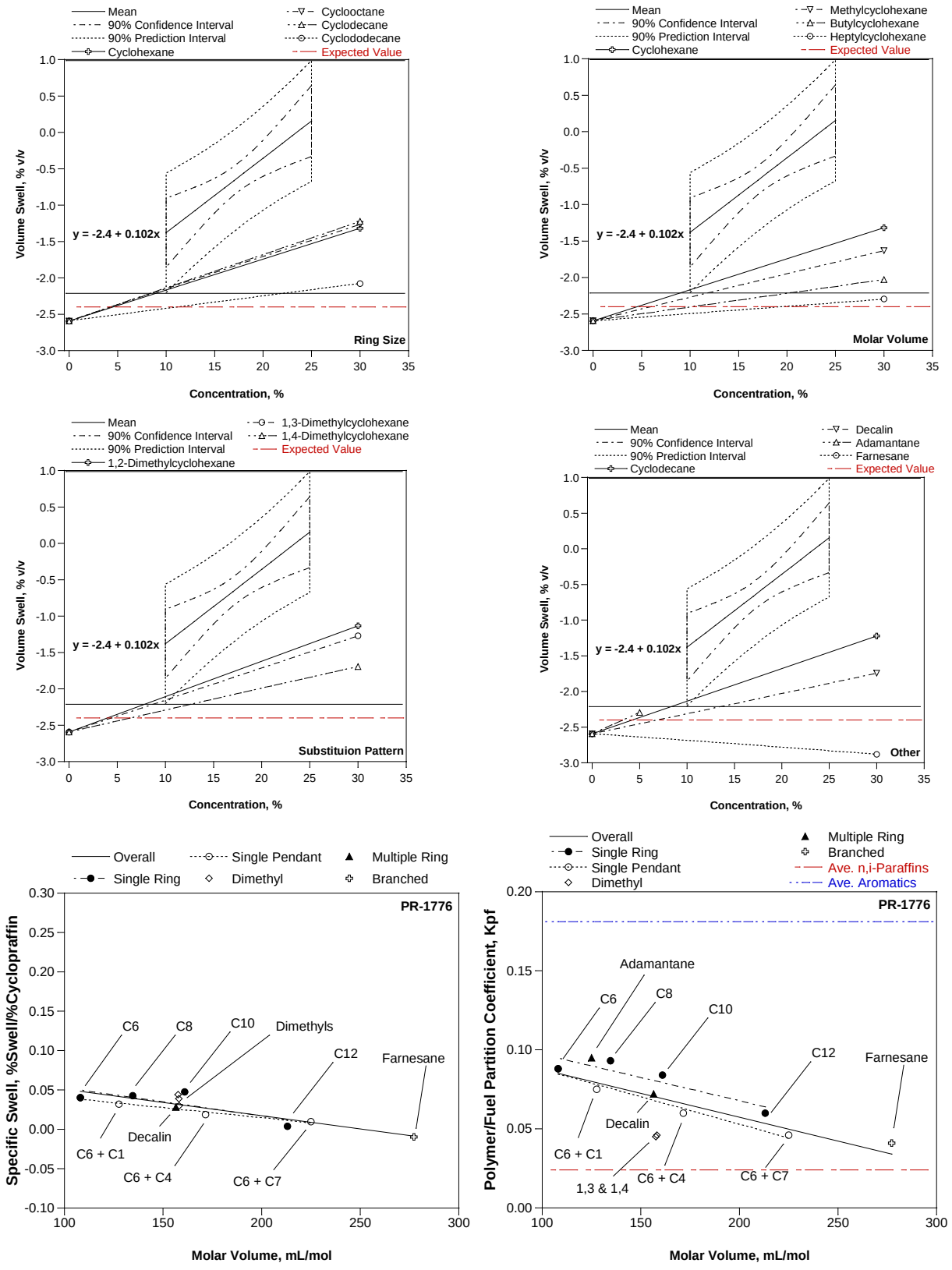

Figure L-15. Polysulfide sealant (PR-1776).

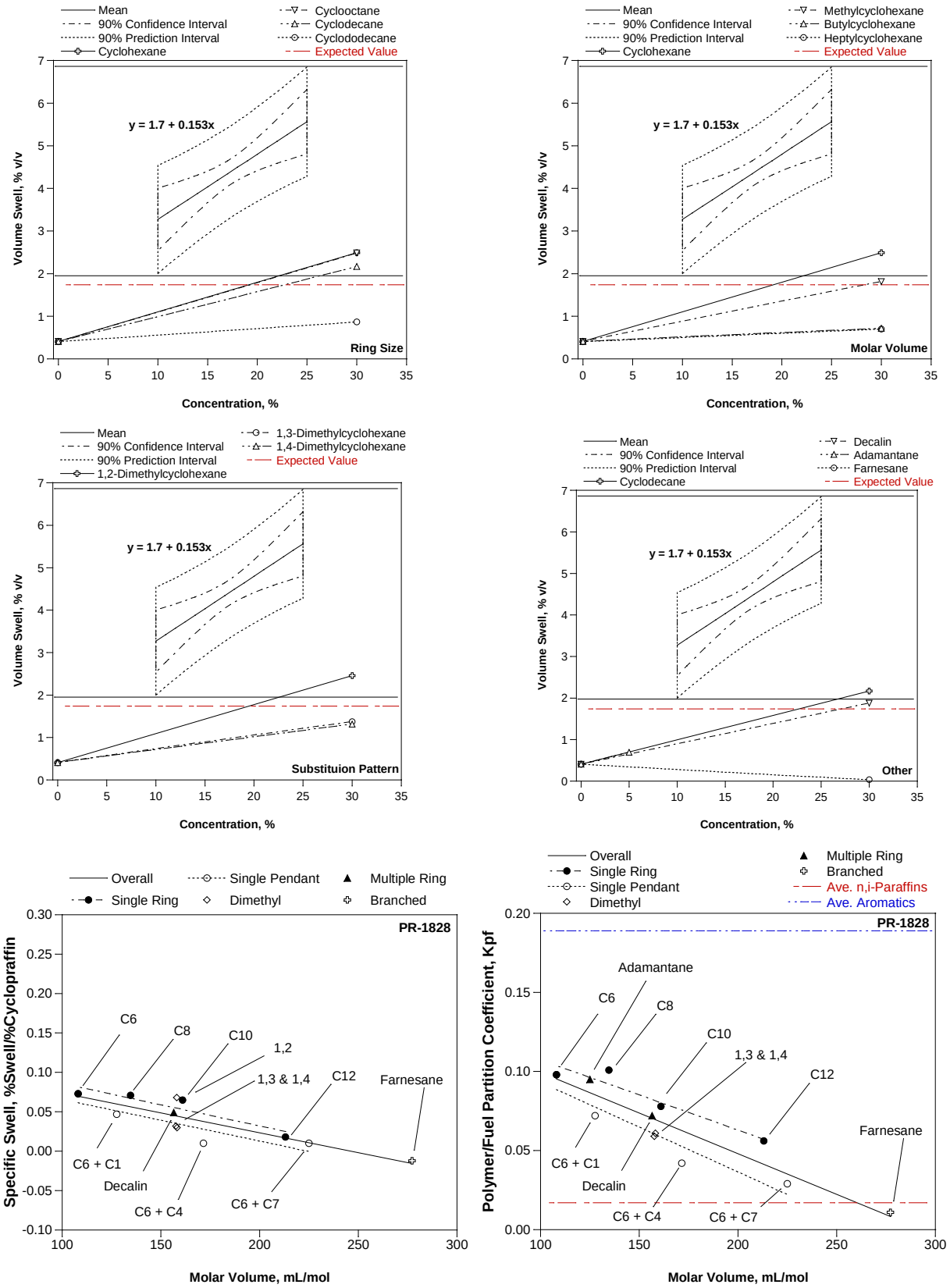

Figure L-16. Polythioether sealant (PR-1828).

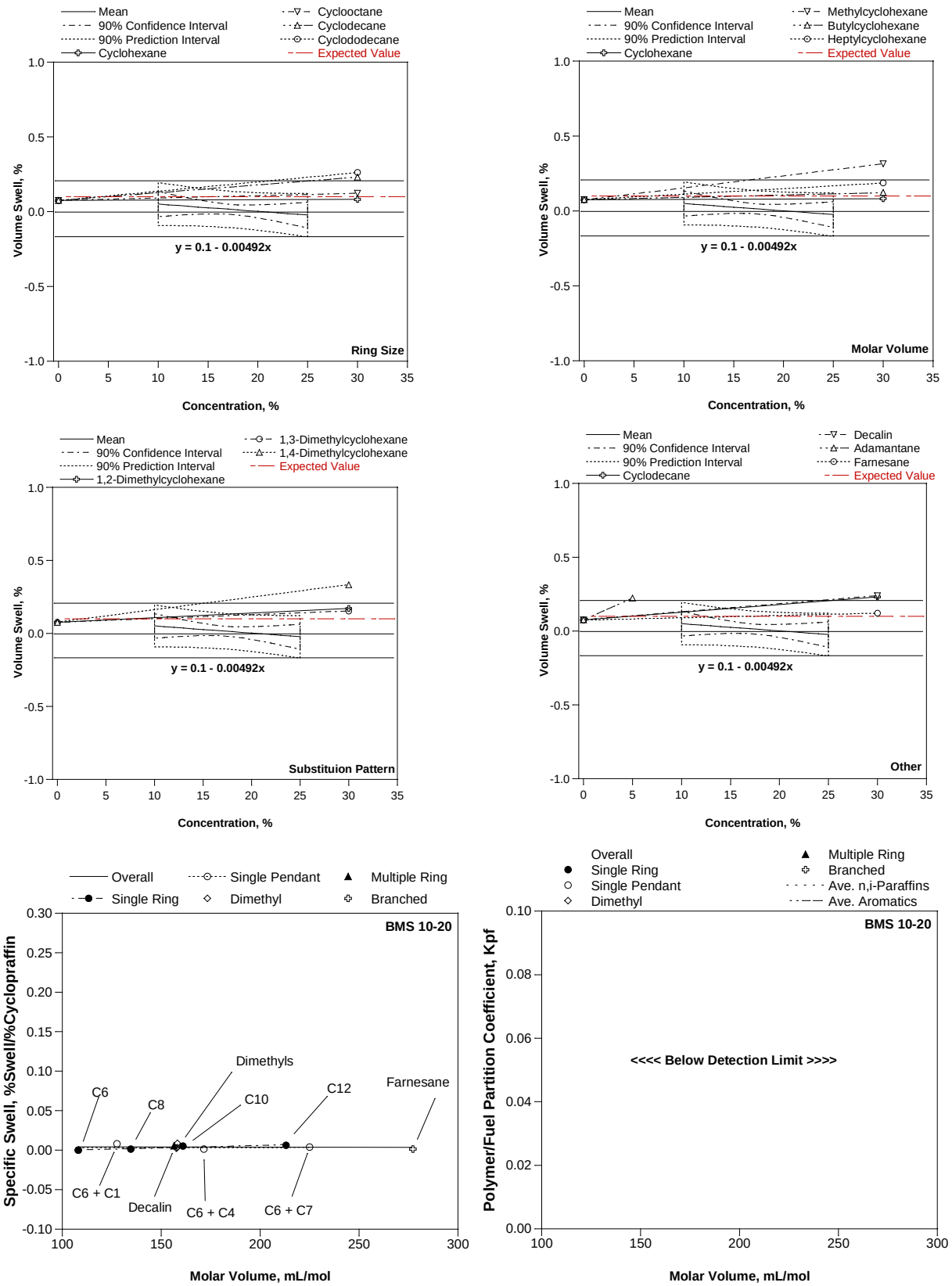

Figure L-17. Epoxy coating (BMS 10-20).

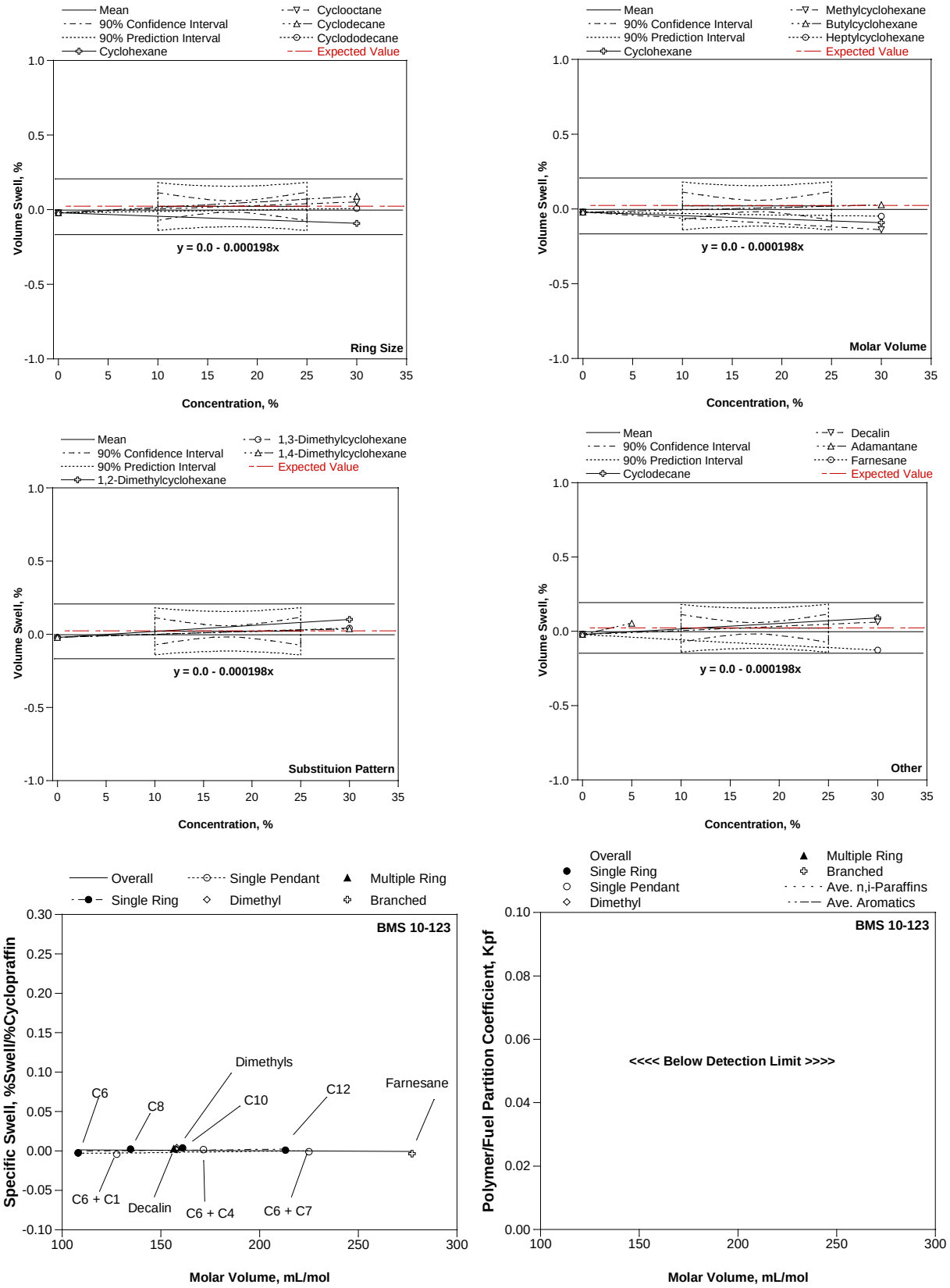

Figure L-18. Epoxy coating (BMS 10-123).

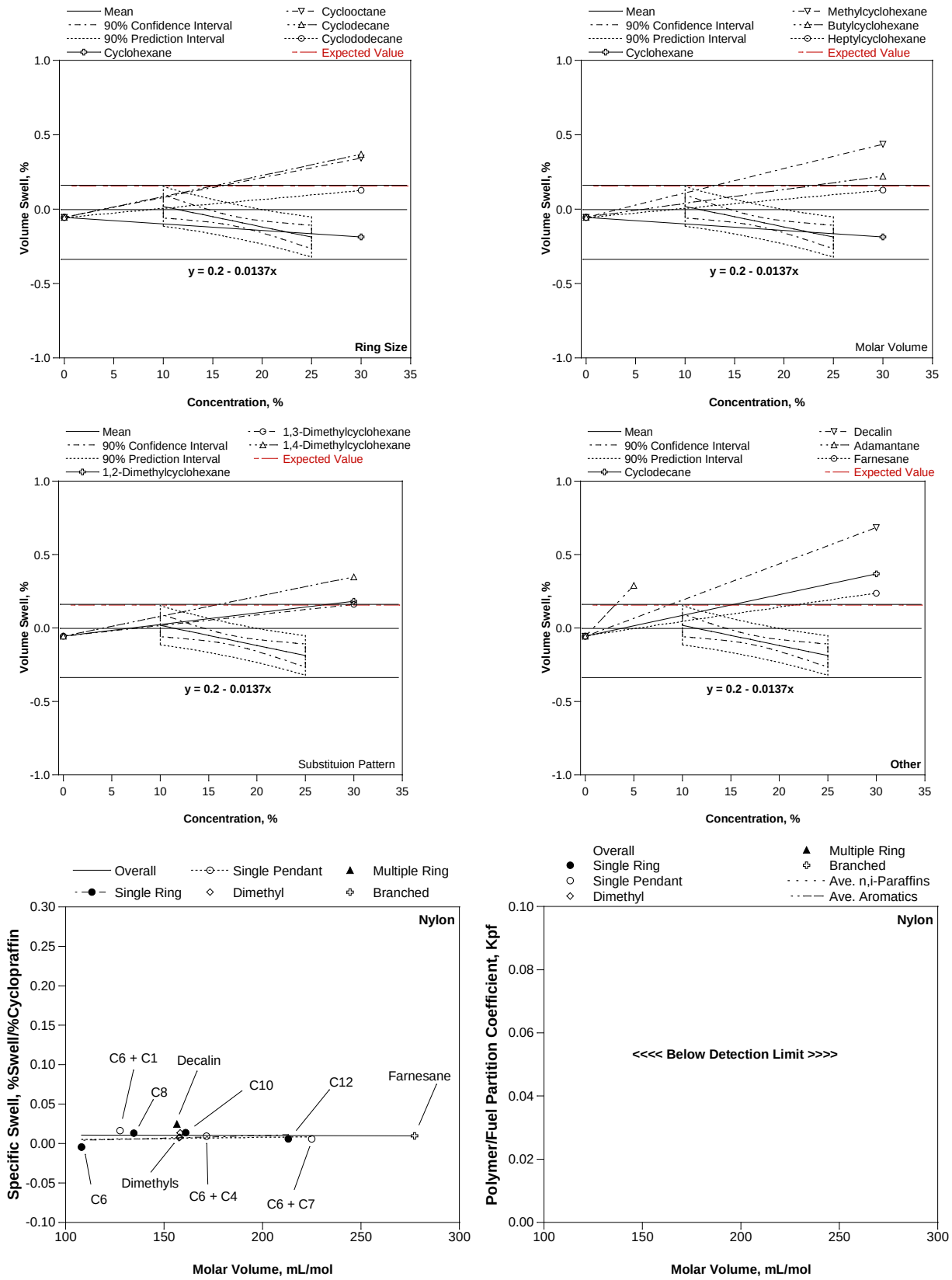

Figure L-19. Nylon film.

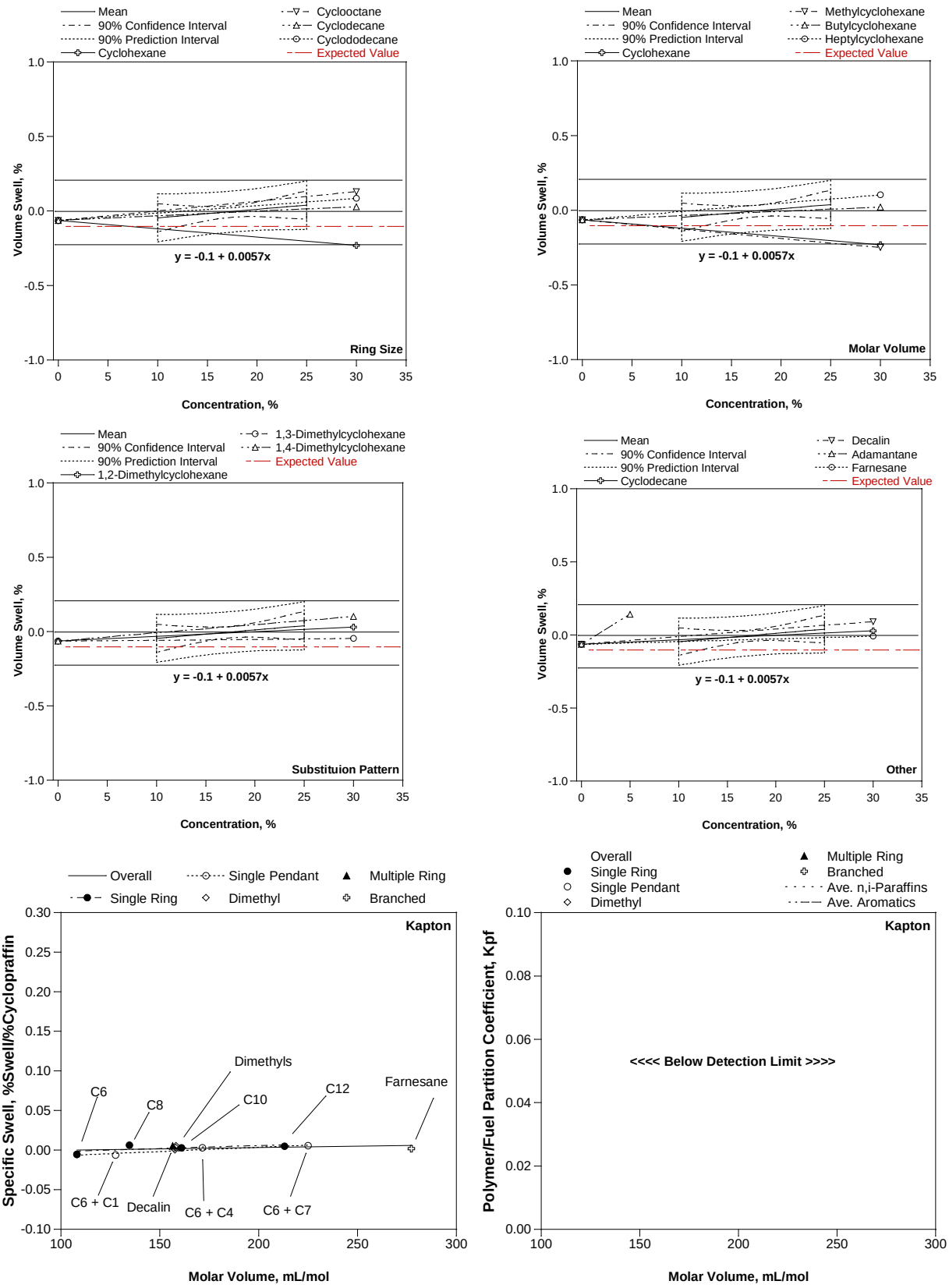

Figure L-20. Kapton film.

Overall, these results show that the volume swell character of the cycloparaffins is higher than the n,i-paraffins, though much less than the aromatics. These results also show that the primary factor influencing the activity of the cycloparaffins is their molar volume, though for some materials there is a degree of selectivity based on molecular structure. Specifically, for the nitrile rubber, polysulfide, and polythioether, the unsubstituted cycloparaffins showed a moderately higher activity as compared to the substituted cycloparaffins and that this activity declined as the ring size (molar volume) increased. The fluorocarbon showed a weak response to the cycloparaffins (though higher than the n,i-paraffins in the SPK-1) that declined as the molar volume increased with the unsubstituted cycloparaffins being slightly less active than the substituted cycloparaffins, thought the absolute value of the difference is quite small. The coatings and films showed little response to the fuels and remained relatively inert in the presence of the cycloparaffins. The Nylon film material showed the greatest response to the fuels, but the absolute values were very small and did not correlate with molar volume or any other factors such as molecular structure. The fluorosilicone showed significant volume swell in all fuels includes the SPK-1 blended with the cycloparaffins, Interestingly, the volume swell correlated strongly with the molar volume of the cycloparaffins, but without any significant selectivity based on other factors such as molecular structure.

With respect to the substitution pattern, the 1,2-dimethylcyclohexane generally showed higher activity as compared to the 1,3- and 1,4-dimethylcyclohexanes, where the activity of the later were similar.

The activity of decalin compared well with the activity of cyclodecane as did the activity of Adamantane. This indicates that there are no significant benefits with respect to the volume swell of multi-ring cycloparaffins, though they may have other favorable characteristics such as a relatively high density as compared to other paraffins. This suggests that the inclusion of cycloparaffins in general, and multi-ring cycloparaffins in particular, may offer a means of increasing the volume swell character as well as the density of SPK fuels.

5.12.4.3 Volume Swell of 50% SPK/Jet-A Fuel Blends with a Selected Cycloparaffin

Considering several factors including performance, availability, cost, and the fact that it has been demonstrated that it can be made from non-petroleum sources (coal) decalin was selected as the example paraffin to be blended with SPK-1 to demonstrate the use of a biofuel that contains a significant amount of a cycloparaffin as a blending stock with Jet-A fuels. Specifically, a blending stock was prepared with 30% v/v decalin (cis and trans) in SPK-1 and re-designated SPK-1a. The volume swell of the test materials was measured in SPK-1a and a set of 50% blends made with SPK-1a and the reference Jet-A fuels.

The volume swell results for the blends prepared from the original SPK-1 and SPK-1a are summarized in Figure L-21, Figure L-22, and Figure L-23, for the O-rings, sealants, and coatings and films, respectively. The overlap in the 90% prediction intervals are summarized in Table L-

9. Overall, these results show that the inclusion of the 30% decalin in the SPK-1 performed as expected; it elevated the volume swell of the SPK blending stock and the 50% fuel blends prepared from this base fuel to the point where all of the 50% fuel blends with 8% aromatics exhibited volume swell that was within the normal range for each of the test materials (see Table L-9). Most notable is the improvement in the performance of nitrile rubber, which tends to be one of the most problematic materials. Specifically, the overlap in the 90% prediction intervals improved from an average of 29% (29% of 50% SPK-1/Jet-A fuels having volume swell within the normal range for Jet-A) to 100%. Also, these data show that those materials that are relatively inert in Jet-A remain relatively inert in the 50% SPK-1a/Jet-A blends, so while the addition of decalin to the SPK-1 blending stock improved the volume swell of the challenging materials such as nitrile rubber, it did not adversely affect the volume swell behavior of the fuel resistant materials.

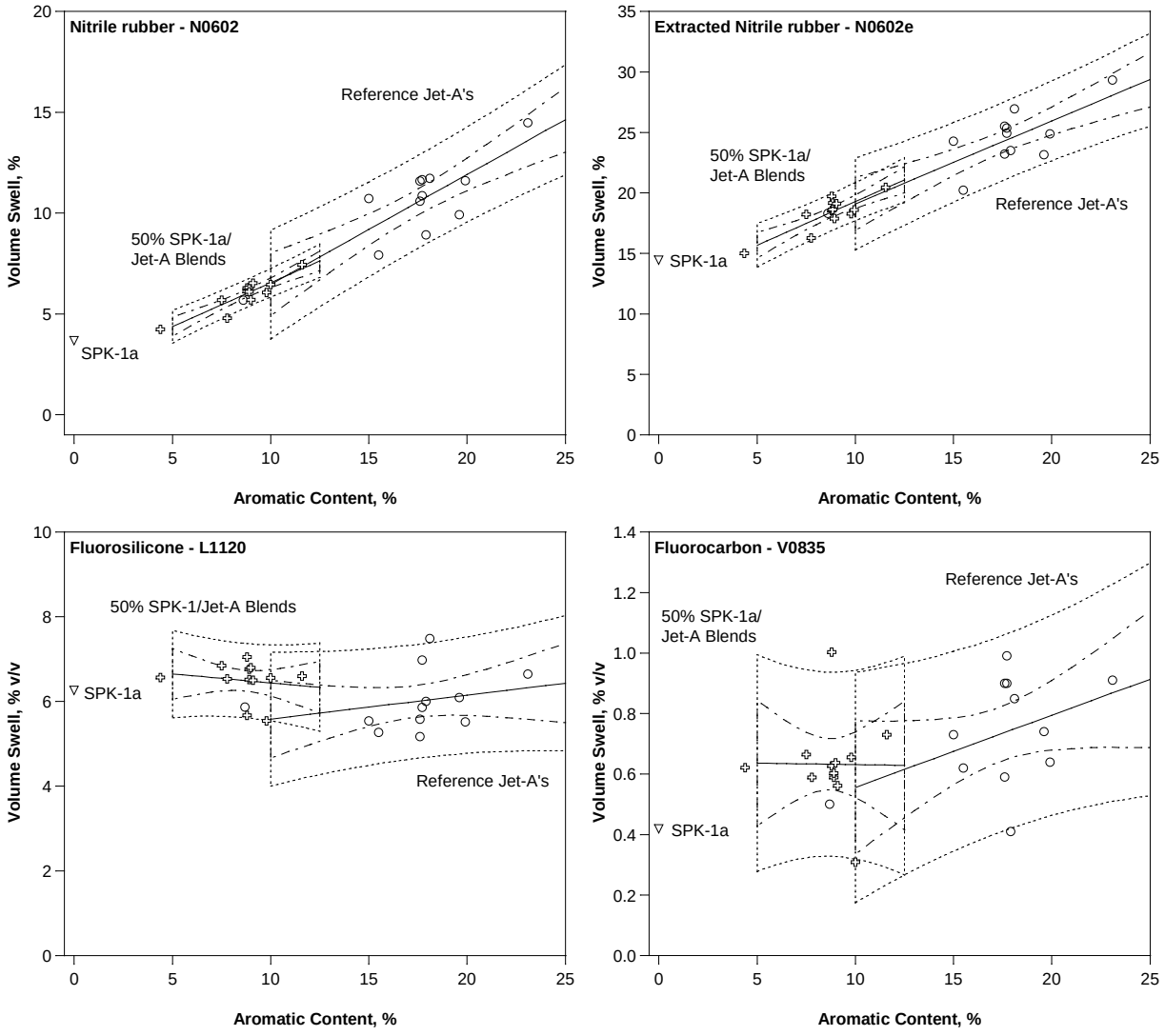

Figure L-21. Volume swell of the O-ring materials in SPK-1 with 30% decalin, 50% blends of this modified SPK-1 and Jet-A, and the reference Jet-As.

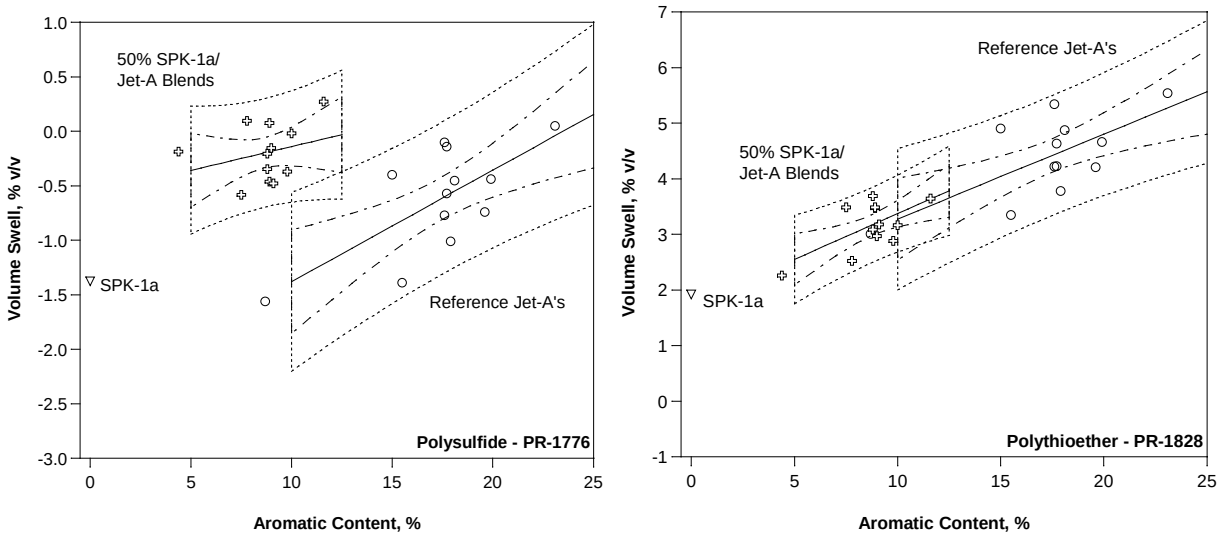

Figure L-22. Volume swell of the sealant materials in SPK-1 with 30% decalin, 50% blends of this modified SPK-1 and Jet-A, and the reference Jet-As.

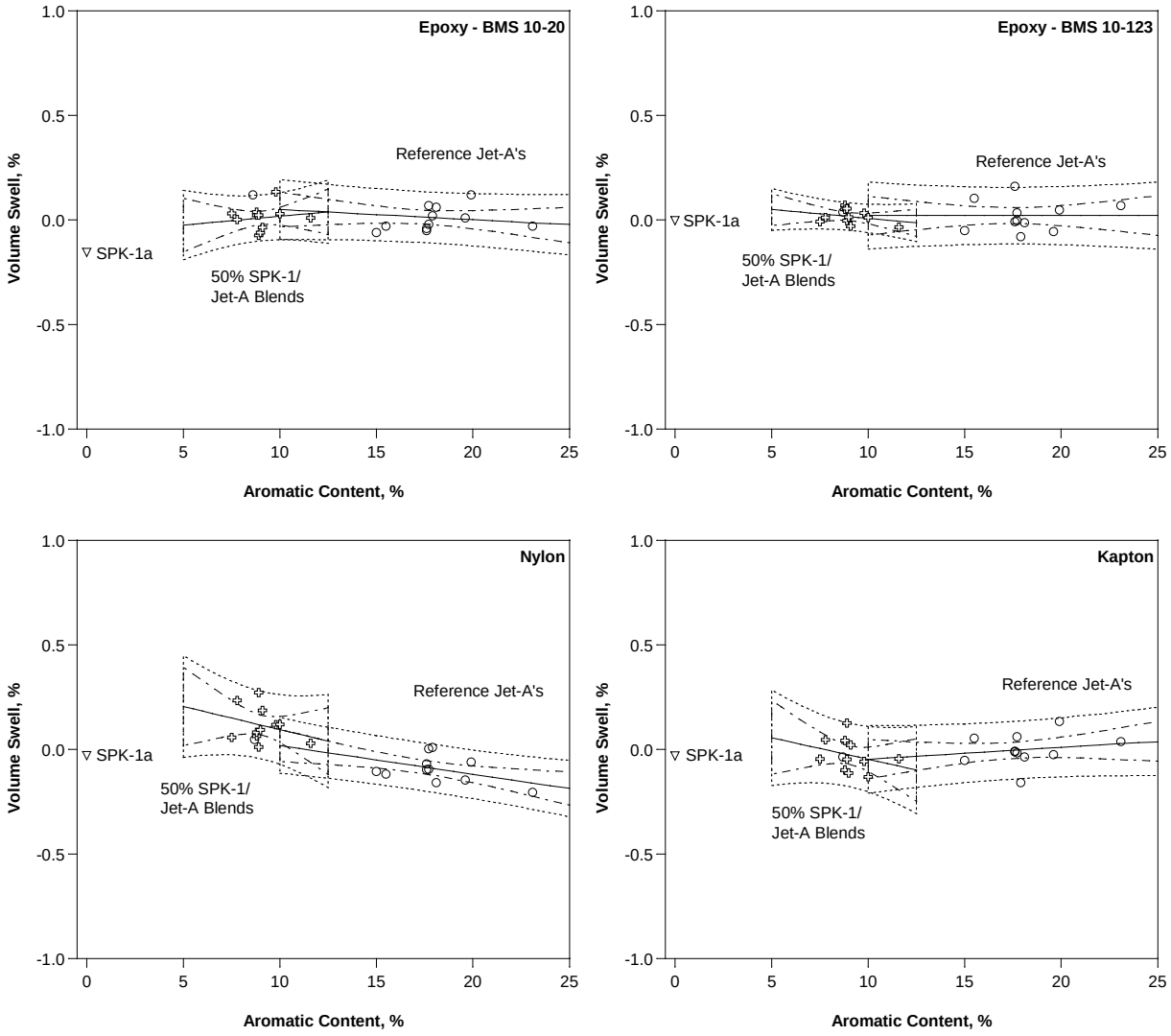

Figure L-23. Volume swell of the coatings and film materials in SPK-1 with 30% decalin, 50% blends of this modified SPK-1 and Jet-A, and the reference Jet-As.

Table L- 9. Overlap in the 90% Prediction Intervals for 50% Jet-A Fuel Blends Prepared with SPK-1 and SPK-1a

Component	Sample ID	50% SPK-1 5-12.5% Aro.	50% SPK-1a 5-12.5% Aro.	50% SPK-1 8% Aro.	50% SPK-1a 8% Aro.
O-Ring	N0602	44%	97%	23%	100%
	N0602e	51%	85%	34%	100%
	L1120	100%	100%	100%	100%
	V0835	100%	100%	100%	100%
Sealant	PR 1776	88%	100%	100%	100%
	PR 1828	57%	91%	56%	100%
Coating	BMS 10-20	100%	95%	100%	100%
	BMS 10-123	96%	100%	100%	100%
Film	Nylon	80%	100%	100%	100%
	Kapton	100%	84%	100%	100%

5.12.4.4 Analysis of Absorbed Fuel by Thermogravimetric Analysis

The mass fraction of absorbed fuel was analyzed using thermogravimetric analysis (TGA) as it was done in the core study (see section 3.2). The mass fraction of absorbed fuel versus volume swell is summarized in Figure L-24 and Figure L-25 for the O-rings and sealants, respectively. (Note that the coatings and films did not absorb enough for this analysis.) Overall, these results show good agreement for the materials that absorb a significant amount of fuel such as the nitrile rubber and fluorosilicone O-rings. The agreement is relatively poor for materials that are fuel-resistant, such as the fluorocarbon O-ring material, or have significant interferences that make discriminating the mass fraction of fuel from other semi-volatile components, such as the sealants. This suggests that TGA may be used to measure the mass fraction of absorbed fuel in some materials, though caution is warranted if this technique is to be used in place of measuring he volume swell directly.

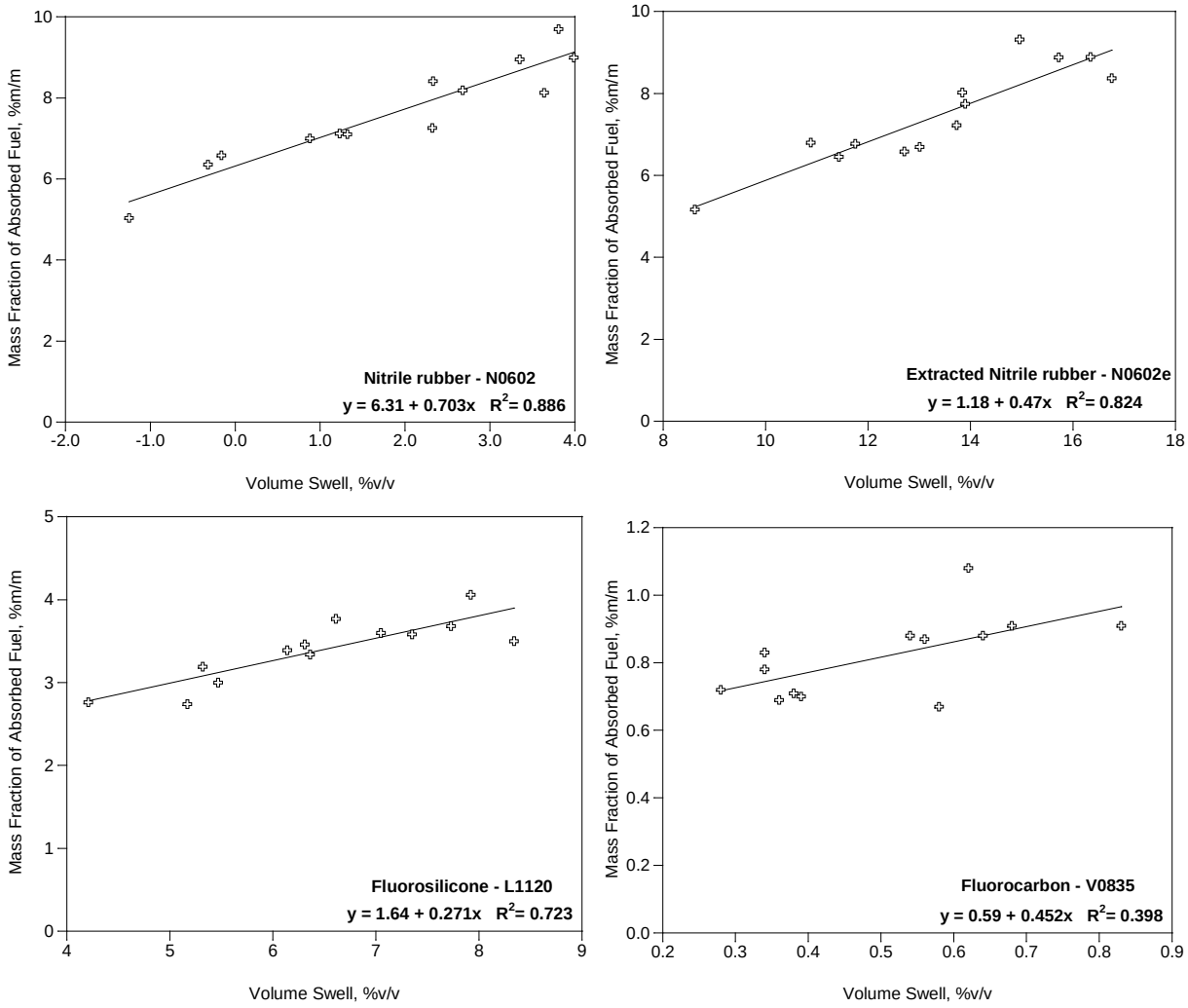

Figure L-24. The mass fraction of absorbed fuel versus volume swell for the O-ring materials.

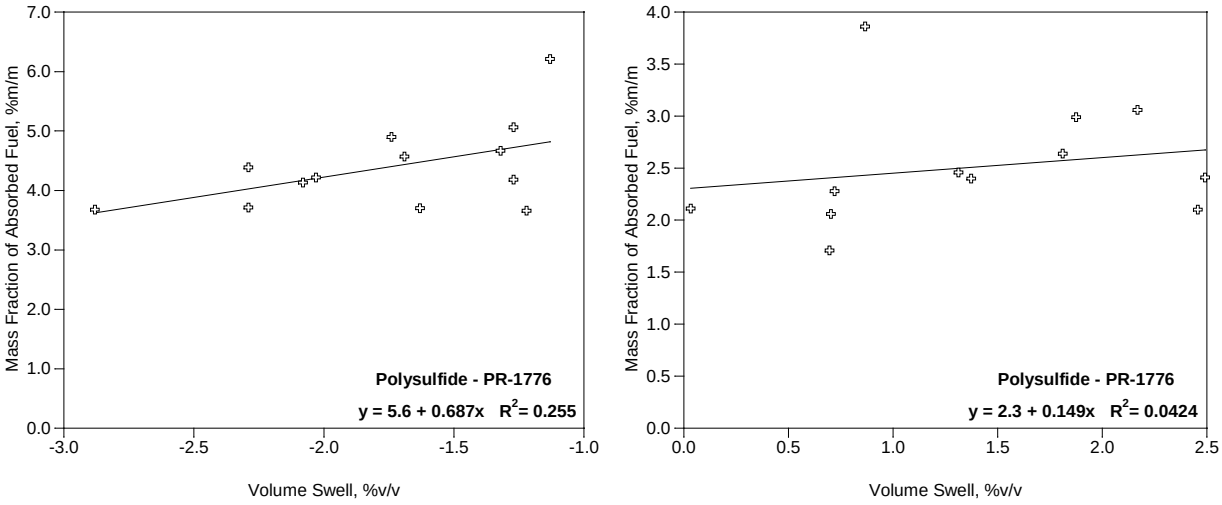

Figure L-25. The mass fraction of absorbed fuel versus volume swell for the sealant materials.

5.12.5 Conclusions

This study shows that cycloparaffins obey the same basic rules as other fuel components. Specifically, the ability of cycloparaffins to impart volume swell character into a fuel such as an SPK or Jet-A increases as the polarity of the cycloparaffin increases and as molar volume decreases (cycloparaffins do not exhibit any hydrogen bonding character). The activity of cycloparaffins is higher than that of linear and branched paraffins by virtue of their relatively small molar volume and slight polar character. The later has been directly observed using techniques such as GCxGC analysis and likely arises from the restricted conformations of the cycloparaffins structure. Molar volume appears to be the main factor influencing the performance of cycloparaffins, there is some differentiation based on structure. Specifically, non-substituted cycloparaffins show a modest increase in activity as compared to substituted cycloparaffins. The volume swell is weakly influenced by the substitution position of pendant groups with the 1,2 substitution pattern being the preferred configuration. The activity of multi-ring cycloparaffins such as decalin and Adamantane does not appear to be exceptionally high as compared to other non-substituted cycloparaffins of similar molecular weight. The addition of decalin at 30%v/v to the SPK used here significantly improved the material compatibility of the 50% fuel blends used in this study. The results suggest it may be possible to develop a fuel that is high in cycloparaffins with very low, or even zero, aromatic content. Cycloparaffins may also offer a means of contributing to the density to SPKs without degrading their performance.